

THE THERMODILUTION TECHNIQUE  
DURING ARTIFICIAL VENTILATION

DE THERMODILUTIEMETHODE  
TIJDENS BEADEMING

PROEFSCHRIFT  
TER VERKRIJGING VAN DE GRAAD VAN DOCTOR  
AAN DE ERASMUS UNIVERSITEIT ROTTERDAM  
OP GEZAG VAN DE RECTOR MAGNIFICUS  
PROF.DR. A.H.G. RINNOOY KAN  
EN VOLGENS BESLUIT VAN HET COLLEGE VAN DEKANEN.  
DE OPENBARE VERDEDIGING ZAL PLAATSVINDEN OP  
WOENSDAG 29 JUNI 1988 OM 13.45 UUR

DOOR

JOZEF REINIER CORNELIS JANSEN

GEBOREN TE NOORDWIJKERHOUT

## Promotiecommissie

Promotor: Prof. Dr. A. Versprille

Overige leden: Prof. Dr. Ir. N. Bom  
Prof. Dr. J. A. Poulis  
Prof. Dr. P. R. Saxena

Co-promotor: Dr. J. M. Bogaard

Financial support by the Netherlands Heart Foundation for the publication of this thesis is gratefully acknowledged.

Voor *Betty, Reinier en André*, aan mijn ouders

# CONTENTS

<b>1. The indicator dilution technique</b>	<b>7</b>
1.1 Introduction . . . . .	7
1.2 Historical aspects of the indicator dilution methods . . . . .	7
1.3 Theory of indicator dilution methods . . . . .	9
1.4 The assumption of constant blood flow . . . . .	11
1.5 Outline of the thesis . . . . .	12
<b>2. A computerized respiratory system for ventilation, lung function and circulation testing</b>	<b>17</b>
2.1 Introduction . . . . .	17
2.2 System description . . . . .	18
2.2.1 <i>Pump and valve assembly</i> . . . . .	18
2.2.2 <i>The motor servo system</i> . . . . .	18
2.2.3 <i>Computer system</i> . . . . .	21
2.2.4 <i>Communication</i> . . . . .	21
2.2.5 <i>Ventilatory settings</i> . . . . .	21
2.2.6 <i>Software</i> . . . . .	23
2.3 Applications . . . . .	24
2.3.1 <i>Automatic operations</i> . . . . .	24
2.3.2 <i>Lung function testing</i> . . . . .	26
2.3.3 <i>Circulation testing</i> . . . . .	29
2.4 Comments . . . . .	31
<b>3. Thermodilution for measurement of cardiac output during artificial ventilation</b>	<b>33</b>
3.1 Introduction . . . . .	33
3.2 Methods . . . . .	34
3.2.1 <i>Surgical procedure</i> . . . . .	34
3.2.2 <i>Measurements</i> . . . . .	35
3.2.3 <i>Data acquisition and analysis</i> . . . . .	37
3.2.4 <i>Experimental procedures</i> . . . . .	38
3.3 Results . . . . .	38
3.3.1 <i>Assessment of steady state</i> . . . . .	38
3.3.2 <i>Variation of cardiac output with phase of ventilatory cycle</i> . .	39
3.3.3 <i>Estimation of cardiac output under changing circumstances</i> . .	39
3.3.4 <i>Comparison of thermodilution and Fick method</i> . . . . .	41
3.4 Discussion . . . . .	41

3.4.1	<i>Thermodilution technique</i> . . . . .	41
3.4.2	<i>Ventilatory modulation</i> . . . . .	45
<b>4.</b>	<b>Improvement of cardiac output estimation by the thermo- dilution method during mechanical ventilation</b>	<b>49</b>
4.1	Introduction . . . . .	49
4.2	Methods . . . . .	50
4.2.1	<i>Experimental techniques</i> . . . . .	50
4.2.2	<i>Catheters</i> . . . . .	50
4.2.3	<i>Fick method</i> . . . . .	50
4.2.4	<i>Thermodilution method</i> . . . . .	51
4.2.5	<i>Series of observations and conditions</i> . . . . .	52
4.2.6	<i>The averaging procedures</i> . . . . .	53
4.2.7	<i>Statistical analyses</i> . . . . .	55
4.3	Results . . . . .	56
4.3.1	<i>Pattern of blood flow estimation</i> . . . . .	56
4.3.2	<i>Amplitude of the estimated flow</i> . . . . .	56
4.3.3	<i>Comparison of thermodilution and Fick method</i> . . . . .	59
4.3.4	<i>Average procedure</i> . . . . .	60
4.4	Discussion . . . . .	60
4.4.1	<i>Cyclic modulation</i> . . . . .	61
4.4.2	<i>Accuracy of estimates</i> . . . . .	62
4.4.3	<i>Clinical application</i> . . . . .	64
<b>5.</b>	<b>Extrapolation of thermodilution curves obtained during a pause in artificial ventilation</b>	<b>67</b>
5.1	Introduction . . . . .	67
5.2	Methods . . . . .	68
5.2.1	<i>Surgical procedure</i> . . . . .	68
5.2.2	<i>Measurements and estimation of cardiac output</i> . . . . .	69
5.2.3	<i>Model fitting</i> . . . . .	70
5.2.4	<i>Experimental protocol</i> . . . . .	71
5.2.5	<i>Data analysis</i> . . . . .	71
5.3	Results . . . . .	72
5.4	Discussion . . . . .	78
<b>6.</b>	<b>Discrepancies between models as a basis for cardiac output estimation and medical practice</b>	<b>83</b>
6.1	Introduction . . . . .	83

6.2	Methods . . . . .	84
6.2.1	<i>Animal experiments</i> . . . . .	84
6.2.2	<i>Analysis of the thermodilution curves</i> . . . . .	84
6.2.3	<i>Flow averaging of concentration and of time</i> . . . . .	85
6.2.4	<i>Pulse contour method</i> . . . . .	85
6.2.5	<i>Model fitting</i> . . . . .	87
6.3	Results . . . . .	88
6.4	Discussion . . . . .	92
6.4.1	<i>Flow averaging of time or concentration with a direct flow measurement</i> . . . . .	92
6.4.2	<i>Flow averaging of time or concentration with the pulse contour method</i> . . . . .	93
<b>7.</b>	<b>Verification of the experimental results by model simulations</b>	<b>97</b>
7.1	Introduction . . . . .	97
7.2	Methods . . . . .	97
7.2.1	<i>Constant blood flow and ideal bolus injections</i> . . . . .	99
7.2.2	<i>Nonstationary flow</i> . . . . .	99
7.2.3	<i>The simulation model</i> . . . . .	99
7.3	Results . . . . .	101
7.3.1	<i>Variation of cardiac output with the moment of injection in the cycle</i> . . . . .	101
7.3.2	<i>Effect of the amplitude of modulation of flow on the cardiac output estimates</i> . . . . .	103
7.3.3	<i>Prolonging the injection time</i> . . . . .	103
7.4	Discussion . . . . .	104
7.4.1	<i>Estimation of mean cardiac output under changing circumstances</i> . . . . .	106
7.4.2	<i>Improvement of cardiac output estimation</i> . . . . .	107
<b>8.</b>	<b>Summary</b>	<b>113</b>
<b>9.</b>	<b>Samenvatting</b>	<b>117</b>
	Curriculum vitae	125
	Nawoord	126
	List of abbreviations	127

# CHAPTER 1

## THE INDICATOR DILUTION TECHNIQUE

### 1.1 Introduction

*"It is a source of regret that the measurement of flow is so much more difficult than the measurement of pressure. This has led to an undue interest in blood pressure measurements. Most organs, however, require flow rather than pressure".* This statement from Jarisch [11] in 1881, cited by Prys-Roberts (1969), is still fully accepted. Many methods of flow or cardiac output measurements have been developed, but the number of methods for application in animal and, particularly, human studies is limited. In this thesis the indicator dilution method will be considered because this method attained an extensive application in clinical practice, even under circumstances (e.g. during mechanical ventilation) which do not fulfill the theoretical conditions required for the method.

### 1.2 Historical aspects of the indicator dilution methods

The concept of indicator dilution has already been used by Hering [8] in 1829 to determine the circulation time. He injected potassium ferricyanide intravenously and collected timed samples of blood from a contralateral vein. To detect the time of arrival of the first indicator he added ferric chloride to these samples to obtain the Prussian Blue reaction. Such a determination reflected only the shortest pathway taken by the blood between the site of injection and the site of sampling.

Stewart extended the application of the indicator dilution technique to the determination of cardiac output and of central blood volume. He was the first (1897) who developed the method for a continuous detection of indicator at the sampling site [21]. He injected a solution of hypertonic saline, 1.5%, into a blood vessel and measured the diluted saline downstream. The detector consisted of a pair of nonpolarizable electrodes, placed in an arm of a Wheatstone bridge. The output of the bridge was connected to a telephone and the bridge was balanced to yield minimal noise. When the blood with higher sodium chloride concentration reached the electrodes, the bridge became unbalanced, and the noise increased. The time between injection and the rise of the audio signal was called the "circulation time". Stewart also

used methylene blue as an indicator and measured its appearance by transillumination of the blood vessel at the detection site. The methylene blue coloured blood overpowered the natural colour of the blood and could be seen through the wall of the vessel.

Subsequently, Stewart [22, 23] refined the method to measure blood flow. He injected a known concentration of NaCl solution with a constant speed for a certain time. A sample of the blood at the detection site was collected when the sound remained steady. *"Sometimes, for comparison, two or even three samples were collected at different parts of time of passage, or collection was made during the whole time of passage including the tapering beginning and end"* [22]. The collection during the whole time of passing is analogous to the mathematical integration of the dilution curve by the sudden single injection technique. The concentration of NaCl in the blood was measured by adding NaCl solution to a blood sample obtained before injection until the noise was equal to that of the measurement sample. From the injected concentration, the injection speed and the measured concentration in the blood cardiac output was calculated.

Hamilton and his group [5, 6, 7, 12, 14] continued the work of Stewart and made it possible to correct for the effect of recirculation on the primary curve after a single injection of indicator. They eliminated the recirculation of indicator by a semilogarithmic plotting of the decay of the curve with use of a linear extrapolation of the upper part of the descending limb. This resulted in a more accurate estimation of cardiac output. They assessed the reliability of the single injection method, since then known as the Stewart-Hamilton technique, by comparison of their results with those of direct flow measurements in models without any recirculation [12]. Besides the agreement between both estimations of cardiac output no significant differences were found with estimates of cardiac output obtained according to direct Fick procedures [14].

In 1948 Hamilton's group joined with Cournand's group to perform a comparative study of cardiac output measurement in man by using the direct Fick and the dye dilution technique [6]. This study established the Stewart-Hamilton technique as a reliable method for the estimation of cardiac output.

A more mathematical approach of the indicator dilution technique was introduced by Stephenson [20], who considered the dilution curve as a frequency distribution of indicator particles. To eliminate recirculation he analyzed the whole first part of the curve, instead of Hamilton's linear extrapolation technique which only used a part of the downslope of the curve.



Other mathematical models were introduced; Newman et al. [16] presented a compartmental model, Sheppard [19] a random walk model, and Stow and Hetzel [24] a log-normal distribution. However, Meier and Zierler [13] are generally cited, nowadays, for the clearly presented theoretical basis of both the single injection technique and the technique of constant infusion of indicator including the limitations of this techniques for measuring flow and volume.

The theoretical basis of the thermodilution method is identical to that described for NaCl and dye. The indicator is a cold fluid with respect to the blood temperature. The sensor of the temperature change of the blood is a thermistor probe. The thermodilution catheter technique was first described by Fegler in 1954 [4]. Subsequently, it was studied and improved by a number of investigators. After the introduction of the flow-guided pulmonary artery catheter by Swan and Ganz in 1970 [25] the thermodilution method for estimation of cardiac output became a common clinical tool.

### 1.3 Theory of indicator dilution methods

For a reliable application of a dilution technique several conditions have to be fulfilled.

As a first main condition steady state of the biological system can be mentioned. One of the most important stationary variables is of course the variable to be estimated, which is blood flow. In a stationary system the distribution of transit times of all parts of indicator will be constant from moment to moment. Therefore, with similar input of indicator into the system at different times the output responses will have to be the same. Precautions have to be taken that the injection of indicator does not alter the steady state significantly.

A second main condition to be fulfilled is linearity. This linearity implies a proportional increase in response when the injected amount of indicator is increased. So, during the passage of indicator no loss of indicator from the circulatory system can be tolerated.

Stationarity and linearity have to be fulfilled for a theoretical accurate derivation of most equations including the convolution principle. This principle is an important concept in the different indicator dilution methods: the single injection technique, the constant infusion method without recirculation, and the constant infusion technique with a constant recirculation. We will consider here the single injection technique.



Fig. 1. Outflow concentration of indicator versus time after a bolus injection without recirculation.

#### *Single injection of indicator*

A typical thermodilution curve recorded from the pulmonary artery, after injection of cold near the entrance of the right atrium, is seen in Fig. 1. Conservation of mass requires that the blood flow,  $\dot{Q}(t)$ , times the concentration,  $C(t)$ , summated over time is equal to the injected mass,  $m_i$ , i.e.

$$m_i = \int_0^{\infty} \dot{Q}(t)C(t)dt \quad (1)$$

At the injection site ( $i$ ) the same equation counts for the injectate,

$$m_i = \int_0^{\infty} \dot{Q}_i(t).C_i dt \quad (2)$$

However, when the injection is done in an infinitely short time, which is an impulse input, the injected amount of indicator is the product of injection volume,  $V_i$ , and concentration  $C_i$ , or,

$$m_i = V_i.C_i \quad (3)$$

Infinitely short time for injection of an amount of fluid cannot be realized. However, a short injection time (about 300 ms) with respect to the time period of a dilution curve (4 s) is satisfactory. Under the circumstances of the two main conditions, i.e. stationarity and linearity, and the flow,  $\dot{Q}$ , is calculated from e.g. 1 and 3 according to:

$$\dot{Q} = \frac{V_i.C_i}{\int_0^{\infty} C(t)dt} \quad (4)$$

This formula should be corrected for recirculation of indicator. There are, however, some indicators, such as the temperature, hydrogen, and xenon, whose recirculation is minimal, and where extrapolation techniques of the dilution curve are not required.

For temperature as an indicator, equation 4 becomes:

$$\dot{Q} = \frac{S_i \rho_i (T_b - T_i) V_i}{S_b \rho_b \int_0^\infty \Delta T_b(t) dt} \quad (5)$$

where  $T$  is the temperature,  $\rho$  the density,  $S$  the specific heat of blood ( $b$ ) and injectate ( $i$ ) respectively, and  $V_i$  the injected volume of indicator.

#### 1.4 The assumption of constant blood flow

Zierler [29] studied the effect of violation of the assumptions underlying the generally accepted Stewart-Hamilton equation. For the assumption of stationary blood flow and volume, he stated: "*The sudden-injection method cannot measure either flow or volume, if flow or volume changes during the course of the indicator dilution curve, unless the changes are rapid and phasic*". If cyclic changes in flow occur, as in mechanical ventilation, the dilution curve will be differently influenced by the phases of low and high flow. When the main part of the dilution curve coincides with the phase of high flow mean flow will be overestimated, when it coincides with the phase of low flow mean flow will be underestimated.

As was shown in theoretical and physical models [1, 17, 18, 28] the errors in the estimation of mean flow by the bolus injection technique are potentially very large, especially if the frequency content of the dilution curve is similar to that of the flow modulation as occurs during artificial ventilation.

The presence of such fluctuations has been shown by several authors. Hering [9], already in 1869, demonstrated the influence of mechanical ventilation on the circulation in a paper, entitled: "*Über den Einfluß der Athmung auf den Kreislauf*". Hoffman et al. [10] and Vermeire and Butler [26] reported the presents of cyclic blood flow changes during spontaneous breathing. Morgan et al. [15] were the first who demonstrate the cyclic modulation of blood flow during mechanical ventilation. In humans, pulmonary capillary flow during inspiration could be as much as four times the flow during expiration [26]. In pigs the amount of modulation of blood flow during artificial ventilation appeared to be reversely related to mean flow [27]. This means that during hypovolemia and during ventilation with positive end expiratory pressure, PEEP, an increased modulation will occur.

Thus, variations in blood flow will be met in physiological and clinical conditions when mechanical ventilation is applied. These variations jeopardize an accurate measurement of blood flow by means of the thermodilution method.

A theoretical attempt to correct for the influence of flow modulation on the dilution curve was made in 1962 by Gonzales-Fernandez [3] and in 1970 by Bassingthwaight et al. [1]. Gonzalez-Fernandez [3] suggested to use in such circumstances a "flow-averaged" sampling. This means that the contribution of the indicator concentration to the area of the dilution curve would be made proportional to the flow passing the sampling site.

Bassingthwaight et al. suggested to use a catheter tip sensor for blood velocity together with a high dynamic response detector for the indicator to provide the theoretical "flow-average" sampling technique. For that reason they modified the Stewart-Hamilton equation to

$$\dot{Q} = \frac{m_i}{\int_0^{\infty} \frac{v(t) \cdot C(t) dt}{\bar{v}}} \quad (6)$$

where  $\bar{v}$  is mean blood velocity and  $v(t)$  the instantaneous velocity of the blood. The two important conditions to be fulfilled for such a method are a proportional relationship between blood flow and blood velocity, and no phase shift between the signals of velocity and indicator concentration.

## 1.5 Outline of the thesis

In this thesis the errors due to nonstationarity of blood flow on the estimation of mean blood flow by the standard thermodilution technique are studied in artificially ventilated pigs. Also the effects of other errors, such as loss of indicator and poor mixing, will be considered. Three different approaches to improve accuracy of the estimation of mean flow by the thermodilution technique have been studied. The thesis contains the following items.

- In the majority of the experiments a computer controlled ventilator of our own design was used. This ventilator is described in Chapter 2. It allows a variety of breathing maneuvers. Furthermore, the moment of injection of indicator in the ventilatory cycle can be controlled by this ventilator.
- In Chapter 3 the errors due to the straight forward application of the Stewart-Hamilton equation on the estimation of mean blood flow

during nonstationary flow conditions, as during artificial ventilation, have been analyzed for both the right and left side of the heart. A suggestion is made for the most appropriate moments in the ventilatory cycle to estimate mean cardiac output.

- This suggestion was the aim of the study in Chapter 4. The accuracy of the estimation of mean cardiac output by the thermodilution technique was improved by averages of 2-6 estimates spread equally over the ventilatory cycle. Such a procedure appeared far superior to the averaging of random observations.
- In Chapter 5 the thermodilution technique was studied during breath holding procedures. Under these conditions the feasibility of three different mathematical models for description of the dilution curve and for extrapolation of the downslope of the curve was tested. Cardiac output estimates during a prolonged expiratory pause were compared to mean flow.
- In Chapter 6 the modified Stewart Hamilton equation as theoretically presented by Bassingthwaighe et al. (eq. 6) was experimentally tested.
- In Chapter 7 cardiac output estimation by the thermodilution is generally considered. Model simulations were used to test the theoretical basis.

## References

- [1] Bassingthwaighe, J.B., T.J. Knopp, and D.U. Anderson. Flow estimation by indicator dilution. (Bolus injection): Reduction of errors due to time-averaged sampling during unsteady flow. *Circ. Res.* 27: 277-291, 1970.
- [2] Cropp, G.J.A., and A.C. Burton. Theoretical considerations and model experiments on the validity of indicator dilution methods for measurements of variable flow. *Cir. Res.* 18: 26-48, 1966.
- [3] González-Fernández, J.M. Theory of the measurement of the dispersion of indicator in indicator-dilution studies. *Circ. Res.* 10: 409-428, 1962.
- [4] Fegler, G. Measurement of cardiac output in anaesthetized animals by a thermodilution method. *Quart. J. Exptl. Physiol.* 39: 153-164, 1954.

- [5] Hamilton, W.F., J.W. Moore, J.M. Kinsman, and R.G. Spurling. Studies on the circulation. IV. Further analysis of the injection method, and of changes in hemodynamics under physiological and pathological conditions. *Am. J. Physiol.* 99: 534-551, 1932.
- [6] Hamilton, W.F., R.L. Riley, A.M. Attyah, A. Courmand, D.M. Fowell, A. Himmelstein, R.P. Noble, J.W. Remington, D.W. Wheeler, and A.C. Witham. Comparison of Fick and dye injection methods of measuring the cardiac output in man. *Am. J. Physiol.* 153: 309, 1948.
- [7] Hamilton, W.F., and J.W. Remington. Comparison of the time concentration curves in arterial blood of diffusible and nondiffusible substances when injected at a constant rate and when injected instantaneously. *Am. J. Physiol.* 148: 35, 1947.
- [8] Hering, A. Versuche, die Schnelligkeit des Blutlaufs und der Absonderung zu Bestimmen. *Ztschr. Physiol.* 3: 85-126, 1829.
- [9] Hering, A. Über den Einfluß der Athmung auf den Kreislauf. *Sitzungsb. d. k. Akad. d. W. math. naturw.* CI LX Bd II Abth. 1869 (829-855).
- [10] Hoffman, J.I.E., A. Guz, A.A. Charlier, and D.E.L. Wilcken. Stroke volume in conscious dogs: effect of respiration, posture and vascular occlusion. *J. Appl. Physiol.* 20: 865-877, 1965.
- [11] Jarisch, A. Kreislauffragen. *Deut. med. Wschr.*, 54, 1213 1928. In: Prys-Roberts C. The measurement of cardiac output. *Brit. J. Anaesth.* 41: 751, 1969.
- [12] Kinsman, J.M., J.M. Moore, and W.F. Hamilton. Studies on the circulation, I. Injection method: Physical and mathematical considerations. *Am. J. Physiol.* 89: 322, 1922.
- [13] Meier, P., and K.L. Zierler. On the theory of the indicator-dilution method for measurement of blood flow and volume. *J. Appl. Physiol.* 6: 731-744, 1954.
- [14] Moore, J.W., J.M. Kinsman, W.F. Hamilton, and R.G. Spurling. Studies on the circulation, II. Cardiac output determinations: Comparison of the injection method with the direct Fick procedure. *Am. J. Physiol.* 89: 331-339, 1929.
- [15] Morgan, B.C., W.E. Martin, T.F. Hornbein, E.W. Crawford, and W.G. Guntheroth. Hemodynamic effects of intermittent positive pressure ventilation with and without an end-expiratory pause. *Anesthesiology* 27: 584-590, 1966.
- [16] Newman, E.V., M. Merrell, A. Genecin, C. Monge, W.R. Milnor, and W.P. McKeever. The dye dilution method for describing the central circulation: An analysis of factors shaping the time-concentration curves. *Circulation* 4: 735-746, 1951.
- [17] Scheuer-Leeser, M., A. Morquet, H. Reul, and W. Inrich. Some aspects to the pulsation error in blood-flow calculations by indicator dilution technique. *Med. Biol. Eng. Comput.* 15: 118-123, 1977.

- [18] Sherman, H. On the theory of indicator-dilution methods under varying blood flow conditions. *Bull. Math. Biophys.* 22: 417-424, 1960
- [19] Sheppard, C.W. Mathematical considerations of indicator dilution techniques. *Minn. Med.* 37: 93, 1954.
- [20] Stephenson, J.L. Theory of the measurement of blood flow by the dilution of an indicator. *Bull. Math. Biophys.* 10: 117-121, 1948
- [21] Stewart, G.N. Research on the circulation time and on influences which affect it. IV. The output of the heart. *J. Physiol.* 22: 159 1897.
- [22] Stewart, G.N. The output of the heart in dogs. *Am. J. Physiol.* 57: 27-50, 1921.
- [23] Stewart, G.N. The pulmonary circulation time, the quantity of blood in the lungs and the output of the heart. *Am. J. Physiol.* 58: 20-44, 1921.
- [24] Stow, R.W., and P.S. Hetzel. An empirical formula for indicator-dilution curves as obtained in human beings. *J. Appl. Physiol.* 7: 161-167, 1954.
- [25] Swan, H.J.C., W. Ganz, J. Forrester, H. Marcus, G. Diamond, and D. Chonette. Catheterization of the heart with use of a flow-directed balloon-tipped catheter. *New. Eng. J. Med.* 283: 447-451, 1970.
- [26] Vermeire, P., and J. Butler. Effect of respiration on pulmonary capillary blood flow in man. *Circ. Res.* 22: 299, 1968.
- [27] Versprille, A., J.R.C. Jansen, and J.J. Schreuder. Dynamic aspects of the interactions between airway pressure and circulation. In: Prakash, O. (ed.) *Applied physiology in clinical respiratory care*. Martinus Nijhoff, The Hague, p. 447, 1982.
- [28] Reth, E.A. von, J.C.J. Aerts, A.A. van Steenhoven, and A. Versprille. Model studies on the influence of nonstationary flow on the mean flow estimate with the indicator-dilution technique. *J. Biomech.* 16: 625-633, 1983.
- [29] Zierler, K. L. Circulation times and the theory of indicator-dilution methods for determining blood flow and volume. In: *Handbook of Physiology. Circulation*. Washington, DC: Am. Physiol. Soc., sect. 1, vol I, chap. 18, p. 585-615, 1962.





## CHAPTER 2

# A COMPUTERIZED RESPIRATORY SYSTEM FOR VENTILATION, LUNG FUNCTION AND CIRCULATION TESTING

JOS R.C. JANSEN, ED HOORN, JEROEN VAN GOUDOEVER,  
AND ADRIAN VERSPRILLE

Department of Pulmonary Diseases, Pathophysiological Laboratory,  
Erasmus University, 3000 DR Rotterdam, The Netherlands  
Submitted for publication

### 2.1 Introduction

Mechanical ventilation sustains an important vital function in patients during anesthesia and intensive care. A large number of ventilators is commercially available. They range from simple devices with restricted possibilities to complicated systems with an array of facilities [7]. Most of these ventilators are primarily designed for conventional mechanical ventilation. In many cases they are unsuitable for procedures of lung function and circulation tests which require special patterns of breathing.

In this paper we describe the development of a ventilator which combines most of the facilities of conventional ventilators with the possibility to perform series of different special breathing maneuvers. The ventilator was made for animal studies, but contains the potentials for clinical use. The ventilator was designed with the following features:

1. volume controlled ventilation;
2. the applicability of a wide range of single and multiple ventilatory patterns, changing from one breath to the next;
3. the possibility to change from one gas concentration to another between two successive breaths;
4. facilities for communication with a remote computer system.

The ventilator was composed with the use of a commercial microcomputer system, an electrical-mechanical servo system, a valve assembly and a

pair of concertina bellows. Since the microcomputer guarantees great flexibility in function control, the valve and servo system could be designed relatively simple.

## 2.2 System description

### 2.2.1 Pump and valve assembly

A scheme of the mechanical part of the ventilator is given in Fig. 1. The two concertina bellows (A1 and A2) work in parallel. The effective diameter of a bellows is 120 mm with a length of 55 mm at full extension. During the insufflation the solenoid valves E1 and E2 open. The expiratory valves D1 and D2 and the inlet valves F1 and F2 remain closed. The motor M turns the ball screw K and drives the moving plate. The gas mixture is forced from the bellows via the tubes I1 and I2 into the lungs of the animal. At the end of the insufflation the plate is in the ultimate forward position, almost against the 'soft filling elements' mounted on the fixed front plate. The concertina bellows are folded around these soft elements, which minimizes dead space.

During an end-inspiratory pause all valves are closed. The inspiratory valves E1 and E2 close when the expiratory phase starts and either the expiratory valve D1 or D2 is opened. This juncture the expiratory gas flows passively through either the valve P1 or P2 to atmosphere. With these valves a positive end expiratory pressure can be applied. Expiration can be changed from P<sub>1</sub> to P<sub>2</sub> within one ventilatory cycle. During expiration the valves F1 and F2 are open and the motor expands the bellows, which results in an inflow of fresh gas into the bellows. When the bellows have expanded again to the tidal volume for the next insufflation the next cycle starts. The animal and concertina bellows are protected against over-pressure by the safety valves C1 and C2 and against under-pressure by the valves B1 and B2. Valves D,E,F and the motor are controlled by the computer.

### 2.2.2 The motor servo system

The volume controlled ventilator is based on a motor servo system. A power amplifier drives the low inertia DC motor M, which turns the ball screw K and drives the moving plate forward and backward. The moving plate is connected to a potentiometer for indication of its position (Fig. 2), which is read in by the computer via an analog to digital converter. Based on the difference between commanded position and actual position the micro-

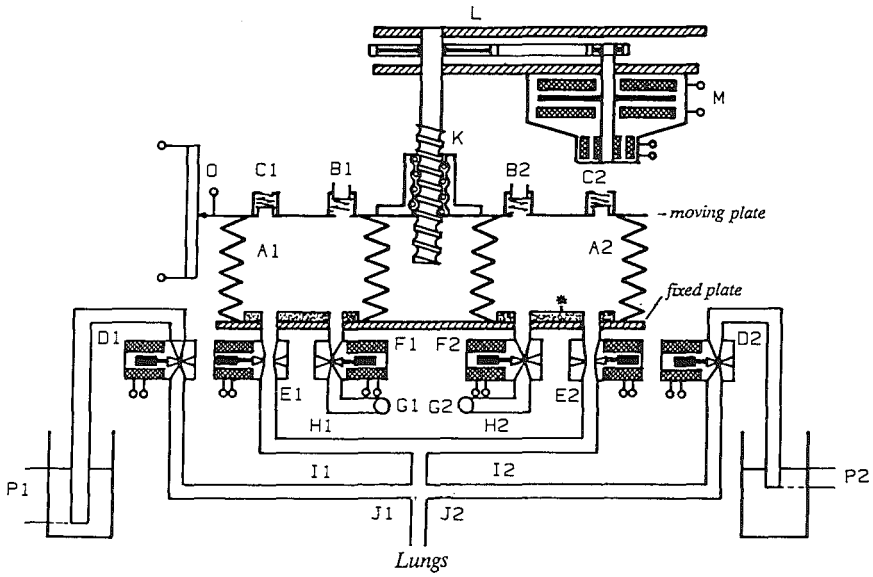


Fig. 1. Diagram of the pump assembly. A1,A2 teflon concertina bellows; B1,B2 safety valves for under pressure; C1,C2 safety valves for over pressure; D1—F2 solenoid valves; G1—J2 tubes; K lead screw; L transmission; M low inertia motor; O potentiometer for piston position; P1,P2 positive end expiratory pressure valves; \* soft filling element.

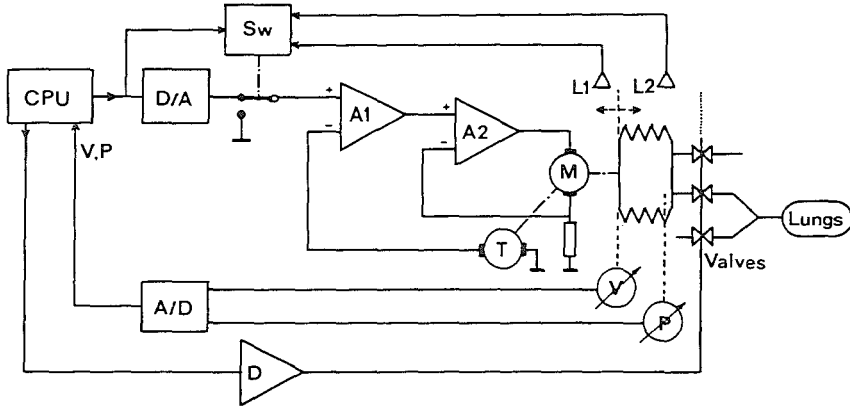


Fig. 2. Schematic diagram of the respiratory servo system. CPU, microcomputer; D/A, digital to analog converter; A/D, analog to digital converter; A1, pre-amplifier; A2, power amplifier; M, motor; T, tachometer; V, position potentiometer; P, pressure signal; Valves, solenoid valves; D, drivers for the valves; L1, L2, optical end limits; Sw, electronic switch. For explanation, see text.

computer calculates the desired speed value for the servo amplifier. This information of speed is updated 100 times per second. The calculated speed signal is corrected by the actual speed, measured by the tachometer, before it is led to the power-amplifier and motor. By this servo principle the moving plate follows the time changing commanded position given by the computer. A measurement of the volume delivered to the lungs by this ventilator is not necessary because the servo system is highly accurate, and the bellows have hardly any dead space at the end of insufflation. So, the compliance based on compression of air is almost zero. Calibration procedures showed that the ventilator will deliver what will be ordered by the operator.

The motor, the ball screw and the bellows are protected against software and hardware failure by two optical end position sensors. When the ultimate forward position is reached the forward command is switched off. Then, the motor could only be started again for the backward movement of the moving plate. The opposite reasoning is valid for the end position of maximal backward movement.

The power unit (320 W), formed by a linear four quadrants transistor amplifier, is designed to work in combination with the low inertia DC motor (Mavilor 80).

### 2.2.3 Computer system

To control the servo ventilator a general personal computer (PC) with MS-DOS is used (Olivetti M24). This computer system is equipped with a co-processor (Intel 8087), 640 K memory, a serial interface, a dual floppy disk drive and a noncommercial pump-interface module. This module contains a 16 bit digital input and output port, four analog inputs and two analog outputs, and a programmable clock. The analog output is used to drive the servo system. The analog inputs are used to sense the position of the bellows, to measure the pressure in the bellows of the ventilator, and to provide a hardware protection for failure in the pump-servo system and the computer program. The digital output controls the solenoid valves and additional external devices and is also used to trigger external processes, as data collection by another computer and the injection of cold fluid for thermodilution cardiac output measurements.

### 2.2.4 Communication

The ventilatory settings are given by either an operator via a keyboard or a remote computer system via the serial interface. The ventilatory input and derived data, the mode of operation and the command signal for the servo system are displayed on the videoscreen of the PC. On request, instructions for a change-over to a different mode, i.e. special ventilation maneuvers for lung function testing or circulatory testing, is displayed. From the input data the command signal of the servo system and the position of the valves are calculated and stored in output buffers.

### 2.2.5 Ventilatory settings

An example of a command signal, which controls the servo system, is given in Fig. 3. The ventilatory cycle in the software starts with a move in the backward direction of the moving plate in order to expand to the volume setting of the next insufflation. The settings for a ventilatory cycle are:

$V_T$ , insufflation volume in ml;

$T_c$ , ventilatory cycle time in seconds;

$X_e$ , expiration time in % of  $T_c$ ;

$X_a$ , duration of the backward movement in % of  $X_e$ ;

$A$ , the pattern of the backward movement, which becomes an effective

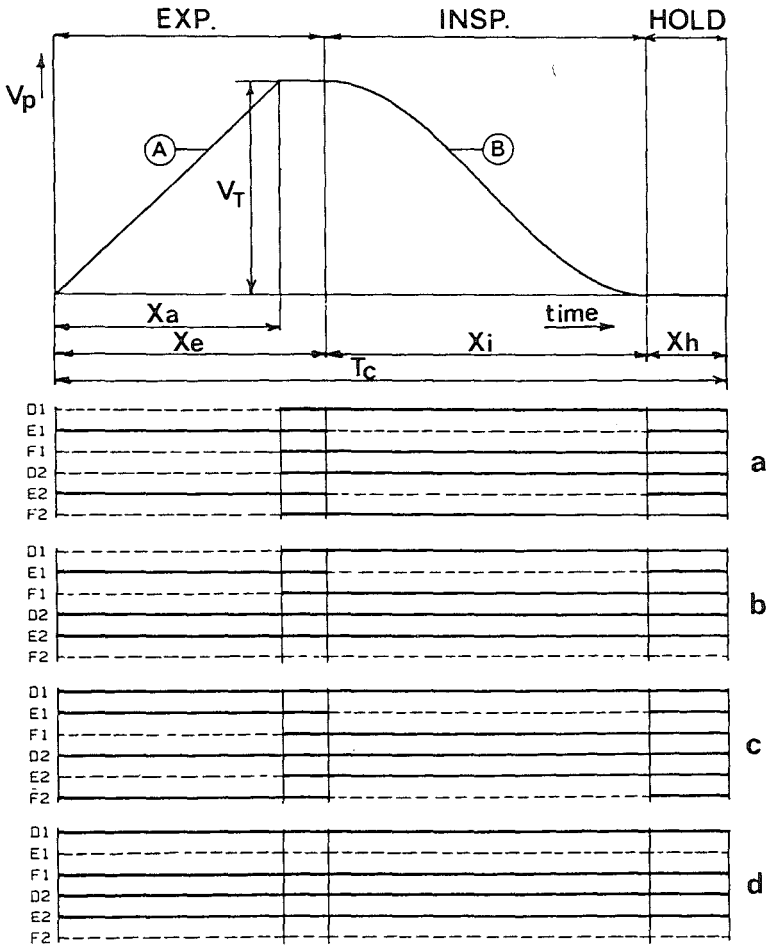


Fig. 3. Command signals for the respiratory servo system.  $V_T$ : tidal volume;  $T_c$ : cycle time; A: pattern of backward movement; B: half sinusoidal pattern of inflation;  $D_1$ - $E_1$ - $F_1$ : valve positions bellows A1;  $D_2$ - $E_2$ - $F_2$ : valve positions bellows A2 (see Fig. 1). Thick lines give closed valve settings and dotted lines open valve settings: a, parallel operation of the bellows; b, normal operation for bellows A1 and flush for bellows A2; c, controlled expiratory flow; d, closed system ventilation. For further symbols and description, see subsection ventilatory settings.

expiratory pattern in case of a controlled expiration, see applications;  
Xi, insufflation time in % of  $T_c$ ;  
Xh, inspiratory hold  $Xh=100 - (X_e + X_i)$ . This is a derived setting  
automatically calculated from the other settings;  
B, the inspiratory flow pattern;  
M, mode of ventilation.

The mode of ventilation determines the control of the valves. The solenoid valves are controlled via the digital output port of the computer.

There are four modes of operation, which can be changed from breath to breath.

- Normal ventilation is performed with bellows A1, whereas bellows A2 can be used in flush mode. The flush mode is used to equilibrate the gas content of bellows A2 with any gas mixture. It allows wash-in and wash-out experiments by changing the operation of bellows A2 and A1 between two successive breaths.
- Both bellows are working in parallel to increase the maximal applied insufflation volume twice for special procedures.
- Bellows A1 is used for insufflation and bellows A2 is used for expiration to control the expiratory flow by the backward movement of the moving plate.
- The expiratory gas is rebreathed with bellows A1, bellows A2 is in the flush mode.

#### 2.2.6 Software

The computer software is written in FORTRAN and in assembly language. The assembly part is used for the interrupt service routines, and Fortran is used for keyboard input, screen output and pattern calculations. The two parts are communicating with each other via a common memory block to improve execution speed. From the input parameters the output signals are calculated and put in an output buffer. This buffer contains the data of the command signal for the servo system, the data for the valve positions and a word for the programmable interrupt timer. The interrupt timer gives the time interval between the data words. Upon a request of the programmable clock the interrupt routine subtracts the actual position from the commanded position, calculates the speed and sets the analog output

accordingly. At the same time also the settings for the valves are updated. For normal ventilation the software pointer of the buffer is reentered at its first position after the last position has been passed at the end of a ventilatory cycle, see Fig. 4. In the ventilator program four output buffers are defined: two (A and B) for normal continuous ventilation to change from one pattern to another and two (C and D) for special ventilations. In contrast to the buffers for normal ventilation a buffer for special ventilation is only passed through once to insert a single breath maneuver during normal ventilation. When the special ventilation has been completed normal continuous ventilation is automatically resumed. A very simple example of such a special maneuver is a sigh, i.e. a ventilation with a large volume in between the normal ventilations. The interrupt structure of the program allows multitasking. Thus, while the interrupt subroutine of buffer A controls the ventilator, the operator has the possibility to change the settings in one of the other buffers. The computer (FORTRAN part) then calculates the content for that other buffer and places this in a common memory block. The interrupt routine is flagged that a new buffer has been filled. A change of ventilatory pattern or a special maneuver follows, when the operator commands so via the keyboard and the pointer has reached the end position in buffer A.

## 2.3 Applications

### 2.3.1 *Automatic operations*

**Closed-loop ventilation.** A closed-loop ventilation [6] can be achieved with use of an additional remote computer system for data collection and analyses (Fig. 5). Based on the analyses of the data collected from an animal the remote computer calculates a set of respiratory parameters. This set is transmitted to the servo ventilator, and a new ventilation pattern starts running. After a prescribed number of ventilation cycles (enclosed in the transmitted parameter set) the ventilator signals the remote computer to start data collection. The remote computer collects the data from the animal and a new set of respiration parameters is calculated. This process can be repeated as often as required.

**Control of experimental observations.** The interconnection between the ventilator and the additional computer, as is described for the closed-loop system, can also be used for the control of a measurement sequence. The protocol of a complete series of observations can be pre-



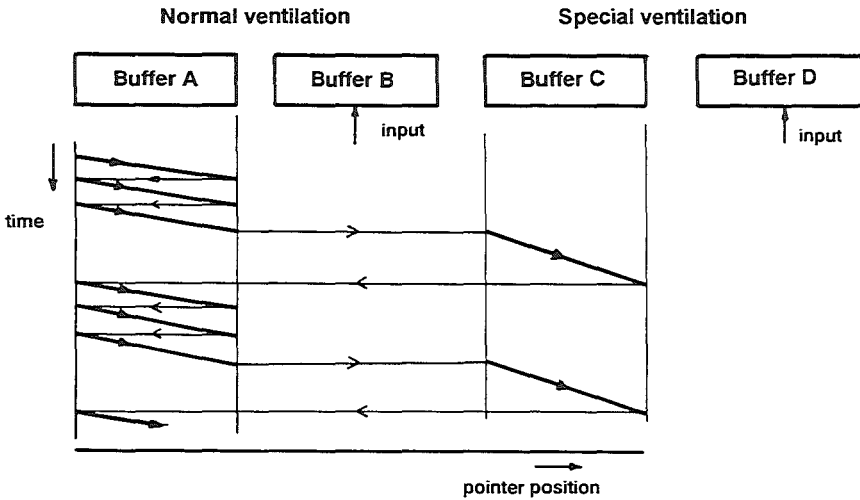


Fig. 4. Buffers for the interrupt routine. The normal ventilation in A is interrupted after a commanded number of cycles by one cycle of the special ventilation buffer C. The buffers B and D are open for input by the operator.

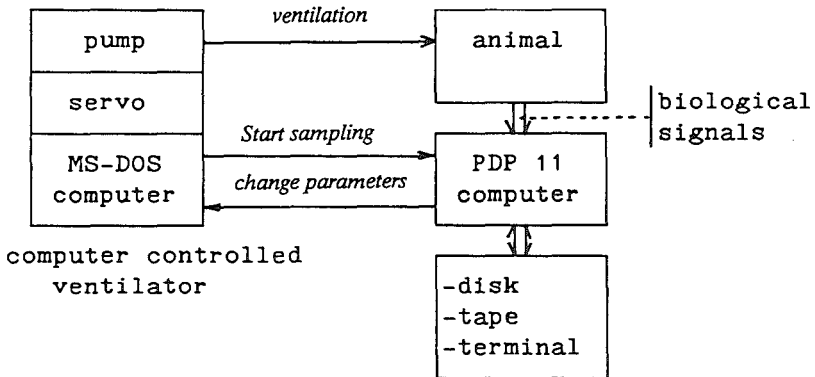


Fig. 5. Closed loop ventilation system. For explanation, see text.

programmed on a remote computer by giving a list of ventilation settings for normal and special ventilations and to set the data collection and parameters for calculations of derived variables. The protocol can be tested on a dummy. After a start command of the remote computer the protocol is carried out automatically. So, the operator needs less attention for the protocol and has more time to observe all experimental conditions. We obtained good results from automatic operations of series of observations during experiments in five different research protocols [2, 3, 3a, 8, 9].

### 2.3.2 Lung function testing

**Multiple-breath test.** For the determination of the end expiratory lung volume with the helium (He) dilution technique, either a closed system (i.e. rebreathing) or an open system (i.e. washin-washout) has been used [4, 5]. An example of the two helium dilution procedures is shown in Fig. 6. Tidal volume, ventilatory rate and pattern and the number of breaths involved in the test were set by the operator. Normal ventilation was performed with one bellows (e.g. A1 Fig. 1), while the other (A2) was flushed through valve F2 (Fig.1) with gas from a Douglas bag containing helium. To start a wash-in procedure the ventilator signalled the remote computer to start data collection one breath before switching ventilation from bellows A1 to bellows A2. During an open washin procedure (Fig. 6a) ventilation continued in a "normal" mode with bellows A2, which was filled each time from the Douglas bag. When a washin procedure was done in a closed system ventilation (Fig. 6b) for the first ventilation the bellows was filled with air from the Douglas bag and all subsequent following ventilations were rebreathing ventilations. Valve settings for this mode are given by Fig. 3d.

After a pre-setted number of breaths, bellows A1 took over again ventilation, conventional ventilation was automatically resumed and a washout was started.

**Controlled expiration.** To study intrapulmonary gas mixing by convection and diffusion or the effects of breathing patterns on the clearance of CO<sub>2</sub>, it will be more useful to plot the gas concentration in the expired air against expired volume than against time. For this study single-breath procedures with controlled expiration were programmed in between normal ventilation [5, 8]. Figure 7 shows a single-breath procedure for CO<sub>2</sub>. By the choice of a linear displacement of the moving plate (i.e. a constant expiratory flow) the shape of CO<sub>2</sub> versus time was equal to the CO<sub>2</sub> curve versus expired volume. One bellows was used for inflation and the other was used

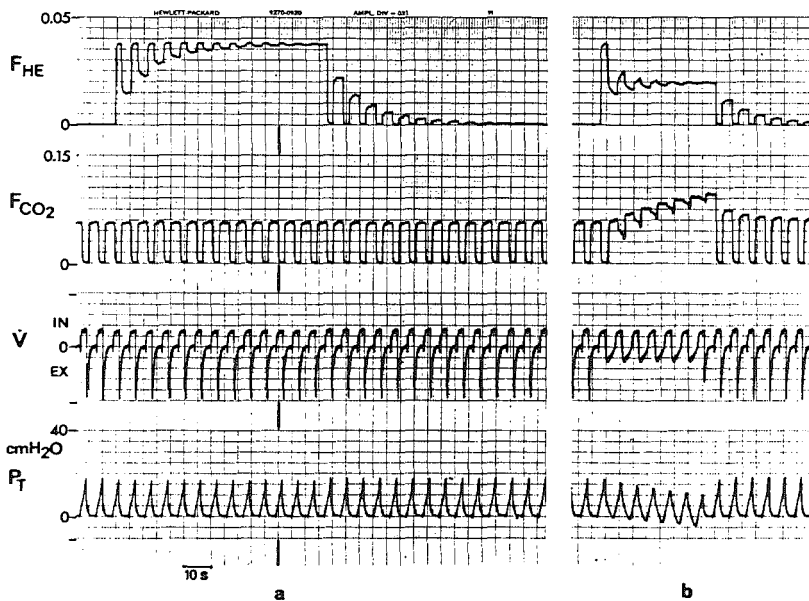


Fig. 6. Functional Residual Capacity (FRC) estimation by a washin and washout technique (a) and a closed rebreathing technique (b) for helium concentrations ( $F_{HE}$ ). The  $F_{HE}$  and  $CO_2$  concentration ( $F_{CO_2}$ ) were simultaneously measured by mass spectrometry.  $\dot{V}$ , air flow measured with a Fleisch pneumotachometer;  $P_T$ , tracheal pressure; s, time in seconds.

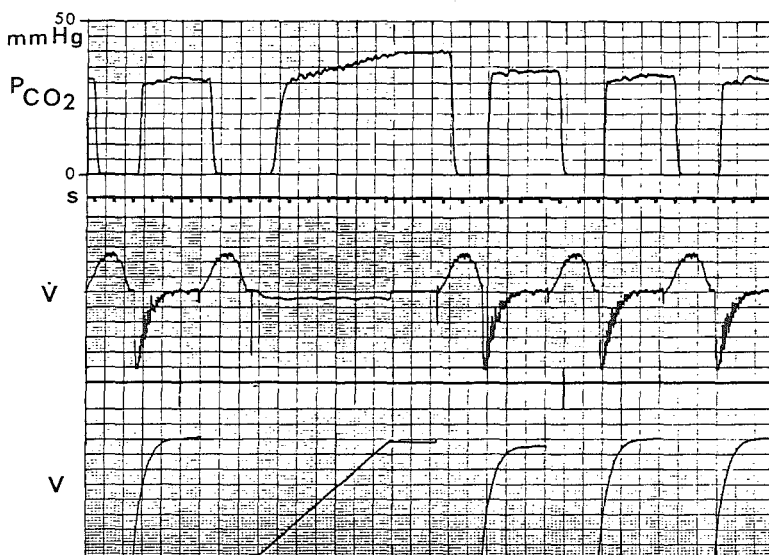


Fig. 7. A recording of a single-breath procedure with controlled expiration.  $\dot{V}$ , air flow measured with a Fleisch pneumotachmeter;  $V$  ventilation volume;  $P_{CO_2}$  partial pressure of carbon dioxide in ventilated air measured with a capnometer (HP-47210A) with a sample chamber in the airway adapter; s, time in seconds.

for the controlled expiration. Controlled expiration, breath to breath is also possible with this two bellows principle. Then, the expiratory valve must be opened to atmosphere before the end of each expiration to compensate for the difference in inspiratory and expiratory volume due to the larger oxygen uptake than the carbon dioxide output of the lung.

**Static compliance.** Three ventilatory procedures for the estimation of total compliance of the lungs and thorax have been tested in an animal study [3a]. Two types of compliance estimates have been derived from special ventilatory maneuvers characterized by an inflation with a constant flow rate followed by an end-inspiratory hold of 9 s. A third type of compliance estimation was derived from a slow inflation-deflation procedure to obtain the quasi static pressure and volume curves over a large range of volume. In this latter procedure the moving plate moved very slowly (33.5 s.) to its front position i.e. inflation, after a short pause followed by a controlled expiration, i.e. deflation, in the same time. Volume could be inflated stepwise (Fig. 8)

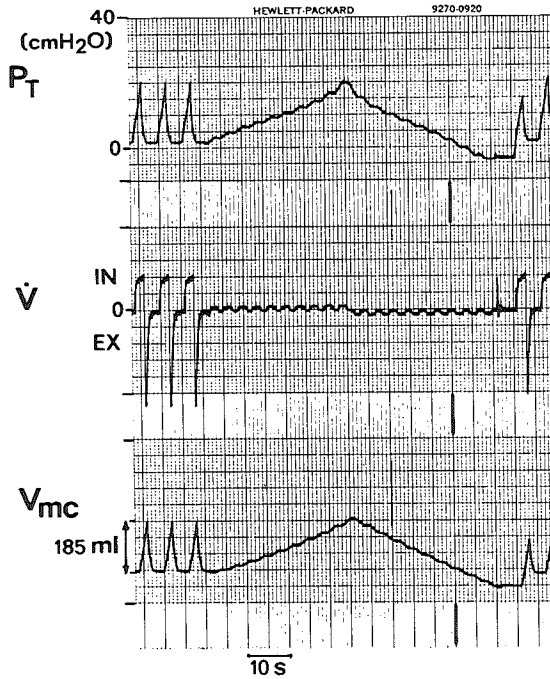


Fig. 8. Slow inflation- deflation procedure.  $P_T$ , tracheal pressure;  $\dot{V}$ , air flow measured with a Fleisch pneumotachometer;  $V_{mc}$ , change in thoracic volume measured with a mercury cord around the thorax at the level of the sternum.

as well as at a constant rate.

### 2.3.3 Circulation testing

**Mean systemic filling pressure.** Guyton's theory on venous return, claiming a linear relationship between blood flow ( $\dot{Q}_{pa}$ ) and central venous pressure ( $P_{cv}$ ), was tested in experiments with closed chest animals [9], i.e. normal circulatory conditions. Single breath procedures with an inspiratory hold of 7.2 seconds were used to change central venous pressure (Fig. 9). The relationship between blood flow and central venous pressure was studied by application of different lung volumes during a series of such single breath



Fig. 9. Inspiratory hold maneuver.  $\dot{Q}_{pa}$ , flow in the common pulmonary artery in arbitrary units;  $P_{cv}$ , averaged central venous pressure;  $P_T$ , airway pressure;  $s$ , time in seconds.

procedures. The settings for these procedures were received from a remote computer which controlled the protocol of the experiment. It also sampled the hemodynamic variables during the special maneuvers. After each single breath procedure the ventilator automatically resumed normal conventional ventilation for 5 minutes before the next procedure was applied.

**Estimation of mean cardiac output.** Cardiac output estimates by thermodilution during mechanical ventilation revealed a cyclic modulation related to the phase of ventilation [2, 3]. The average of estimates equally spread over the ventilatory cycle leads to a much better estimation of mean cardiac output than the average of a similar number of measurements randomly performed [3]. The moment of injection has been controlled by programming a "special" ventilation with the same parameters as the normal ventilation. At the prescribed moment the ventilator commanded the injector and cardiac output computer to start processing.

In an other study [2], thermodilution estimates of cardiac output have been done during prolonged expiratory pauses, where cardiac output was constant.

## 2.4 Comments

The computerized ventilator has shown to fulfill the demands as stated in the introduction. With this ventilator conventional ventilation is possible with a wide range of ventilatory settings. The flexibility of the ventilator allows to generate respiratory maneuvers for lung function and circulation tests. By our knowledge a ventilator as described is not yet commercially available. Only Meyer and Slama [4] have described a respiratory servo system that has several features in common with ours. They used a hydraulically powered one cylinder piston assembly. Their system needs a reservoir of oil and a pump that supplies a pressure of 50 bar. This makes it voluminous and noisy. We have chosen for an electro-mechanical servo system, because it can be kept relatively small and makes hardly any noise. Furthermore, we have made the microcomputer as a part of the servo loop to obtain a digital servo system. A distinct advantage of such a digital servo system above an analog servo system is its larger versatility. The program which controls the servo system can be modified to a large scale of experimental conditions without any modification of the hardware. Such adaptation is done by changes in gain, integration and differentiation time constants, and nonlinear input-output relations. The few applications presented illustrate the potentials of the ventilator. Another application could be the usage of the ventilator to generate respiratory data of flow and gas concentrations for function control of analysis systems as described by Boutellier et al. [1]. The ventilator described has been used in animal research for approximately 6 years now and it appeared to be a very reliable system for long term experiments. Although the ventilator is primarily designed for application in animal studies, it has its merits also for the design of a ventilator for patient care.

Acknowledgements. The authors are indebted to A. Drop, and W.v. Alphen, R. Niesing of the Central Research Workshop of the Erasmus University for their participation.

## References

- [1] Boutellier, U., U. Gomez, and G. Mäder. A piston pump for respiration simulation. *J. Appl. Physiol.* 50: 663-664, 1981.
- [2] Jansen, J.R.C., J.M. Bogaard, and A. Versprille. Extrapolation of thermodilution

- curves obtained during a pause in artificial ventilation. *J. Appl. Physiol.* 63, 1551-1557, 1987
- [3] Jansen, J.R.C. and A. Versprille. Improvement of cardiac output estimation by the thermodilution method during mechanical ventilation. *Int. Care Med.* 12: 71-79, 1986.
- [3a] Goudoever van, J., J.R.C. Jansen, J.M. Bogaard, and A. Versprille *Appl. Physiol.* Submitted for publication.
- [4] Meyer, M. and H. Slama. A versatile hydraulically operated respiratory servo system for ventilation and lung function testing. *J. Appl. Physiol.* 55: 1023-1030, 1983.
- [5] Meyer, M., C. Hook, and H. Rieke. Gas mixing in dog lungs studied by single breath washout of He and SF<sub>6</sub>. *J. Appl. Physiol.* 55: 1795-1802, 1983.
- [6] Mitamura, Y., T. Mikami, H. Sugawara, and C. Yoshimoto. An optimally controlled respirator. *IEEE Trans. Biomed. Eng.* 18: 330-338, 1971.
- [7] Muskin, W.W., L. Rendell-Baker, P. Thompson, and W.W. Mapleson. *Automatic Ventilation of the Lungs* (3rd. ed.) Oxford, UK: Blackwell, 1980.
- [8] Rooyen, W. van, A. Versprille. Beneficial effects of expiratory flow retardation during mechanical ventilation. In: *Update in intensive care and emergency medicine.* Vincent J.L. (ed), Springer-Verlag, Berlin Heidelberg, p. 234-239, 1987.
- [9] Versprille, A., and J.R.C. Jansen. Mean systemic filling pressure as a characteristic pressure for venous return. *Pflügers Arch.* 405: 226-233, 1985.



## CHAPTER 3

# THERMODILUTION TECHNIQUE FOR MEASUREMENT OF CARDIAC OUTPUT DURING ARTIFICIAL VENTILATION

JOS R.C. JANSEN, JAN J. SCHREUDER, JAN M. BOGAARD,  
WILLEM VAN ROOYEN, AND ADRIAN VERSPRILLE  
(with the technical assistance of A. Drop)

Department of Pulmonary Diseases, Pathophysiological laboratory,  
Erasmus University, 3000 DR Rotterdam, The Netherlands.  
Published in *J. Appl. Physiol.* 51: 584-591, 1981.

### 3.1 Introduction

Continuous or frequent monitoring of hemodynamic and respiratory variables during artificial ventilation is important for optimal management of critically ill patients as well as for physiological studies. One of the main variables, cardiac output, can be measured by the thermodilution technique introduced by Fegler [3]. The feasibility of this method has been demonstrated in animals [5, 8, 18, 21] and humans [1, 4, 12]. The method is easy to perform and can be repeated almost without limitations at very short time intervals. However, a few important requirements must be fulfilled: complete mixing [15], no loss of indicator [6, 20, 22] and constant blood flow during the period of measurement [2, 17].

During artificial ventilation, i.e., intermittent and continuous positive-pressure breathing (IPPV and CPPV), a significant modulation of cardiac output, i.e. stroke volume, occurs with each respiratory cycle [10, 11]. Except for our preliminary report [7] we are not aware of any investigation concerning the influence of this fluctuation on the estimate of mean cardiac output with the thermodilution technique.

The purpose of the present study was to estimate the error in the cardiac output measured by thermodilution in anesthetized closed-chest pigs during different phases of the respiratory cycle so as to determine the most appropriate moment of injection. Additionally, the effect of mean cardiac output on the errors were studied by changing the end-expiratory pressure. It is known that positive end-expiratory pressure (PEEP) decreases cardiac

output [10] but increases its modulation [7]. This study was carried out on both sides of the heart. The output of the left side of the heart was measured in order to avoid the influence of nonindicator blood temperature changes during each respiratory cycle [22] and to minimize the errors due to loss of indicator under circumstances of low cardiac output levels [21, 22].

Since routine measurements of cardiac output using thermodilution techniques in clinical medicine are performed by administering the injectate in the right atrium and detecting the thermal changes in the pulmonary artery, we have also included comparable measurements in the present study.

## 3.2 Methods

### 3.2.1 Surgical procedure

Yorkshire pigs (5-7 wk old, weighing 7-11 kg) were anesthetized with pentobarbital sodium (30 mg.kg<sup>-1</sup> ip). The body temperature was maintained at about 38°C by placing the animals on a thermocontrolled operating table. After tracheostomy all pigs were connected to a Fleisch pneumotachograph head (type 0, Godart) and were allowed to breath spontaneously. Two catheters were inserted into the right common carotid artery: a double-walled injection catheter was placed 2.5-3 cm beyond the aortic valves into the left ventricle; the tip of the other, with a thermistor, was positioned in the aortic arch near the origin of the brachiocephalic artery. The length of the intracorporeal part of the injection catheter was 12-15 cm. A four-lumen catheter was inserted via the right internal jugular vein into the superior vena cava to the level of the right atrium. One lumen was used for measuring central venous pressure, and the others were used for infusions. In animals where the output of the right heart was measured, a double-walled injection catheter and a Swan-Ganz 5F catheter with thermistor were placed via the right external jugular vein into the right atrium and the pulmonary artery, respectively. After the experiments the position of each catheter was confirmed at autopsy.

Anesthesia was maintained by a continuous infusion of pentobarbital (7.5 mg.kg<sup>-1</sup>.h<sup>-1</sup> iv). After completion of surgical procedures the animals were paralyzed with *d*-tubocurarine hydrochloride (0.1 mg.kg<sup>-1</sup> loading dose), administered over a period of 3 min, followed by a continuous infusion of 0.2 mg.kg<sup>-1</sup>.h<sup>-1</sup> to avoid spontaneous breathing during the experimental procedures. The animals were ventilated with room air with a constant-volume Starling ventilator (Braun-Melsingen) at a rate of 10 cycles/min. Inflation lasted 44% of the ventilatory cycle and was followed by a spontaneous expi-

ration against a water seal from 0 up to 15 cmH<sub>2</sub>O. The ventilation volume was adjusted to maintain arterial carbon dioxide tension ( $P_{CO_2}$ ) between 38 and 44 Torr. When the arterial  $P_{CO_2}$  was stabilized between these values the tidal volume was not changed further.

### 3.2.2 Measurements

*Fick method.* When blood pressures, heart rate, end-tidal and arterial  $P_{CO_2}$ , and peak tracheal pressure were stable, cardiac output ( $CO_{Fick}$ ) was measured by the direct Fick method for oxygen [19]. Arterial and mixed venous blood and expiratory air from a gas mixing box were sampled over a period of 3 min. The respiratory gases were measured with a mass spectrometer (Perkin-Elmer MGA 1100). The oxygen uptake ( $\dot{V}O_2$ , ml.s<sup>-1</sup> STPD) was corrected for the differences between inspired and expired volumes by assuming no volume change of nitrogen [14]. The oxygen content of mixed venous blood from the pulmonary artery and that of the arterial blood from the aorta was calculated from the directly measured oxygen saturated and hemoglobin (Hb) values (Radiometer OSM 2) and from the physically dissolved oxygen as determined by the  $P_{O_2}$  values. Acid-base values were measured with an automatic analyzer (Radiometer ABL 1). A value of 1.39 ml O<sub>2</sub> STPD.Hb<sup>-1</sup> was used as the oxygen binding capacity (International Committee for Standardization in Haematology, 1965).

*Thermodilution method.* The thermodilution measurements of cardiac output ( $CO_{TH}$ ) were performed by an automatically controlled injection of 0.5 ml saline (0.9%) at room temperature (Fig. 1). Volume reproducibility was checked. The pneumatic cylinder was driven by compressed air, and injection was initiated by an electric signal from the control unit. After each measurement the injector was automatically refilled.

The moment of injection depended on two preset factors: 1) the moment within the ventilatory cycle and 2) a certain number of ventilations between two injections (in our experiments this number was 5). The moment of injection within the ventilatory cycle was derived from two discs on the axis of the Starling ventilator, one with 100 holes and the other with 1 hole. The disc with 1 hole was used to reset the counter at the start of the inspiration. The disc with 100 holes divided a ventilatory cycle in percentages. The control unit controlled the moment of the injection and signaled the computer to start the integration of the temperature-time curve derived from the temperature bridge. The thermistor had the following characteristics: diameter 0.5 mm, resistance at 37°C 5,000 Ω. It was mounted at the tip of a polyethy-

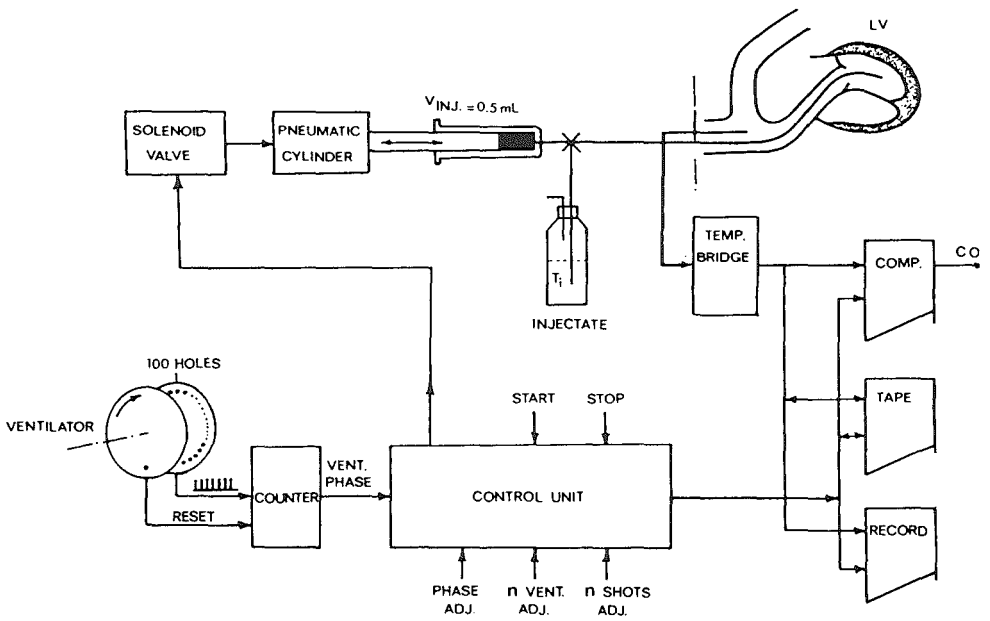


Fig. 1. Schematic diagram of thermodilution technique as applied on left side of heart. LV, left ventricle;  $V_{inj}$ , syringe giving an injection volume of 0.5 ml; Comp, digital computer PDP 11/3; Tape, Ampex FR 1300 A tape recorder; Record, Hewlett-Packard 7758 A recorder.

lene catheter (1.14 mm ID, 1.57 mm OD) and had a 90% thermal response time of approximately 0.2 s. The voltage across the thermistor was kept low to avoid influences due to changes in the velocity of blood. When the bridge was balanced at blood temperature, the voltage-temperature characteristic of the bridge gave a satisfactory linearity within the range of measurements (37-39°C) [4, 9, 13].

### 3.2.3 Data acquisition and analysis

Electrocardiogram (ECG), aortic, pulmonary arterial, and central venous pressures, ventilatory pressure and flow, and thermodilution signals were simultaneously recorded on a Hewlett-Packard 7758 A chart recorder and an Ampex FR 1300 A tape recorder and analyzed on-line with a digital computer PDP 11/03. The sample frequency was 200 Hz for the ECG and blood pressures and 50 Hz for the thermodilution curve, ventilatory pressure, and airflow.

Cardiac output (CO) by thermodilution was calculated according to

$$CO = \frac{Q_i}{\rho_b S_b \int_{t_1}^{t_2} [T_b(t) - T_{b1}] dt - A}$$

where

$$Q_i = \rho_i S_i V_i (T_{b1} - T_i) - C_k l (T_{bi} - T_i)$$

$$A = (T_{b2} - T_{b1})(t_2 - t_1)/2$$

$$T_{b1} = \int_{t_1}^{t_1 + \Delta t} T_b(t) dt / \Delta t$$

and

$$T_{b2} = \int_{t_2}^{t_2 + \Delta t} T_b(t) dt / \Delta t$$

A is the area under the temperature-time curve due to leakage of heat from the injection catheter (see dashed area in Fig. 5);  $Q_i$  is the effective amount of indicator, *cal*;  $V_i$  is the injectate volume, *ml*;  $T_i$  is the temperature of injectate, °C;  $T_b$  is the temperature of blood at the detection site, °C;  $S_i$  and  $S_b$  are specific heat of injectate (0.997) and blood (0.870), respectively, *cal.g<sup>-1</sup>.°C*;  $\rho_i$  and  $\rho_b$  are specific gravity of injectate (1.005) and blood (1.045), respectively, *g.ml<sup>-1</sup>*;  $C_k$  is the caloric value of injection catheter

plus remaining injectate,  $cal.m^{-1}.^{\circ}C^{-1}$ ;  $l$  is the length of the intracorporeal part of the injection catheter  $m$ ;  $t_1 - t_2$  is the integration interval, 9s; and  $\Delta t$  is the heart interval.

$T_b$  and  $T_i$  were determined immediately before and after each series of measurements.  $T_b - T_i$  is the difference between the blood temperature measured with the thermistor and the temperature of the injectate measured with a mercury thermometer. The thermistor had been calibrated against the mercury thermometer. The 99% thermal response time of the double-walled injection catheter was about 26 s. Therefore, an interval of five ventilatory cycles between two injections was used.

### 3.2.4 Experimental procedures

Five pigs were used in which the output of the left side of the heart was measured by administering the injectate into the left ventricle and detecting temperature changes in the aortic arch. At four levels of PEEP [0 (ZEEP), 5, 10, and 15 cmH<sub>2</sub>O ], series of 50 thermodilution measurements were carried out under steady-state conditions at all even phases of the ventilatory cycle (2, 4, ..., 100%). The sequence of the phases was chosen at random (PDP 11 random generator). To evaluate the steady-state throughout a series, not only heart rate and blood pressures, as mentioned, were measured but also cardiac output by the direct Fick method for oxygen. Three such measurements of cardiac output were done before as well as after each series. The measurement of cardiac output from the right side of the heart was performed in a separate group of six animals. The experimental protocol was almost identical to that described above, but, in addition to injections in the right atrium, an extra series of 50 measurements at the left side with a PEEP of 5 cmH<sub>2</sub>O was performed for comparison.

## 3.3 Results

### 3.3.1 Assessment of steady state

After all series of observations at four levels of PEEP the hemodynamic variables returned to the initial base-line levels at ZEEP. Mean values ( $\pm$ SD) for aortic pressure ( $94 \pm 6$  Torr), pulmonary arterial pressure ( $19 \pm 5$  Torr), and central venous pressure ( $0.6 \pm 0.4$  Torr) indicated no deterioration in the animal model.

In Fig. 2,A and B, two series of random measurements at the left and right side of the heart, respectively, are presented with all individual values

consecutively ordered. In both series there was no trend of cardiac output with the order of injection, i.e., with time. There were no changes in the other hemodynamic variables with time. Thus a steady state was accepted.

### 3.3.2 *Variation of cardiac output with phase of ventilatory cycle*

The mean value of cardiac output was calculated from all 50 measurements and taken as the 100% value. Each individual measurement was expressed as a percentage of this mean value. The maximum difference between two measurements within the series was about 40% for the left side. For the right side the maximum difference was about 70%. After measurements were sorted with respect to the phase of the ventilatory cycle at the moment of injection, a cyclic modulation of the values appeared (Fig. 2, C and D). On this modulation a random error was superimposed. In Fig. 3, A and B, all results for left and right sides were then averaged. At a PEEP level of 15 cmH<sub>2</sub>O the results of only four animals were used for the study on the left side. The results from the fifth animal were rejected since the steady state was not present. The average curve of the series of measurements at a PEEP of 5 cmH<sub>2</sub>O performed at the left side of the heart during the study of cardiac output measured from the right side did not show any difference with the corresponding series of the study on the left side (Fig. 3A).

The cyclic modulation at the left side, estimated with thermodilution, does not change with PEEP. During the inflation a decrease of flow was measured with recovery to a plateau with the onset of spontaneous expiration. Also at the right side the amount of the modulation did not significantly change with PEEP, although Fig. 3B suggests a slight decrease. However, the pattern of modulation shifts with PEEP.

### 3.3.3 *Estimation of cardiac output under changing circumstances*

During application of PEEP the cardiac output decreased with respect to the mean value at ZEEP. The absolute and the relative decrease of cardiac output with PEEP is shown in Table 1 for all series. The largest fall was observed between 5 and 10 cmH<sub>2</sub>O of PEEP. At 60% of the respiratory cycle the estimates of cardiac output at the left side are not significantly different from the mean of all 50 thermodilution measurements at all levels of PEEP; at 90% a systematic overestimation of about 6% was observed with a standard deviation of about 5%.

For the right side of the heart the smallest change of cardiac output with PEEP was at about the 90% phase of the ventilatory cycle. Due to the shift

TABLE 1.

Averaged values of cardiac output estimates related to PEEP

PEEP cmH <sub>2</sub> O	n	CO <sub>Fick</sub> ml.s <sup>-1</sup> kg <sup>-1</sup>	$\overline{\text{CO}}_{TH}$ ml.s <sup>-1</sup> kg <sup>-1</sup>	$\overline{\text{CO}}_{TH}$ % $\overline{\text{CO}}_{TH}$ at ZEEP	CO <sub>TH</sub> (60%), % $\overline{\text{CO}}_{TH}$	CO <sub>TH</sub> (90%), % $\overline{\text{CO}}_{TH}$
<i>Left side of heart</i>						
0	5	2.75 ±0.57	2.65 ±0.66	100 ±0	98.8 ±4.6	106.5 ±5.7
5	5	2.25 ±0.37	2.08 ±0.31	82 ±7	99.5 ±3.4	104.9 ±3.8
10	5	1.59 ±0.28	1.62 ±0.21	59 ±4	101.1 ±6.0	106.0 ±3.2
15	4	1.44 ±0.27	1.41 ±0.34	51 ±5	101.4 ±3.2	103.2 ±4.7
<i>Right side of heart</i>						
0	6	2.08 ±0.34	2.12 ±0.23	100 ±0		114.0 ±6.0
5	6	1.78 ±0.34	1.85 ±0.44	88 ±23		102.3 ±7.5
10	6	1.33 ±0.14	1.46 ±0.20	68 ±7		97.3 ±8.2
15	6	1.05 ±0.13	1.12 ±0.07	54 ±5		91.0 ±5.4

Values are means ± SD. PEEP, positive end-expiratory pressure; n, no. of animals; CO<sub>Fick</sub>, mean cardiac output estimated with the Fick method from 3 measurements before and 3 after each series of 50 thermodilution measurements;  $\overline{\text{CO}}_{TH}$ , mean cardiac output estimated from 50 measurements with the thermodilution method; ZEEP, PEEP at 0 cmH<sub>2</sub>O;  $\overline{\text{CO}}_{TH}(60\%)$ , and  $\overline{\text{CO}}_{TH}(90\%)$ , cardiac output measurements at 60 and 90% phase of the ventilatory cycle.



of the modulated curve with PEEP this change of the average value varied from 14% overestimation at ZEEP to 9% underestimation at the PEEP of 15 cmH<sub>2</sub>O.

### 3.3.4 *Comparison of thermodilution and Fick method*

To compare the thermodilution method with the Fick method, the mean of all 50 thermodilution measurements for each series was plotted against the mean of the six Fick measurements performed before and after each thermodilution series (Fig. 4, A and B). The equation of the regression line for the study on the left side is  $y = 0.53 + 0.94x$ . For the right side it is  $y = 1.22 + 0.97x$ . The coefficient of correlation is 0.97 in each case.

## 3.4 Discussion

### 3.4.1 *Thermodilution technique*

To obtain maximum accuracy in the estimation of cardiac output we have developed an automatic injection system, a double-walled injection catheter, and a modification of the usual analysis technique. An automatic injector delivers a highly reproducible injected amount of indicator when compared with manual injections [16]. This we have checked and confirmed. The assumption of complete mixing is supported by the small random error on the modulation of individually estimated cardiac output (Fig. 2,C and D). Complete mixing of the indicator is achieved by turbulence due to mechanical actions of the heart, thermal conduction, and high injection speed through multiple injection holes at the tip of the injection catheter [16].

The uncertainty in determining the amount of indicator contributing to the thermodilution curve has led to many different procedures and a variety of equations used in the calculation of cardiac output from the area subtended by the curve. Vliers et al. [20] have found that two factors mainly determine the total effective amount of indicator: 1) the amount of indicator directly injected into the blood and 2) the amount of indicator passing through the wall of the injection catheter. The loss of indicator between the site of injection and the site of detection appeared to be negligible [2, 4, 20, 21, 22].

The calculation of the cardiac output becomes more accurate if it is possible to eliminate or diminish the effect of the transfer of heat through

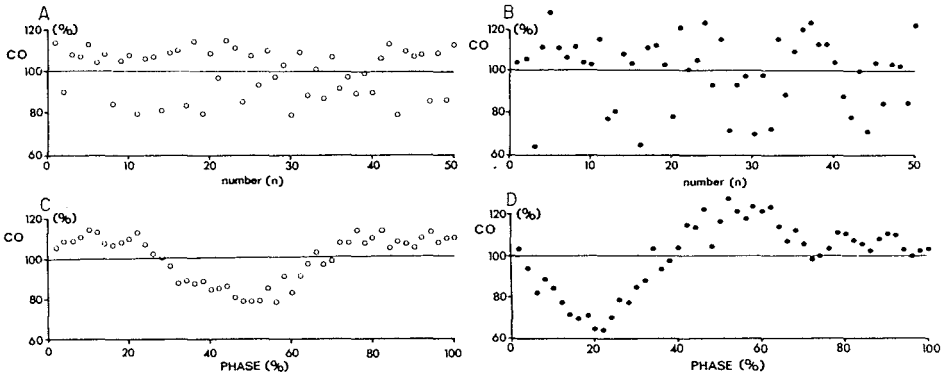


Fig. 2 A and B: series of 50 cardiac output (CO) measurements at the left and right side, respectively, performed at random within the ventilatory cycle; C and D: same series but plotted against moment of injection as a phase of ventilatory cycle.

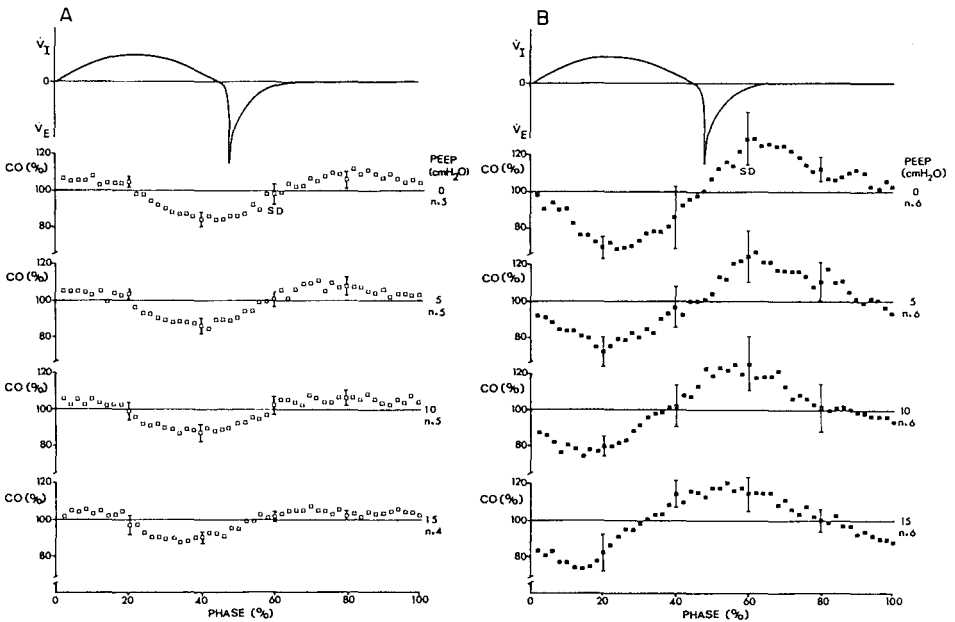


Fig. 3: Estimations of cardiac output (CO) at different levels of positive end-expiratory pressure (PEEP) for left (A) and right (B) side. As a reference pattern of airflow is given:  $\dot{V}_I$  is inflation and  $\dot{V}_E$  outflow. Vertical bars represent standard deviation of mean.

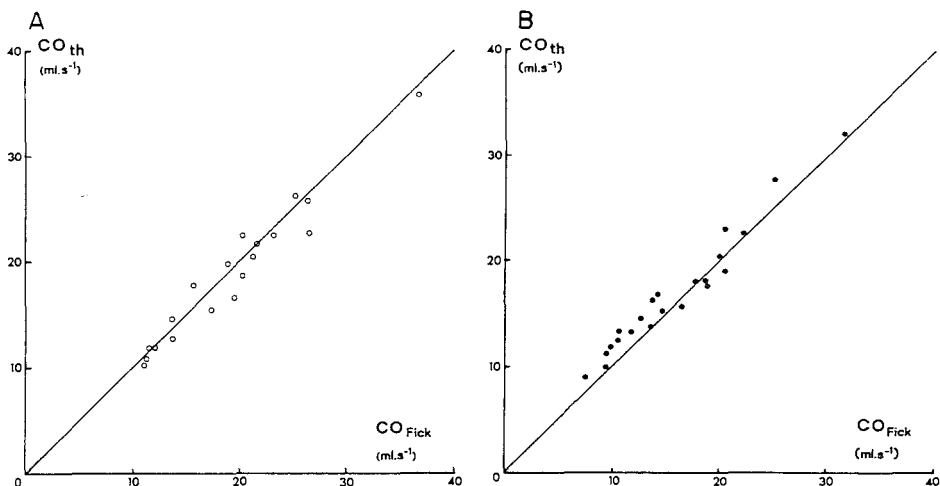


Fig. 4. Correlation of cardiac output (CO) measured with thermodilution (TH) technique and direct Fick method for oxygen. Plot includes 19 series of measurements in 5 different pigs for left side (A) and 24 for right side (B). Line is identity line.

wall of the injection catheter. This can be achieved by partially extrapolating the exponential downslope of the temperature-time curve [20-22] or by neutralizing its effect by rapidly withdrawing the residual injectate from the injection catheter and replacing it with blood [5, 12]. The withdrawal technique was not considered desirable for our automated and computer-controlled injection system because of system complexity. We have avoided the technique of extrapolation of the downslope of the dilution curve. The effects of nonconstant blood flow, due to artificial ventilation, and the bidirectional heat exchange between blood and injection catheter lead to a distortion of the shape of the dilution curve. A semilogarithmic extrapolation is therefore not reliable. Due to the double-walled catheter, heat loss during the injection period could be neglected. In the period after injection, i.e., the measuring period, when the cold fluid remained in the catheter, the time constant of the heat loss was increased considerably. This resulted in a slow injection of a small amount of indicator giving a very dispersed curve ( $W_2$ ) at the detection place (Fig. 5). This curve  $W_2$  is superimposed on the first principal curve  $W_1$  caused by the indicator entering the blood by the injection itself. At the detection site the sum of  $W_1$  and  $W_2$  is measured. For the accuracy of the estimates it is important that the analysis technique separates the areas of  $W_1$  and  $W_2$ . The mean transit time of  $W_2$  is equal to

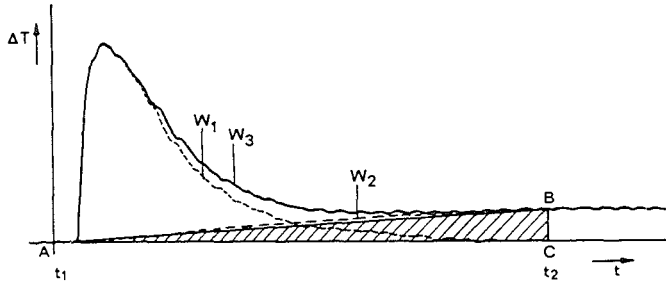


Fig. 5. Schematic representation of different components of thermodilution curve,  $W_3$ . Principal curve,  $W_1$ , is caused by amount of indicator injected through injection holes. Curve  $W_2$  is caused by indicator having left catheter by conduction through the wall. Triangle  $ABC$  is an approximation of the first part of  $W_2$ . Integration interval is from  $t_1$  to  $t_2$ .

the sum of the time constants of the monoexponential temperature decrease of the content of the injection catheter (13-15 s) and the mean transit time of the principal dilution curve  $W_1$  (3-5 s) [23]. As can be shown by linear system theory, the convolution of both temperature-time functions will be nearly symmetrical. The integration time was less than the mean transit time of  $W_2$ , because a part of  $W_2$  can then be approximated by the triangle  $ABC$  of Fig. 5.

The area of the principal curve  $W_1$  is found by subtracting the area of  $ABC$  from the total area. This is valid only if the base-line has neither drift nor fluctuations. After subtracting the area of  $ABC$ , the area of the principal wave corresponds with the effective amount of indicator, which is equal to the total amount of indicator minus the amount of indicator remaining in the injection catheter. If slow temperature drift occurs, the area of triangle  $ABC$  is the sum of the heat transfer  $W_2$  and this drift. So this drift is eliminated together with  $W_2$ . This approach can be applied to curves analyzed by hand or by digital computation. Commercial thermodilution computers are not feasible in this respect, as these instruments assume no base-line drift. During IPPV and CPPV we observed cyclic fluctuations in blood temperature, which were related to ventilation and cardiac pulsation [15, 16, 22]. The respiratory-induced cyclic fluctuations are more pronounced

on the right side, probably due to changes in regional venous inflow into the right atrium and therefore to a continuous redistribution of different heat contents [22]. Variations in base-line were corrected in this study by integration of the area of these fluctuations over an equal time period within the phase of a ventilatory cycle after each dilution curve. This area was then subtracted from the area of the previous dilution curve.

The practice of correction of the effective amount of indicator becomes more complicate when the temperature of the injectate differs from room temperature [20, 22], because that part of the catheter outside the animal will change continuously with room temperature. Injection volumes of 0.5 ml saline at room temperature suited our analyses, as indicated by the small random error superimposed on the modulated signal and the high correlation of the thermodilution and Fick measurements.

#### 3.4.2 *Ventilatory modulation*

The error in the estimate of the cardiac output due to the modulation of blood flow, caused by the artificial ventilation, was tested for both sides of the heart. Although the variations of the thermodilution values are not symmetrically distributed around the arithmetic mean, this latter value appeared to be a reliable estimate of the average value. This is confirmed by the close identity with the Fick values (Fig. 4, A and B).

If the phase of the respiratory cycle at which saline was injected is neglected, differences between estimates of cardiac output of 40 and 70% for left and right side, respectively, are found (Fig. 2, A and B). If this is also true in humans, random thermodilution measurements of cardiac output from both sides of the heart preclude a reliable estimate. However, when the measurements are plotted against the moment of injection in the ventilatory cycle, the large random variations are transformed into a systematic modulation of cardiac output with a much smaller random error superimposed on it. For an estimation of the mean value of cardiac output from the left side, injection at about 60% of the ventilatory cycle appeared to be the best moment. This is true for our experiments, but this may not be entirely valid for measurements under circumstances with other parameters of artificial ventilation. Therefore, in studies during IPPV and CPPV, where very accurate estimations of cardiac output are required, the optimal moment of injection as presented here should be determined. But, in general, a satisfactory moment for the measurement of cardiac output from the left side seems to be near the end of spontaneous expiration, since at this plateau the stan-

dard deviation is only about 5% and the overestimation is systematic and small (about 6%). It is also independent of cardiac output changes induced by PEEP. For the measurements on the right side we could not determine a satisfactory moment of injection for all levels of PEEP, because of the shift of the modulated signal. Thus, taking single estimates of cardiac output as representatives of the mean may be misleading if the PEEP level has been changed.

The degree of modulation of cardiac output obtained with the thermodilution method is similar at all levels of PEEP (Fig. 3). However, the real modulation of flow will increase with PEEP, as demonstrated by measuring flow velocity [7]. This increase is not measured by the thermodilution technique. It might be explained by the phenomenon that every individual thermodilution measurement represents a weighted mean of all actual flows during the time of the dilution curve. The flow values in the first part of the dilution curve contribute the most to this mean and the flow values during the tail of the curve progressively less. Therefore, the real modulation of the cardiac output during a ventilatory cycle will be smoothed by the thermodilution technique. Although an increased averaging effect at lower cardiac output was expected because of longer transit times, it nevertheless was surprising that no increase in modulation at all was observed.

The phenomenon of the forward shift of the modulated curve for the right side of the heart indicates that the decrease of cardiac output, due to inflation of the lungs, is measured earlier in the respiratory cycle. At 10 and 15 cmH<sub>2</sub>O PEEP this decrease manifests itself even before the onset of inflation (Fig. 3B). According to Nordström [11] the phasic decrease of pulmonary artery flow starts at the beginning of inflation. In similar experiments with electromagnetic flow measurements we have recently observed (unpublished data) larger falls of pulmonary artery flow during inflation at increasing levels of PEEP. This will result in the tail of the dilution curve contributing an increasing proportion to the total area of the curve, where injection is made during the preceding end-expiratory phase. Therefore, the cardiac output at that moment will be underestimated.

In conclusion we state that 1) random measurements of cardiac output by thermodilution during IPPV and CPPV can give very unreliable estimates at either side of the heart; 2) the mean of a large series of thermodilution measurements of cardiac output evenly distributed over the respiratory cycle shows excellent correlation with the mean cardiac output measured by the Fick principle; 3) the thermodilution technique is not appropriate for studying modulations of cardiac output dependent on artificial ventilation;

4) for applications on the right side of the heart, comparisons of thermodilution values under changing circumstances, e.g., PEEP, may be inaccurate due to changes of the values based on other mechanisms than decrease of cardiac output itself; and 5) the measurements on the left side of the heart give more reliable estimates of cardiac output, which are comparable and are therefore useful for evaluation of the hemodynamic conditions, at least with changing PEEP.

We thank Prof.dr. J.G. Bovill and Prof.dr. P.R. Saxena for their helpful comments on the manuscript.

## References

- [1] Branthwaite, M.A., and R.D. Bradley. Measurement of cardiac output by thermal dilution in man. *J. Appl. Physiol.* 24: 434-438, 1968.
- [2] Cropp, J.A., and A.C. Burton. Theoretical considerations and model experiments on the validity of indicator dilution methods for measurement of variable flow. *Circ. Res.* 18: 26-49, 1966.
- [3] Fegler, G. Measurement of cardiac output in anaesthetized animals by a thermodilution method. *Q. J. Exp. Physiol.* 39: 153-164, 1954.
- [4] Ganz, W., and H.J.C. Swan. Measurement of blood flow by thermodilution. *Am. J. Cardiol.* 29: 241-246, 1972.
- [5] Goodyer, A.V.N., A. Huvos, W.F. Eckhardt, and R.H. Ostberg. Thermal dilution curves in the intact animal. *Circ. Res.* 7: 432-441, 1959.
- [6] Hosie, K.F. Thermal dilution techniques. *Circ. Res.* 10: 491-504, 1962.
- [7] Jansen, J.R.C., J.M. Bogaard, E. von Reth, J.J. Schreuder, and A. Versprille. Monitoring of the cyclic modulation of cardiac output during artificial ventilation. *Proc. Int. Symp. Comput. Critical Care Pulmonary Med. 1st Norwalk CT, May 26-26, 1979*, p. 59-68.
- [8] Khalil, H.H., T.Q. Richardson, and A.C. Guyton. Measurement of cardiac output by thermal dilution and direct Fick methods in dogs. *J. Appl. Physiol.* 21: 1131-1135, 1966.
- [9] Maruschak, G.F., E.A. Meathe, J.F. Schauble, and A. Fronck. A simplified equation for the thermal dilution cardiac output. *J. Appl. Physiol.* 37: 414-416, 1974.
- [10] Morgan, B.C., W.E. Martin, T.F. Hornbein, E.W. Crawford, and W.G. Guntheroth. Hemodynamic effects of intermittent positive pressure ventilation with and without an end-expiratory pause. *Anesthesiology* 27: 584-590, 1966.
- [11] Nordström, L. Haemodynamic effects of intermittent positive pressure ventilation with and without an end-inspiratory pause. *Acta Anaesth. Scand. Suppl.* 47, 1972.

- [12] Olsson, B., J. Pool, P. van der Mosten, E. Varnauskas, and R. Wassén. Validity and reproducibility of determination of cardiac output by thermodilution in man. *Cardiology* 55: 136-148, 1970.
- [13] Olsson, S.B., R. Wassén, E. Varnauskas, and H. Wallman. A simple analogue computer for cardiac output determination by thermodilution. *Cardiovasc. Res.* 6: 303-308, 1972.
- [14] Otis, A.B. Quantitative relationships in steady-state gas exchange. In: *Handbook of Physiology. Respiration*. Washington, DC: Am. Physiol. Soc., 1964, sect. 3, vol. I, chapt. 27, p. 681-698.
- [15] Pavsek, E., K. Pavsek, and D. Boska. Mixing and observation errors in indicator-dilution studies. *J. Appl. Physiol.* 28: 733-740, 1970.
- [16] Saadjian, A., J.E. Quercy, and J. Torresani. Cardiac output measurement by thermodilution. *Med. Prog. Technol.* 3: 161-167, 1976.
- [17] Scheuer-Leeser, M., A. Morquet, H. Reul, and W. Inrich. Some aspects to the pulsation error in blood-flow calculations by indicator dilution technique. *Med. Biol. Eng. Comput.* 15: 118-123, 1977.
- [18] Silove, E.D., T. Gantez, and B.C. Wells. Thermodilution measurement of left and right ventricular outputs. *Cardiovasc. Res.* 5: 174-177, 1971.
- [19] Stow, R.W. Systematic errors in flow determinations by the Fick method. *Min. Med.* 37: 30, 1954.
- [20] Vliers, A.C.A.P., K.R. Visser, and W.G. Zijlstra. Analysis of indicator distribution in the determination of cardiac output by thermodilution. *Cardiovasc. Res.* 7: 125-132, 1973.
- [21] Warren, D.J., and J.G.G. Ledingham. Cardiac output in the conscious rabbit: an analysis of the thermodilution technique. *J. Appl. Physiol.* 36: 246-251, 1974.
- [22] Wessel, H.U., M.H. Paul, G.W. James, and A.R. Grahn. Limitations of thermal dilution curves for cardiac output determinations. *J. Appl. Physiol.* 30: 643-652, 1971.
- [23] Zierler, K.L. Circulation times and the theory of indicator-dilution methods for determining blood flow and volume. In: *Handbook of Physiology. Circulation*. Washington, DC: Am. Physiol. Soc., sect. 1, vol. I, chapt. 18, p. 585-615, 1962.



## CHAPTER 4

# IMPROVEMENT OF CARDIAC OUTPUT ESTIMATION BY THE THERMODILUTION METHOD DURING MECHANICAL VENTILATION

JOS R. C. JANSEN AND ADRIAN VERSPRILLE  
(with the technical assistance of Arnold Drop)

Pathophysiological Laboratory, Department of Pulmonary Diseases,  
Erasmus University, 3000 DR Rotterdam, The Netherlands.

Published in *Int. Care Med.* 12: 71-79, 1986.

### 4.1 Introduction

The thermodilution technique for the estimation of cardiac output based on the classical Stewart-Hamilton equation has become widely accepted. Although this is valid only for constant blood flow, this method has been applied during artificial ventilation where a characteristic pattern of cyclic fluctuation i.e. modulation occurs in right ventricular output [1, 4, 5, 7, 8, 12, 13]. Few studies have been made of the errors which arise when the thermodilution technique is used during a modulated flow as in artificial ventilation. Cropp and Burton [3] studied the errors in the estimation of cardiac output in a physical model using a constant injection rate of cold indicator. Bassingthwaight et al. [2] simulated a bolus injection in their theoretical studies with a mathematical model. During experiments with pigs we found a cyclic modulation in cardiac output estimates by the thermodilution method [5]. The best moment of injection varied with the level of positive end-expiratory pressure. Snyder and Powner [11] confirmed our results and reported additionally the existence of variation in estimates in a patient.

The objectives of our present study were

1. to investigate the errors in the estimation of mean cardiac output by single measurements during mechanical ventilation with changing conditions of PEEP, ventilatory pattern, ventilatory rate and blood volume, and
2. to search for an averaging technique which maximally reduces the errors

with a minimum of measurements.

## 4.2 Methods

### 4.2.1 *Experimental techniques*

Surgical procedures, measurements, data acquisition and analyses were described in a previous paper [5]. The essentials and additional procedures will be mentioned here. Eighteen Yorkshire pigs, 5-7 wk old, weighing 7-11 kg, were anesthetized with pentobarbital sodium, using a loading dose of 30 mg.kg<sup>-1</sup> i.p followed by a continuous infusion of 7.5 mg.kg<sup>-1</sup>.h<sup>-1</sup>. Muscle relaxation was induced with a loading dose of d-tubocurarine hydrochloride (0.1 mg.kg<sup>-1</sup>) administered over a period of 3 min, followed by a continuous infusion of 0.2 mg.kg<sup>-1</sup>.h<sup>-1</sup>. Heparin (125 I.U. kg<sup>-1</sup>) was given intermittently each hour.

The animals were ventilated with room air using a microprocessor controlled ventilator at rates of 10 and 20 cycles min<sup>-1</sup>. Ventilation volume was adjusted to achieve an arterial carbon dioxide tension between 38 and 44 Torr and was subsequently kept constant for the applied pattern of ventilation. Body temperature was maintained at about 38 °C on a thermo-controlled operating table.

### 4.2.2 *Catheters*

Catheters were positioned under fluoroscopic control and pressure monitoring. A four-lumen catheter was inserted into the vena cava at the level of the right atrium for measuring central venous pressure and for drug infusions. A double-walled injection catheter (inner tube 0.86mm ID, 1.27mm OD, outer tube 1.40mm ID, 1.90mm OD) was inserted into the right atrium for injections of 0.5 ml of saline. The length of the intracorporeal part of this catheter was 12-15 cm. A Swan-Ganz 5F catheter with a thermistor was positioned in the pulmonary artery. After the experiments the position of each catheter was confirmed at autopsy.

### 4.2.3 *Fick method*

Cardiac output ( $CO_{Fick}$ ) was measured by the direct Fick method for oxygen [5]. Inspiratory and mixed expiratory gases were sampled over 3 min with a mass spectrometer (Perkin-Elmer MGA 1100) from a mixing box with a volume equal to 5 times tidal volume. Oxygen content of the arterial and

venous blood was calculated from the directly measured oxygen saturation and hemoglobin values (Radiometer OSM2) and the oxygen pressure ( $P_{O_2}$ ) (Radiometer ABL3). Blood was continuously sampled over three ventilatory cycles. The OSM2 was recalibrated for pig blood by tonometry for the saturation and for hemoglobin (Hb) checked by the Hb cyanide method.

#### 4.2.4 Thermodilution method

When a hemodynamic stability was achieved, cardiac output measurements by thermodilution ( $CO_{TH}$ ) were carried out by injection of 0.5 ml saline (0.9% NaCl) at room temperature. The cold fluid was injected through the double walled catheter within 300 msec by a pneumatically driven syringe. After 12 seconds the syringe was automatically refilled.

The temperature-time curve ( $\Delta T_b(t)$ ) was derived from the thermistor of the Swan-Ganz catheter. The thermistor response was linear within the range of measurements (37-39°C). The temperature-time curve was sampled on-line and analysed with a sample frequency of 50 Hz by a PDP 11/23 computer.

The cardiac output (CO or  $\bar{Q}$ ) was derived from a mass balance equation [15].

$$\rho_i S_i \int \dot{Q}_i(t)(T_b - T_i)(t)dt = \rho_b S_b \int \Delta T_b(t)\dot{Q}(t)dt \quad (1)$$

where  $\dot{Q}(t)$  is the blood flow,  $\dot{Q}_i(t)$  the injectate flow,  $T$  the temperature,  $\rho$  the density and  $S$  the specific heat of blood ( $b$ ) and injectate ( $i$ ) respectively.

For a bolus injection, assuming  $\dot{Q}$  is constant, equation (1) can be written:

$$\bar{Q} = \frac{V_i \rho_i S_i (T_b - T_i)}{\rho_b S_b \int \Delta T_b(t)dt} \quad (2)$$

where  $V_i$  is the injected volume minus the volume of the intracorporeal part of the catheter.

For a reliable estimation of the area of  $\int \Delta T_b(t)dt$  several corrections have to be made [5] (Fig. 1).

The recorded thermodilution curve (Fig. 1a) has to be corrected for variations in base-line temperature concomitant with the ventilatory cycle (Fig. 1b) [14], slow trends in body temperature (Fig. 1c) and the leakage of cold from the intracorporeal part of the double walled injection catheter (Fig. 1d).

No corrections for specific heat were made during hypervolemic and hypovolemic condition since calculations based on the equations of Rosen et

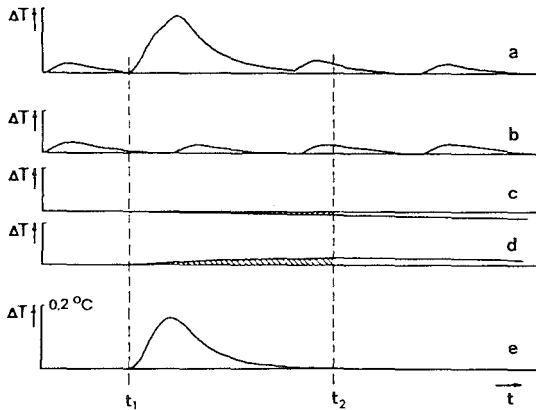


Fig. 1a - e. Corrections to the thermodilution curve. a the curve as actually measured; b base-line fluctuations during each ventilatory cycle; c long-term baseline drift; d loss of cold from the catheter dead space and e the corrected dilution curve after subtraction of b, c and d from the original curve a.

al. [9] showed that the errors introduced were smaller than 1%.

#### 4.2.5 Series of observations and conditions

Series of 50 thermodilution measurements were carried out during hemodynamically stable conditions [5]. Five ventilatory cycles were inserted between two measurements, which implies that the series of 50 measurements was performed in 25 min. The ventilatory cycle was divided into 100 equal intervals. The beginning of insufflation was chosen as the start of the first interval (phase 0%). The injections of indicator for the thermodilution measurements were performed at the even numbered percentage phases of the cycle.

The sequence of injection moments in the ventilatory cycle was randomly chosen. The mean of all 50 measurements was taken as the 100% value. For the evaluation of the stationary state heart rate, aortic, central venous and pulmonary artery pressures were monitored throughout a series. Moreover, the random estimates were tested on their trend in time [5]. A negative or positive trend was assumed to indicate a nonstable condition. Two or three cardiac output estimates were made by Fick's method for oxygen just before and after each series. The interval between two series was about 30 min. Series without hemodynamically stationary conditions were rejected.

Three patterns of ventilation were applied:

1. a sinusoidal like inspiratory flow (I) followed by a spontaneous expiration (E) with an I:E ratio of 44:56 (Fig. 4a);
2. a constant inspiratory flow followed by a spontaneous expiration after an inspiratory pause (IP) with an I:IP:E ratio of 25:5:70 (Fig. 4b);
3. the same pattern as 2. with an I:IP:E ratio of 15:5:80 (Fig. 4c).

Patterns (1-3) were applied at a ventilatory rate of  $10 \text{ min}^{-1}$ , pattern (2) was also applied at a rate of  $20 \text{ min}^{-1}$  (Fig. 4d).

Three volemic conditions were applied with ventilation pattern (2) and a ventilatory rate of  $10 \text{ min}^{-1}$ :

1. hypervolemia was obtained by infusion of  $15 \text{ ml.kg}^{-1}$  6% Macrodex solution in 5% glucose;
2. normovolemia by bleeding the animal  $15 \text{ ml.kg}^{-1}$ ;
3. hypovolemia by a further bleeding of  $15 \text{ ml.kg}^{-1}$ .

These changes were used to study the effects of changes in amplitude of the modulations in real output [13] on the amplitude of the thermodilution estimates.

Four levels of PEEP [0 (ZEEP), 5, 10, 15  $\text{cmH}_2\text{O}$ ] were studied at a ventilatory rate of  $10 \text{ min}^{-1}$  and with inflation pattern (1).

#### 4.2.6 The averaging procedures

Averages were calculated according to a *systematic* and a *random* selection of single estimates. In both procedures the averages were derived from 2, 3, 4, 5 and 6 single measurements of each series of 50, and will be called two, three, four, five and six-point-averages respectively.

In the systematic procedure these averages were calculated from single values equally spread in the ventilatory cycle (Fig. 2). Thus, for each series 25 two-point-averages were attained from the phases 0 + 50%, 2 + 52%, etc. The total number for all 55 series is  $n = 1375$ . Sixteen three-point-averages per series were calculated from the phase 0 + 34 + 68 ( $n = 880$ ). The 12 four-point-averages per series were taken from the phases 0 + 24 + 50 + 76%; etc., where the phases 48 and 74% were left out ( $n = 660$ ). Ten five-point-averages per series were obtained from the phases 0 + 20 + 40 + 60 + 80%, etc. ( $n = 600$ ) and eight six-point-averages from the phases 0 + 34 + 50 + 66 + 82%, etc. without the phases 32 and 98% ( $n = 440$ ).

In the random procedure the same number of averages was calculated as for the corresponding averages of the systematic procedure, e.g. for the five-point averages within each series 10 times a random selection of five

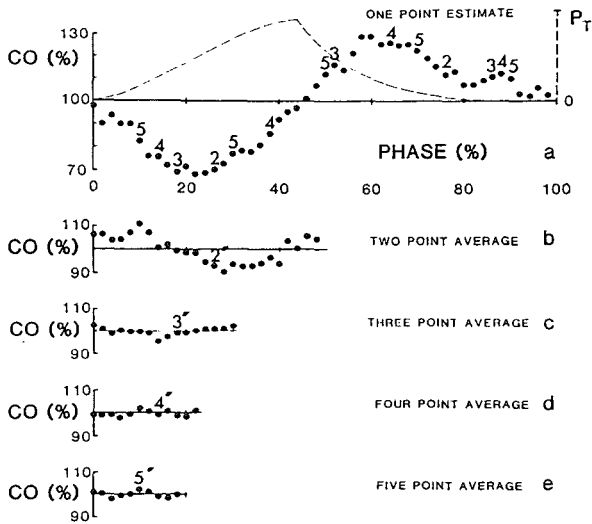


Fig. 2a - e. An example of averaging techniques. Values are given in % of the mean, which is 100% for all 50 single estimates. a 50 single estimates of cardiac output related to the moment of injection in the ventilatory cycle. b 25 two-point-averaged values. For example the dot marked with 2' is the averaged value of two (equally spread) single estimates marked with sign 2. This average value is plotted on the phase axis at the same phase moment of the first dot 2, in Fig.a. c 16 three-point-averaged values. The dot marked with 3' is the averaged value of the three (equally spread) dots 3 in Fig. a. Again the average value is plotted at the same phase of the first dot. d 12 four-point-averaged values. The dots marked with 4' is the averaged value of the four equally spread points 4 in Fig. a. e 10 five-point-averaged values.

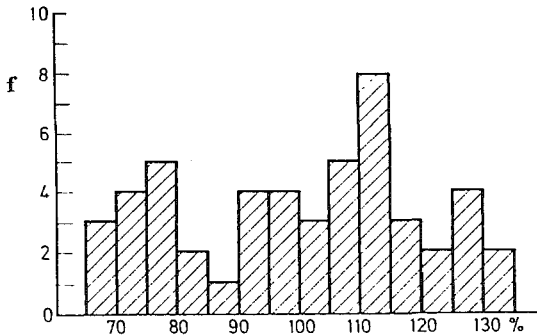


Fig. 3. Frequency distribution of the cardiac output estimates of Figure 2 a.  $f$  is the frequency of estimates for the given %-interval.

estimates was made. Each selection of a single estimate was done with replacement, implying that the same estimate could be selected more than once for one averaged value. This was done in order to simulate random estimations of cardiac output, where the same moment (or phase) in the ventilatory cycle can be taken.

#### 4.2.7 Statistical analyses

The Figures 2, 4 and 5 demonstrate that the series of 50 single estimates have a sinusoidal-like pattern within the timeperiod of the whole ventilatory cycle. In the systematically obtained two-point-averages (Fig. 2) a second sinusoidal-like pattern with a lower amplitude can be observed. Thus, the pattern of single estimates seems to be composed of two harmonic waves.

In a sinusoidal pattern the values, positioned on the curve at equally spaced places on the horizontal phase axis, are concentrated around the maximal and minimal values, i.e. the largest amplitudes. When a second harmonic is present a third concentration around the mean will be present, which can be verified from a composed wave of two harmonics with a frequency ratio of 2. In such a pattern the distribution of values will not be normal either, which is demonstrated in Figure 3 for the single data of Figure 2. In this single series the range of  $\pm 1SD$  around the mean contains 55% of the 50 data, which is far below the theoretical value of 68% for a normal distribution.

However, the aim of our study was to analyse the accuracy of estimation of mean cardiac output under a diversity of ventilatory and hemodynamic

conditions. For that reason we lumped the data of all series and studied the distribution patterns of the single estimates and those of the different averages. Moreover, mean values, standard deviations, number of values within the range of  $\pm 1SD$  around the mean and the number of data within the accuracy limits of 5 and 10% around the mean were calculated.  $p$ -levels for differences between measurements within the same animals were calculated according to a paired Student t-test for small samples.

## 4.3 Results

### 4.3.1 Pattern of blood flow estimation

In 6 animals cardiac output was estimated during 4 different modes of ventilation. The averaged estimates at all 50 phases are shown in Figure 4. Series without stationary conditions were excluded. The mean value of cardiac output over the whole ventilatory cycle was calculated from all 50 estimates and taken as the 100% value. In all series there was a cyclic variation of cardiac output estimates with a periodicity equal to that of the ventilatory cycle. In each ventilatory mode the pattern of estimates was approximately sinusoidal.

The observations under different volemic conditions are presented in Figure 5. The only result was a forward shift of the estimated flow pattern during bleeding from hypervolemia via normovolemia to hypovolemia, which is a shift to earlier phases in the ventilatory cycle. The occurrence of a shift was tested by comparing the points at the same phases. In Figure 5c 29 points were significantly different ( $p < 0.05$ ) from those in Figure 5a. These points were mainly in the slopes of the modulation. Between the phases 0-20% the points of 5c were higher than those of 5a and between 70 and 100 they were lower.

### 4.3.2 Amplitude of the estimated flow

In table I the averaged amplitude of the single estimates is given for the different ventilatory modes and hemodynamic conditions.

For all PEEP levels in the series with a sinusoidal like inspiratory flow a similar value was found for the positive and negative amplitudes with respect to the mean,  $CO_{max}/\overline{CO}_{TH}$  and  $CO_{min}/\overline{CO}_{TH}$  respectively. Differences in amplitude were not observed for the two constant flow patterns (square wave) at rates of  $10 \text{ min}^{-1}$  or for the three volemic conditions at a level of  $p < 0.05$ .



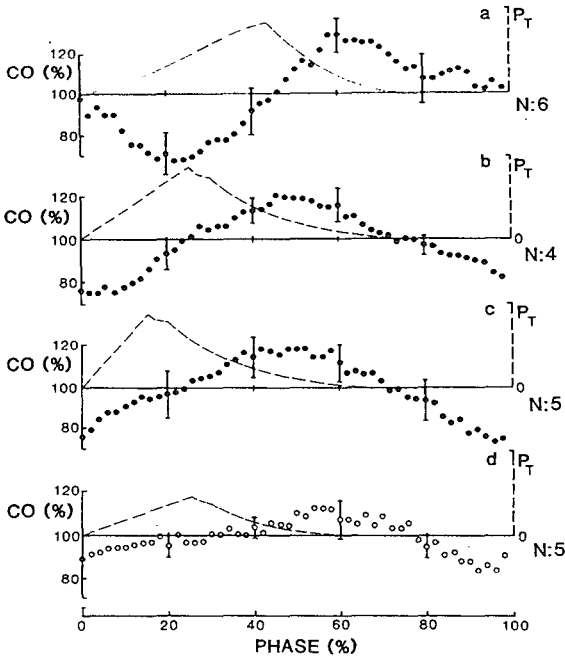


Fig. 4a - d. Estimation of cardiac output (CO) as a function of the injection phase during different ventilatory conditions. Vertical bars represent standard deviations from the mean. The ventilatory mode is given in broken lines as airway pressure ( $P_T$ ). N is the number of animals.

**TABLE 1.**  
Cardiac output data for ventilatory and hemodynamic conditions.

Conditions						$CO_{Fick}$	$\overline{CO}_{TH}$	$\frac{\overline{CO}_{TH}}{CO_{Fick}}$	$\frac{CO_{max}}{\overline{CO}_{TH}}$	$\frac{CO_{min}}{\overline{CO}_{TH}}$	
I	P	E	RR	Vol.	PEEP	n	ml.s <sup>-1</sup> kg <sup>-1</sup>	ml.s <sup>-1</sup> kg <sup>-1</sup>			
%	%	%		ml/kg							
<i>Sinus</i>											
44	0	56	10	0	0	6	2.08 ±0.34	2.12 ±0.23	1.03 ±0.12	1.30 ±0.15	0.69 ±0.09
44	0	56	10	0	5	6	1.78 ±0.34	1.85 ±0.44	1.04 ±0.08	1.23 ±0.13	0.72 ±0.06
44	0	56	10	0	10	6	1.33 ±0.14	1.46 ±0.20	1.09 ±0.11	1.24 ±0.11	0.75 ±0.05
44	0	56	10	0	15	6	1.05 ±0.13	1.12 ±0.07	1.07 ±0.11	1.22 ±0.10	0.74 ±0.05
<i>Square</i>											
15	5	80	10	0	0	5	2.31 ±0.58	2.38 ±0.41	1.05 ±0.11	1.19 ±0.13	0.75 ±0.05
25	5	70	10	0	0	4	2.71 ±0.51	2.61 ±0.50	0.96 ±0.08	1.22 ±0.05	0.75 ±0.05
25	5	70	20	0	0	5	2.87 ±0.43	2.44 ±0.49	0.86 ±0.11	1.13 ±0.06	0.85 ±0.05
25	5	70	10	+15	0	6	3.86 ±0.41	3.62 ±0.32	0.95 ±0.06	1.18 ±0.10	0.71 ±0.08
25	5	70	10	0	0	5	2.66 ±0.39	2.66 ±0.31	1.00 ±0.07	1.19 ±0.08	0.71 ±0.11
25	5	70	10	-15	0	6	1.92 ±0.27	2.16 ±0.29	1.13 ±0.09	1.20 ±0.14	0.74 ±0.03
						55			1.02		±0.09

Sinus is sinusoidal air flow; Square is constant air flow; Values are means ±SD; n, the number of animals; I, P, E, the duration of inspiration, inspiratory pause and expiration as a percentage of the ventilatory cycle; PEEP, positive end-expiratory pressure in cmH<sub>2</sub>O; R.R., respiration rate in breaths per min; VOL, volemic state of the animals;  $CO_{Fick}$ , mean cardiac output estimated by the Fick method from the measurements before and after each series;  $\overline{CO}_{TH}$ , mean cardiac output estimated from 50 thermodilution measurements;  $CO_{max}$  and  $CO_{min}$ , the mean highest value and the mean lowest value of the series respectively.

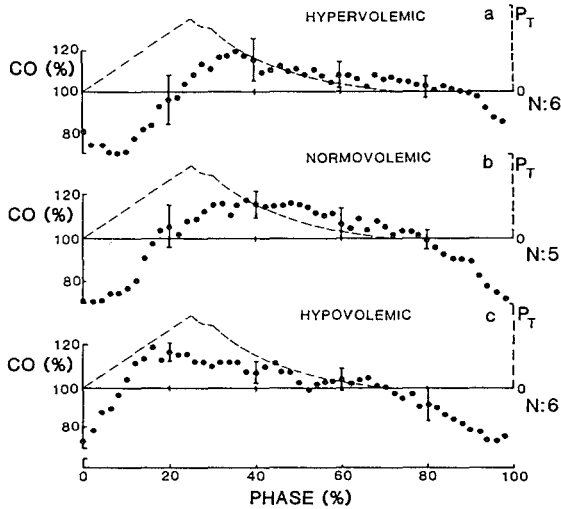


Fig. 5a - c. Estimation of cardiac output (CO) as a function of the injection phase during hypervolemic a, normovolemic b and hypovolemic c conditions. Vertical bars represent standard deviations from the mean. The ventilatory mode is given in broken lines as airway pressure ( $P_T$ ). N is the number of animals.

However, under all these conditions mean cardiac output changed substantially, implying that the relative fluctuations in estimated flow are independent of mean flow.

At a higher ventilatory rate ( $20 \text{ min}^{-1}$ ), however, the amplitudes of fluctuations were smaller than the corresponding values during ventilation at a rate of  $10 \text{ min}^{-1}$ .

#### 4.3.3 Comparison of thermodilution and Fick method

The ratios of the mean of all 50 thermodilution estimates to the corresponding mean of the Fick estimates ( $\overline{CO}_{TH}/\overline{CO}_{Fick}$ ), are shown in table I. Comparing all circumstances for all animals  $\overline{CO}_{Fick}$  and  $\overline{CO}_{TH}$  were not different at a  $p$ -level equal to 0.05. However, the mean of all 50 thermodilution measurements underestimated mean cardiac output during ventilation at a rate of  $20 \text{ min}^{-1}$  and overestimated it during hypovolemia.

#### 4.3.4 Average procedure

The derived data of all single estimates are presented under "systematic procedure" in Table 2, where the data of randomly selected single estimates are given under "random procedure". This selection was done 50 times from each complete series. In the systematic procedure the mean value is by definition 100%. In the randomly selected population of 2750 single estimates the mean value shows a slight difference due to the fact that some data are selected more than once and others not at all.

The distribution of the single estimates was symmetrical in both procedures and much more concentrated around the mean than those of Figure 3. The random selection of single estimates gave approximately similar data for the mean, for SD, for the number of estimates within  $\pm 1$  SD around the mean and for the number of estimates within the accuracy limits of  $\pm 5$  and  $\pm 10\%$  respectively.

The distributions of averages were also symmetrical in both procedures and became increasingly concentrated around the mean when more single points were used for calculation of the averages. The SD-values decreased when the number of points for the averages increased. This decrease in SD was much more pronounced in the averages of the systematic procedure than that in the random procedure.

In all populations of single estimates and averaged values the percentage of estimates around the mean  $\pm 1$  SD were close to 68%, the theoretical value for a normal distribution. Another indication of the increasing concentration of data around the mean was the percentage of estimates within the accuracy limits of  $\pm 5$  and  $\pm 10\%$  around the mean.

The decrease of SD and the increase in percentage numbers within the accuracy limits were much larger in the systematic averaging procedures than those in the random procedure.

## 4.4 Discussion

The mean values in  $\text{ml}\cdot\text{s}^{-1}$  of the series of 50 thermodilution estimates represent reliable values for mean cardiac output [5], which was again demonstrated by comparing them with the Fick values (Table 1). For each series the mean of the 50 thermodilution estimates was normalized to 100% in order to lump all series for the study, independent of the absolute level of cardiac output.

Studying the effects of modulation on the estimation of cardiac output by thermodilution using the Stewart-Hamilton equation, which is common

clinical practice, we conclude that this method is too inaccurate for the estimation of mean cardiac output, even when systematic errors are accepted. The reason is that the errors are not constant when mean cardiac output is changed. The pattern of flow estimates will shift forward in the ventilatory cycle when cardiac output decreases. This is shown for changes in ventilatory pattern (Fig. 4) and volemic conditions (Fig. 5). Similar findings have been reported for changes in PEEP [5].

The shift in the volemic group does not seem to be related to the dilution of blood neither to the order of observations. We did not observe any difference between the results presented in Figure 4b and those in Figure 5b, where the differences between both series is another order of circumstances. In another study [10] we demonstrated similar hemodynamic state and responses on PEEP in animals before and after hemodilution, even when a period of hypervolemia was inserted. When the conditions are changing also the moments in the cycle will change for estimation of mean cardiac output by one single measurement.

#### 4.4.1 *Cyclic modulation*

The ventilatory pattern hardly influences the amplitude of the modulation in the cardiac output estimates. The constant amplitude of modulation in the thermodilution estimates might be due to the same basic frequency of all three ventilatory patterns. Probably these patterns differ only in their effect on real flow fluctuations in the range of the higher harmonics. The influence of higher harmonics in the real flow on the modulation of thermodilution estimates will decrease progressively [2].

The amount of modulation is also similar for the three different volemic conditions (Fig. 5 and Table 1) and, hence, for different values of mean flow. This is shown by the ratios of maximum to mean estimates ( $CO_{max}/\overline{CO}_{TH}$ ) and of minimum to mean estimates ( $CO_{min}/\overline{CO}_{TH}$ ). It could be due to two counteracting phenomena. First, electromagnetic recordings showed that the amplitude of the modulation during mechanical ventilation was reversely proportional to mean flow [13]. Second, according to Knopp and Bassingthwaite [6] the dispersion of indicator is also reversely proportional to flow over a wide range of values. Consequently, during hypervolemia, when flow is high, the dilution curves are peaked, resulting in an estimation of flow over a shorter period of the ventilation than during hypovolemia, when indicator is spread out. In that case a flow is estimated which is a weighted mean over a longer period of the ventilatory cycle, causing a larger smoothing effect

on real modulation than during hypervolemia. Apparently this leads to the coincidence of an almost equal modulation in the thermodilution estimates. We expect that the larger dispersion of indicator in low flow conditions causes the forward shift of the modulation of estimates during PEEP and bleeding. As suggested by us in a previous study [5], a low cardiac output during insufflation will contribute relatively more to the area of a dilution curve corresponding to an injection phase in the end-expiratory period of the preceding cycle because the curve is more spread out.

During shorter insufflation we also observed a forward shift of the modulation (Fig. 4a - c). In these three patterns of ventilation, however, mean flow was the same. The more pronounced fall in actual flow during a faster insufflation will contribute more to the area of a dilution curve after injection in the preceding endexpiratory period than a more gradual fall in actual flow during a slower insufflation.

Increasing ventilatory rate decreases the amplitude of the cyclic variation of the estimates (Fig. 4). This reduction will be caused by two mechanisms. Firstly, tidal volume and therefore intrathoracic pressure rise is smaller leading to a reduction in real amplitude of modulation. Secondly, the duration of a dilution curve is constant, when cardiac output is constant, and independent of the duration of a ventilatory cycle. This implies an estimation of cardiac output by the thermodilution over a larger part of ventilatory cycle when this cycle is shortened. Therefore, the estimated value will deviate less from the mean cardiac output over the whole ventilatory cycle [2].

#### 4.4.2 Accuracy of estimates

In this study a series of different conditions, usually found in intensive care medicine, were applied to different groups of animals in order to evaluate the accuracy of the thermodilution method for estimation of mean cardiac output for a diversity of conditions.

A normal distribution of data around a mean value is characterized by an SD-value containing 68% of all data. A single series of 50 thermodilution measurements did not show a normal distribution (Fig. 3). The SD-value of 55% is much lower than the theoretical value. We conclude that also other series of the total of 55 will not be characterized by a normal distribution.

The total population of single estimates over all 55 series was characterized by a *symmetrical* distribution and an SD value of 68% (Table 2). Testing the number of estimates for  $\pm 2$  SD revealed 96% of all data within these limits.

**TABLE 2.**  
Averaging procedures

	n	Mean	SD	Number of data within $\pm 1$ SD		% of data within	
				n	%	$\pm 5\%$	$\pm 10\%$
<i>Systematic procedure</i>							
Single data	2750	100.0	17.5	1865	68	23	43
2-p-a	1375	100.0	8.6	983	71	47	79
3-p-a	880	99.9	4.2	620	70	79	98
4-p-a	660	100.0	3.3	486	72	89	99
5-p-a	550	100.0	2.6	378	69	93	100
6-p-a	440	99.9	2.4	318	74	95	100
<i>Random procedure</i>							
Single data	2750	100.8	17.0	1876	68	23	43
2-p-a	1375	100.8	11.9	982	71	31	58
3-p-a	880	100.3	10.1	614	70	40	69
4-p-a	660	100.3	8.9	449	68	45	75
5-p-a	550	100.8	8.1	385	70	46	79
6-p-a	440	100.3	7.5	307	70	48	84

2-p-a is two-point-average, 3-p-a is three-point-average, etc. n is the number of measurements. Procedures are explained in text.

Therefore, we considered this total population as a normal distribution of data around the mean. The number of data within SD-values of the populations of averages were all but two close to 68%. The exceptions were the systematic four-point- and six-point-averages with SD values containing 72 and 74% of data within  $\pm 1$  SD respectively. In such populations the SD-value underestimates the concentration of data around the mean. To avoid such underestimation of the reliability of a measurement accuracy limits were used and the percentages estimates within these limits were calculated.

The reliability of a single measurement for estimation of mean cardiac output was low, because 57% of all measurements deviated more than 10% from the mean. Only 68% was within  $\pm 17.5\%$  from the mean implying that in 5% of all measurements a deviation larger than 35% from the mean can be predicted. A random sampling of the single data gave the same results as the original population of estimates. Such a random sampling imitates the random performance of a series of single estimates, independent of the phases of a ventilatory cycle.

An improvement of the accuracy in estimating mean cardiac output was obtained when randomly selected estimates from the series were averaged.

Within the accuracy range of 10% around the mean the percentage of all estimates gradually increased from 43 to 84% going from single estimates to the six-point-averages (Table 2, "random procedures"). But more than 50% of all random six-point-averages were beyond the accuracy limits of 5%.

A much better result was found by the systematic averaging procedure. Two estimates differing half a ventilatory cycle in phase gave averages with an accuracy which was similar to that of the random five-point-averages. However, 21% of the systematic two-point-averages and the random five-point-averages deviate more than 10% from the mean. The largest improvement in the accuracy of mean cardiac output estimation was found in the systematic averaging procedure up to the four-point-averages. Above this number progress in accuracy was much smaller.

The averages of four cardiac output estimates equally spread in the ventilatory cycle will give almost 100% of all measurements within the accuracy limits of 10% and will have a chance of 9 to 1 to be within the 5% limits.

When 10% limits are sufficient a systematic averaging procedure of three single estimations is satisfactory, because that probability is 98%. From Table 2 we concluded that the systematic averaging procedure is far superior to the random averaging procedure. The reliability of the random averages is insufficient even when 6 single estimates are used.

#### 4.4.3 *Clinical application*

The amplitude of an indicator dilution curve depends on the amount of indicator entering the bloodstream within a certain time and the level of blood flow [15]. As an example we have calculated the ratio between the amount of cold ( $^{\circ}\text{C}\cdot\text{ml}$ ) entering the blood stream per second and per kg body weight, and the blood flow in ml per second and per kg body weight (Table 3). For both patients and pigs these calculated ratios approximate the temperature change of blood at the injection site. The values are in the same order of magnitude. Thus, injection of a relatively low amount of indicator will give only an acceptable amplitude of the dilution curve when injection time is short.

The shorter injection time leads to a shorter dilution curve which approximates mean flow over a shorter period. In a flow with cyclic variations a procedure with short injection time will approximate real variation better than a procedure of longer injection time. Studying the differences between single estimates and mean cardiac output during cyclic variation of blood flow, and, searching for reduction of these errors by averaging techniques,



**TABLE 3.**

	$V_i$ ml	$t_i$ s	$T_b - T_i$ °C	W kg	CO ml/s kg <sup>-1</sup>	$q_i$ °C.ml/s kg <sup>-1</sup>	$\Delta T_{injsite}$ °C
Patient	10(5)	3(1.5)	37	70	1.19	1.76	1.5
Pig	0.5	0.3	17	10	2.0	2.83	1.4

$V_i$ : volume of injection fluid;  $t_i$ : duration of injection;  $T_b - T_i$ : difference between blood and injectate temperature; W: body weight;  $q_i$ : indicator flow [ $V_i \cdot (T_b - T_i)/(t_i \cdot \text{weight})$ ];  $\Delta T_{injsite}$ : the change in blood temperature at the injection site; (indicator flow / blood flow)

we used a short injection time to accentuate the errors. Using a longer injection time will certainly reduce but not eliminate the errors. However, the differences in the reduction of errors of both averaging techniques will also count for longer injection times.

Phase controlled injection of indicator needs an equipment, which is not (yet) available for clinical purposes. For those ventilators which deliver a constant number of pulses during each ventilatory cycle, development of a phase selecting system is satisfactory. Such a system can be used in combination with an injector system, which discharges automatically on a signal from the phase selector. As a power supply for the discharge of the syringe airpressure routinely available in the hospital can be used.

We conclude in general that during mechanical ventilation the average of four estimates spread equally over the ventilatory cycle, is preferable to single estimates or to averages of single estimates obtained randomly in the ventilatory cycle. For patients with contra-indications to volume loading a regime of three or two estimates could be adopted, reducing correspondingly the accuracy of the estimation of mean cardiac output.

## References

- [1] Abel F.L., and J. A. Waldhausen. Respiratory and cardiac effects on venous return. *Am. Heart J.* 78: 266, 1969.
- [2] Bassingthwaighte J. B., T. J. Knopp, and D. U. Anderson. Flow estimation by indicator dilution (bolus injection): Reduction of errors due to time-averaged sampling during unsteady flow. *Circ. Res.* 27: 277, 1970.
- [3] Cropp G. J. A. and, A. C. Burton. Theoretical considerations and model experiments on the validity of indicator dilution methods for measurements of variable flow. *Circ. Res.* 18: 26, 1966

- [4] Hoffman J. I. E., A. Guz, A. A. Charlier, and D. E. L. Wilcken. Stroke volume in conscious dogs: effect of respiration, posture and vascular occlusion. *J. Appl. Physiol.* 20: 865, 1965.
- [5] Jansen J. R. C., J. J. Schreuder, J. M. Bogaard, W. van Rooyen, and A. Versprille. Thermodilution technique for measurement of cardiac output during artificial ventilation. *J. Appl. Physiol.* 51: 584, 1981.
- [6] Knopp T. J., and J. B. Bassingthwaighe. Effect of flow on transpulmonary circulatory transport functions. *J. Appl. Physiol.* 27: 36, 1969.
- [7] Morgan B. C., W. E. Martin, T. F. Hornbein, E. W. Crawford, and W. G. Guntheroth. Hemodynamic effects of intermittent positive pressure respiration. *Anesthesiology* 27: 584, 1966.
- [8] Nordstrom L. Haemodynamic effects of intermittent positive pressure respiration. *Acta Anaesth. Scand. Suppl.* 47 1972.
- [9] Rosen A. L., S. A. Gould, L. R. Seghal, H. L. Seghal, and G. S. Moss. Errors in calculating cardiac output due to administration of perfluorochemicals. *J. Appl. Physiol.* 54: 318, 1983.
- [10] Schreuder J. J., J. R. C. Jansen, and A. Versprille. Hemodynamic effects of PEEP applied as a ramp in normo-, hyper- and hypovolemia. *J. Appl. Physiol.* 59: 1178, 1985.
- [11] Snyder J. V., and D. J. Powner. Effects of mechanical ventilation on the measurement of cardiac output by thermodilution. *Crit. Care Med.* 10: 677, 1982.
- [12] Vermeire P., and J. Butler. Effect of respiration on pulmonary capillary blood flow in man. *Circ. Res.* 22: 299, 1968.
- [13] Versprille A., J. R. C. Jansen, and J. J. Schreuder. Dynamic aspects of the interactions between airway pressure and the circulation. In: Prakash O, (ed). *Applied Physiology in Clinical Respiratory Care*. Martinus Nijhoff, The Hague, p. 447, 1982.
- [14] Wessel H. U., G. W. James, and M. H. Paul. Effects of respiration and circulation on blood temperature of the anesthetized dog. *Am. J. Physiol.* 211: 1403, 1966.
- [15] Zierler K. L. Circulation times and the theory of indicator dilution methods for determining blood flow and volume. In: Zierler KL, (ed). *Handbook of Physiology, Circulation*. Am. Physiol. Soc., Washington, DC, sect. 1, vol.I, Chapt. 18; p. 585, 1962.

## CHAPTER 5

# EXTRAPOLATION OF THERMODILUTION CURVES OBTAINED DURING A PAUSE IN ARTIFICIAL VENTILATION

JOS R.C. JANSEN, JAN M. BOGAARD AND ADRIAN VERSPRILLE  
(with the technical assistance of Arnold Drop)

Pathophysiological Laboratory, Department of Pulmonary Diseases,  
Erasmus University, P.O. Box 1738, 3000 DR Rotterdam, The Netherlands  
Published in J. Appl. Physiol. 63(3):1551-1557, 1987

### 5.1 Introduction

ESTIMATION OF MEAN CARDIAC OUTPUT by the thermodilution method can be applied only under conditions of constant flow, complete mixing, and no loss of indicator, when the Stewart-Hamilton equation is used [1, 20, 21]. Nevertheless, the method has been used extensively in mechanically ventilated patients, where cyclic modulation of pulsatile flow exists. Flow variations at frequencies in the range of heart rate will produce little error [1, 12], but cyclic flow modulations with a periodicity in the range of duration of the thermodilution curve, as caused by conventionally mechanical ventilation, can lead to differences of more than 100% between individual measurements [5, 6]. To avoid such errors, cardiac output estimation by thermodilution has been done during prolonged expiratory pauses [4, 7], which might result in overestimation [15, 16].

During prolonged expiratory pauses as well as during inspiratory hold maneuvers in healthy pigs, constant hemodynamic conditions are present. However, the decay of a dilution curve to the initial base-line value may take more time than the period of the hold procedures, especially at low levels of cardiac output. When an inspiratory hold is suddenly released, right ventricular flow is increased, and consequently the tail of the dilution curve will be deflected downward. When flow decreases during insufflation after a prolonged expiratory hold, the curve will incline to a less steep slope. An undisturbed curve can be found by fitting a model to the undisturbed part of the curve by taking the truncation point just before the flexion point.

The objective of our study was to compare the feasibility of three models, which extrapolate the tail of the curve beyond the truncation point: a local density random walk distribution, a log-normal distribution, and a two-compartmental model. These models stand for a diffusion with drift approach, a mathematical description of the curve, and a compartmental approach, respectively. Thermodilution curves were fitted with these models and the estimates were compared with electromagnetic flow measurements which were simultaneously performed. First, two undisturbed curves with different skewness and duration were collected during constant-flow conditions. On the decay of these curves five truncation points were chosen to test the effect of a decreasing number of data samples available for the model fits on the accuracy of the estimates. Second, inspiratory hold procedures were applied for 10 s at different inspiratory volumes to create different flow values [16] leading to dilution curves of different duration. As a result the position of the truncation point shifted upward and downward on the decay of the curve when flow decreased and increased, respectively.

Furthermore, the estimates by thermodilution found during prolonged expiratory pauses were compared with mean cardiac output in order to evaluate the amount of overestimation.

## 5.2 Methods

### 5.2.1 Surgical procedure

Figs (7- 11 kg body wt) were anaesthetized with pentobarbital sodium. The initial dose ( $30 \text{ mg}\cdot\text{kg}^{-1}$  i.p.) was followed by a continuous infusion of  $7.5 \text{ ml}\cdot\text{kg}^{-1}\cdot\text{h}^{-1}$ . After muscle relaxation with tubocurarine (initial dose  $0.1 \text{ mg}\cdot\text{kg}^{-1}$  followed by a continuous infusion of  $0.2 \text{ mg}\cdot\text{kg}^{-1}\cdot\text{h}^{-1}$ ) mechanical ventilation was started. Ventilation was set on  $10 \text{ breaths min}^{-1}$  and tidal volume was adjusted to an end-tidal  $\text{CO}_2$  of 38-42 Torr. A positive end-expiratory pressure of 2-3  $\text{cmH}_2\text{O}$  was given to avoid atelectasis. Body temperature was maintained at  $\sim 38^\circ\text{C}$  by placing the animals on a thermocontrolled operating table. Every hour thrombolytine ( $125 \text{ I.U. kg}^{-1}$  Organon, Oss, The Netherlands) was given.

A polythene catheter was inserted into the aortic arch via the right common carotid artery, a Swan-Ganz 5-F catheter with thermistor was placed into the pulmonary artery, a double-walled injection catheter into the right atrium, and a four-lumen catheter near the entrance of the right atrium for measurement of central venous pressure and for infusions. All these catheters were inserted via the right external jugular vein, which was ligated on the

catheters at two places. To avoid bleeding, vaseline was injected into the small compartment in between both ligatures, before the distal ligature was fixed. A left-sided thoracotomy was performed between the second and third rib to place an electromagnetic (EM) flow probe intrapericardially around the pulmonary artery. Subsequently, the pericardium was sutured and the thorax was closed airtight. Thereafter pneumothorax was eliminated by suction at a pressure of -15 cmH<sub>2</sub>O and by application of a PEEP of 10 cmH<sub>2</sub>O for 1-1.5 min.

### 5.2.2 Measurements and estimation of cardiac output

Electrocardiogram, aortic pressure, pulmonary arterial pressure, central venous pressure, tracheal pressure, and ventilatory flow were monitored on a chart recorder (HP 7758A) to check stability of the animal preparation during the observations.

During the observation periods electromagnetically measured flow curves ( $\dot{Q}_{EM}$ ) were sampled at 250 Hz by a PDP 11/23 computer. The areas under the curves were digitally integrated. Zero level for integration was indicated on the curves at a graphics terminal by cross-hair control. The maximal total area during a ventilatory cycle was found from the beats of all complete heart cycles within that ventilatory cycle. This sum was divided by total interval time for these beats and calibrated against the mean cardiac output as measured by the Fick method [5], resulting in the number of area units per milliliter. Dividing the area of a beat by this calibration factor gives stroke volume. Mean flow during a cardiac cycle was found when stroke volume was divided by the heart interval.

Thermodilution curves were obtained by injection of 2 ml saline of room temperature (20.5-22.5°C) into the right atrium. The temperature-time curves were measured in the pulmonary artery, sampled (50 Hz), and digitally integrated, accounting for base-line drift and heat capacity of the injection catheter, as described elsewhere [5, 6]. To obtain maximum accuracy in the estimation of cardiac output, an automatic injection system was used. This system delivers a highly reproducible injected amount of indicator [5].

Cardiac output was calculated according to the modified Stewart-Hamilton formula

$$\dot{Q}_{rv} = \frac{S_i \rho_i (V_i - V_D)(T_{b_1} - T_i)}{S_b \rho_b \int_{t_1}^{t_2} (T_b - T_{b_1}) dt} \quad (1)$$

The areas under the curves  $\int_{t_1}^{t_2} (T_b - T_{b_1}) dt$  were derived from the fitted curves of the three different models, and in case of undisturbed curves directly

from computer sampling where  $\dot{Q}_{rv}$  = cardiac output ( $ml/s$ );  $V_i$  = injected volume ( $ml$ ) of indicator;  $V_D$  = volume ( $ml$ ) of the intracorporeal part of the injection catheter;  $T_i$  = temperature ( $^{\circ}C$ ) of injectate;  $T_b$  = temperature ( $^{\circ}C$ ) of the blood at the detection site;  $T_{b_1}$  = temperature ( $^{\circ}C$ ) of the blood at the moment of injection;  $S_i$  and  $S_b$  = specific heat ( $cal.g^{-1}.^{\circ}C^{-1}$ ) of injectate (0.997) and blood (0.870), respectively;  $\rho_i$  and  $\rho_b$  = specific gravity ( $g/ml$ ) of injectate (1.005) and blood (1.045), respectively;  $t_1$  = injection time (s);  $t_1 - t_2$  = integration interval.

### 5.2.3 Model fitting

The tail of the dilution curve was determined using three different mathematical models.

*A Local Density Random Walk (LDRW) model.* A local density random walk (LDRW) model, which is essentially equal to a diffusion with drift model, is mathematically described by a nonnormalized probability distribution function of indicator transit times [2, 3, 10, 11, 19, 21]. The changes in blood temperature were expressed as follows

$$\Delta T_b(t) = \alpha \frac{\exp(\lambda)}{\mu} \left| \frac{\lambda}{2\pi} \right|^{1/2} \left| \frac{\mu}{t'} \right|^{1/2} \exp \left\{ -1/2 \lambda \left( \frac{t'}{\mu} + \frac{\mu}{t'} \right) \right\} \quad (2)$$

where  $t' = t - t_0$ ,

and  $\Delta T_b$  is the blood temperature related to base-line value before injection of cold fluid;  $\alpha$  is the area under the curve;  $\lambda$  is the skewness parameter, increasing with decreasing asymmetry;  $\mu$  is the median transit time;  $t_0$  is the *time 0* of the distribution, which is a virtual injection moment before the appearance of the curve. Real injection time is no model parameter because of convective transport of indicator, (i.e., delay time).

*Log-normal distribution.* Unlike the previous model, the log-normal distribution does not imply a physical model behind the processes of indicator transport. Instead it is based on a mathematical description of the curve [19].

$$\Delta T_b(t) = \Delta T_{b(max)} \exp \left\{ -\left[ \ln(t - t_0) - \ln t_L \right]^2 / 2\sigma^2 \right\} \quad (3)$$

where  $\Delta T_{b(max)}$  is the maximum amplitude of dilution curve;  $\sigma$  is the standard deviation;  $t_L$  is the transformed time scale; and  $t_0$  is the *time 0* of the distribution, as defined earlier.

*Compartmental distribution.* A compartmental distribution function for two mixing chambers in series is described by the sum of two exponential

washout processes in series [8-10, 12, 14, 21].

$$\Delta T_b(t) = c \left| \exp\left(-\frac{1}{\tau_1} t_n\right) - \exp\left(-\frac{1}{\tau_2} t_n\right) \right| \quad (4)$$

where  $t_n = t - t_a$ ,

and  $t_a$  is the appearance time;  $\tau_i$  is the time constant of a single chamber, volume-flow ratio;  $c$  is  $m/(V_1 + V_2)$  scaling factor, mass over volume ratio; and  $V_1, V_2$  are the volumes of the two mixing chambers.

The fitting procedures were programmed in FORTRAN IV on a PDP 11/23 microcomputer and based on a Gauss-Newton subroutine for nonlinear least squares fitting. The initial values of the parameters were obtained from the dilution curves [10, 19].

#### 5.2.4 *Experimental protocol*

In each of four pigs two series of observations were done: one series before and one after thoracotomy. Each series began and ended with two estimations of mean cardiac output by the Fick method for  $O_2$ , and with four thermodilution measurements at equally spread intervals of the ventilation (0, 25, 50, and 75% of the ventilatory cycle) in order to compare thermodilution with Fick for reasons of accuracy in estimation of mean cardiac output [6]. The four estimates were done with intervals of 1 min.

These estimates were followed by a series of seven thermodilution measurements at different cardiac output levels using inspiratory hold maneuvers at different inspiratory volumes between 0 and 300 ml in steps of 50 ml. The volumes were randomly applied. An inspiratory volume of 0 ml resulted in a prolonged expiratory pause of the preceding ventilatory cycle. The injections during these observations were controlled by computer and were made 1 s after the onset of the inspiratory hold when the blood flow was stabilized from the previous insufflation. The interval between two succeeding observations was 5 min. To correct thermodilution curves for changes in base-line temperature during an inspiratory hold maneuver the series of seven inspiratory hold maneuvers was duplicated without an injection of indicator. After thoracotomy the series was similar to that before. Additionally, flow was measured using a pulmonary artery EM flow probe.

#### 5.2.5 *Data analysis*

To evaluate the various aspects of the three applied models, the data were analyzed as follows. First, the stability of the extrapolation was studied

by varying the truncating point at five locations in two typical complete (undisturbed) curves with different skewness.

From the inspiratory hold procedures in the series after thorax surgery, a direct comparison was made between the cardiac output estimates by the model fits of the thermodilution curves and those from the EM flow measurements. Truncation points were taken at the last QRS complex of the ECG signal before the end of the inspiratory hold. For all thermodilution curves, including those before thoracotomy, the LDRW, log-normal, and two-compartment, estimates were compared with each other and the number of unable fits was noted. The goodness of fit of the models was evaluated by comparing the root-mean-square errors for the different models with respect to each other. These errors were calculated over the time available for the fit procedures.

### 5.3 Results

An example of a dilution curve obtained during an inspiratory hold maneuver (Fig. 1) illustrates the constancy of the pulmonary arterial flow during an inspiratory pause. A main part of the dilution curve coincides with this pause. The sudden release of the inspiratory hold is followed by a sudden increase in flow, causing a deflection of the dilution curve. The breath-hold procedure without injection of cold saline causes an increase in base-line temperature, indicating a slightly increasing contribution of blood from colder regions with respect to blood from warmer parts of the body.

The performance of the three different models in relation to the position of five truncating points on the undisturbed curve (i.e., the available part of the curve used for the calculations) is shown in Fig. 2 and Table 1. These undisturbed curves were recorded for 14 s during two different flow situations in the same animal. *Curve A* is sampled during normal flow condition (14.7 ml/s) and *curve B* during low flow condition (9.2 ml/s). Note the difference in appearance time and skewness between both curves.

For the curve of Figure 2A an estimation of the area of the curve with an accuracy <6% is possible with all three approaches when data are available until 3.9 sec. after the moment of injection or until the decay of the curve had reached 39% of the peak value. For the more symmetrical curve (Fig. 2B) the fit accuracy of the two-compartment model became more dependent on the site of truncation. Truncation at 9.8 s, i.e., 38% of the top, led to an error that exceeded more than 10% for the estimated area under the curve when the two-compartment model was used. This inaccuracy



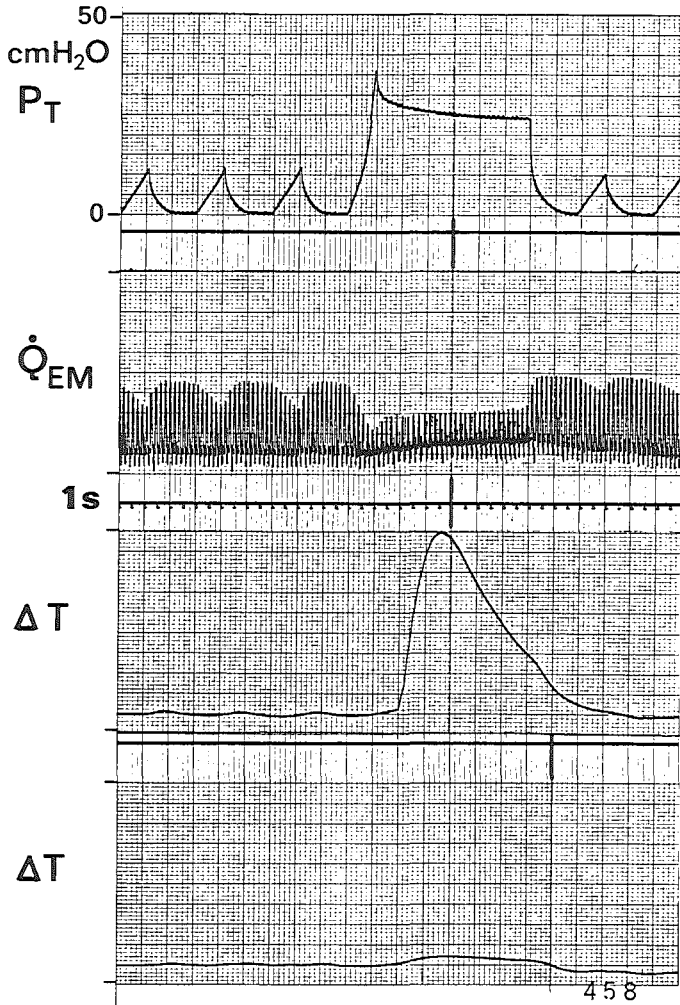


Fig. 1. Typical recording during an inspiratory hold of 12 s.  $P_T$ , tracheal pressure.  $\dot{Q}_{EM}$  electromagnetic measured pulmonary arterial flow (AU). Slight increase in peak value coincides with a parallel increase of 0 line. Beat-to-beat analyses have shown constancy of stroke volume throughout pauses of this duration.  $\Delta T$  3rd, trace, dilution curve. Note the deflection of the tail of the curve; full-scale deflection is  $0.8^\circ\text{C}$ .  $\Delta T$ , bottom trace, base-line temperature curve without injection of indicator, from the same procedure in 2nd series.

**TABLE 1.**

Accuracy of fit procedures with three models depending on the truncation point of the dilution curve

Point	Time	$h_{tp}/$ s	LDRW			Log Normal			Two-compartment		
			A	A/A <sub>1</sub>	rms	A	A/A <sub>1</sub>	rms	A	A/A <sub>1</sub>	rms
Curve from Fig. 2A											
1	9.9	0	2.30	1.00	231	2.33	1.00	45	2.29	1.00	242
2	5.8	11	2.26	0.98	261	2.31	0.99	24	2.27	0.99	438
3	4.8	25	2.22	0.96	185	2.28	0.98	14	2.25	0.98	682
4	3.9	39	2.15	0.94	81	2.22	0.95	5	2.31	1.01	1383
5	2.8	87	2.07	0.90	56	2.17	0.93	1	2.65	1.16	1288
Curve from Fig. 2B											
1	14.0	8	3.84	1.00	240	3.89	1.00	12	4.17	1.00	5007
2	9.8	38	3.93	1.02	22	3.98	1.02	29	4.64	1.11	5229
3	7.8	66	3.84	1.00	13	3.89	1.00	15	5.19	1.25	4557
4	6.8	83	3.75	0.98	10	3.82	0.98	4	6.33	1.52	3713
5	5.8	97	3.54	0.92	6	3.70	0.95	1	10.38	2.49	2345

Time, time after injection of cold, when truncation was chosen, see also Fig. 2, A and B ;  $h_{tp}$  height of curve at the truncation point;  $h_{max}$ , peak value of the curve; A, area under curve predicted by the model; A/A<sub>1</sub>, A<sub>1</sub> related to area of fit for longest time available (fitted area A<sub>1</sub> is equal to area of the unfitted curve Fig. 2A and is almost equal for Fig. 2B); rms, root-mean square error of fit by the model compared with original curve for period of fit (i.e., until the truncation point).

increased progressively when truncation points were taken earlier. However, using the LDRW or the log-normal model, the area was estimated with an error smaller than 2% when 6.8 s (83% of the top) of the curve were available starting at the moment of injection. The difference in the shape of the actual curves and the curves predicted by the models can be observed from Fig. 2. The root-mean-square error of the fit is summarized in Table 1. The root-mean-square error is much larger for the two-compartment model than for both other models.

In Fig. 3 cardiac output data obtained from the inspiratory hold maneuvers and calculated from the three different models are compared with the data obtained from the EM flow measurements. A good correlation without statistical differences ( $p > 0.05$ ) was found for all models. Differences between the feasibility of the models were apparent in the number of failed fittings. With the two-compartment model 12 out of 56 fits failed. These failures were 4 and 2 with the LDRW model and the log-normal model, respectively.

Mutual comparison of the three models (Figs. 4 and 5) showed the same accuracy ( $p < 0.01$ ) in estimation of cardiac output for the LDRW approach and the log-normal distribution. Although the residual error (root-mean square error) of the fit for the LDRW was slightly higher than that for the log-normal model, significant differences were not found ( $p > 0.05$ ). The cardiac output estimates with the two-compartment model were not statistically different ( $p > 0.05$ ) from the LDRW or the log-normal distribution, but the differences in root-mean-square error were highly significant ( $p > 0.01$ ).

The effect of a breath-hold procedure on the temperature of blood in the pulmonary artery (i.e., the baseline of the dilution curve) is illustrated in Fig. 1. The actual curve for a given procedure was found by subtracting the temperature curve without injection of cold from the dilution curve. The errors on estimation of cardiac output by omitting this subtraction are given in Fig. 6. For the applied procedures the error was maximally ~10%. The error decreased with an increase of cardiac output.

Cardiac output estimates during a prolonged expiratory pause are given in Table 2 and are compared with mean cardiac output during normal mechanical ventilation. The estimates during the prolonged expiratory pause were significantly higher than the mean ( $p < 0.01$ ) with an overestimation of 5-50% [on average  $19 \pm 16\%$  (SD)].

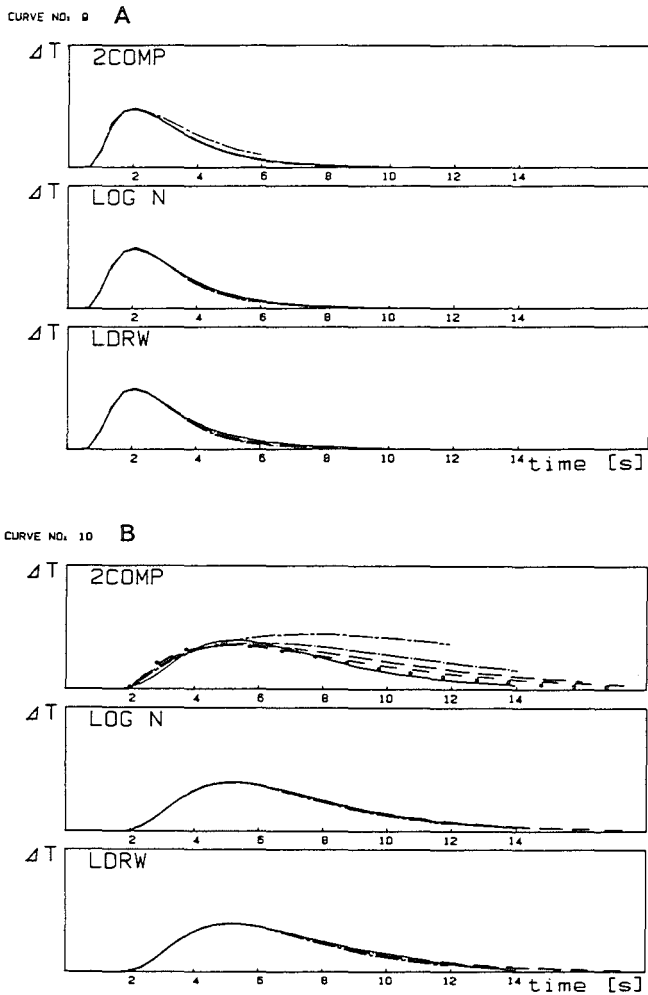


Fig. 2. Fits of 2 curves with the 3 models for different truncating points.  $\Delta T$ , the change in temperature due to injection of cold; full scale deflection is  $0.8^{\circ}\text{C}$ . Time scale is started at the moment of injection. Fitted lines with corresponding truncation point are A: 9.9, 5.8, 4.8, 3.9, and 2.8 s, corresponding to B: 14.0, 9.8, 7.8, 6.8, and 5.8 s.

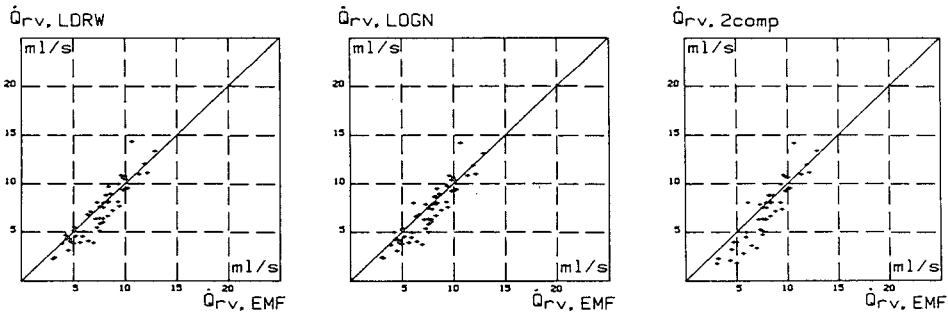


Fig. 3. Comparison between electromagnetically measured mean flow and flow estimates based on local random walk (LDRW) model, log-normal distribution (LOGN) and two-compartment model (2comp).

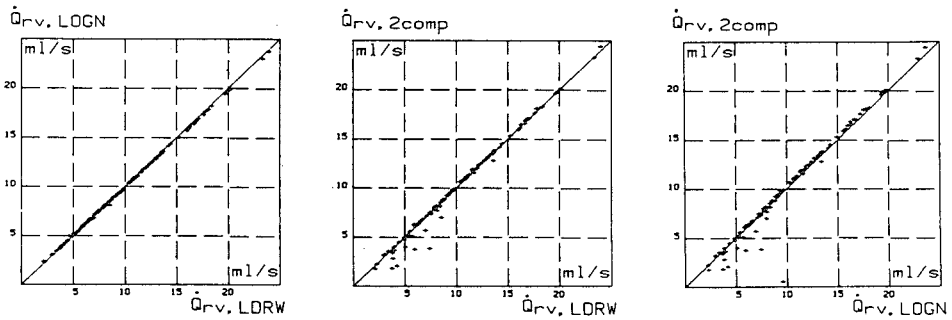


Fig. 4. Comparison of cardiac output estimates ( $\dot{Q}_{rv}$ ) based on fits of models in relation to each other. Abbreviations as in Fig. 3.

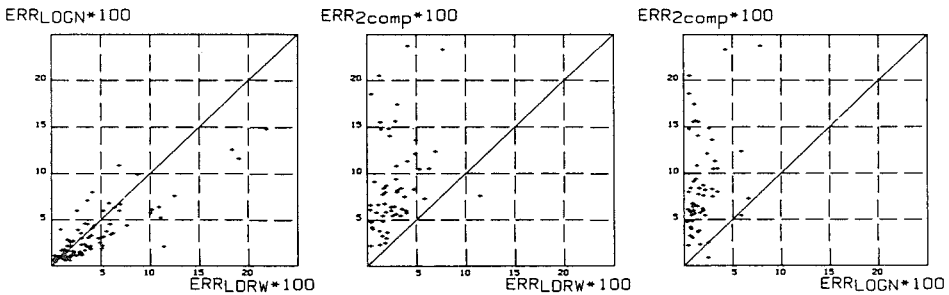


Fig. 5. Comparison of root-mean-square errors (ERR) for 3 different models in relation to each other. Root-mean-square errors were measured over duration of fits.

**TABLE 2.**

Flow estimation during expiratory pauses compared with mean flow

A: $\dot{Q}_{TH,ee}$ ml/s	19.58	10.57	17.97	12.85	22.70	13.90	17.05	10.12
B: $\dot{Q}_{TH,Ap}$ ml/s	17.76	7.76	16.86	12.24	19.73	9.24	15.11	9.25
A/B	1.10	1.36	1.10	1.05	1.15	1.50	1.13	1.09

$\dot{Q}_{TH,ee}$ , flow estimates during 8 series of prolonged expiratory pauses in 4 pigs, estimated with the log-normal model.  $\dot{Q}_{TH,Ap}$ , mean of 4 estimates equally spread over the ventilatory cycle [5,6].

## 5.4 Discussion

Estimation of the area under indicator-dilution curves, which are either truncated or disturbed by recirculation, is usually accomplished by log-linear extrapolation of the upper part of the descending limb [3, 21]. However, we did not focus on that approach, because often too small a part of the descending tail is available for extrapolation, causing a systematic overestimation of the area under the curve. Moreover, random noise on the curve also causes a positive bias of the estimated area [3]. In these cases it is recommended to use all the information of the nondisturbed part of the curve, thus including the ascending limb, as is done by application of a model describing the whole curve.

We first studied the consequences of the site of truncation on the descending limb for the accuracy of such fits. From the results given in Fig. 2 and Table 1 we concluded that the log-normal and LDRW fits were more accurate for early truncation on the descending limb than the two-compartment model. Especially more symmetrical curves were fitted less accurately with the two-compartmental model. An explanation could be that the process is better described with at least some dispersion of indicator. This feature is not incorporated in the compartmental model. The two-compartment model predicts a sharp upward deflection after the first appearance of indicator. To compensate for this mismatch this model needs more information from the descending limb of the curve than the other models in order to reach the same level of accuracy in estimating the area under the curve.

The estimates of mean flow over the period of the breath-hold by the three models tested against an EM flow probe showed that the accuracies of the three models were comparable for the high-flow range. In the low-flow range, underestimation of flow occurred, especially with the two-

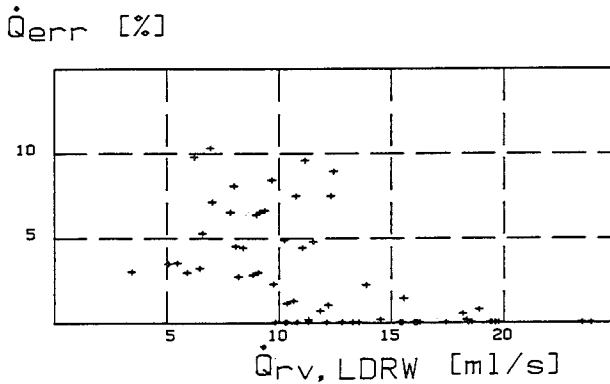


Fig. 6. Underestimation of cardiac output in percent ( $\dot{Q}_{err}$ ), when base-line drift is neglected in relation to cardiac output corrected for base-line drift and estimated with the local random walk (LDRW) model ( $\dot{Q}_{rv, LDRW}$ ).

compartment approach. This underestimation cannot be explained by loss of cold over the wall of the right ventricle and pulmonary artery because a loss of cold would lead to a small area of the curve, resulting in an overestimation of flow. Moreover, Wessel et al. [18] and Vliers et al. [17] showed experimentally that the loss of indicator between right atrial injection and pulmonary sampling appeared to be negligible, when an injectate at room temperature is used. The goodness of fit is similar for the log-normal and LDRW models but less accurate in the two-compartment approach, especially in the low-flow range. Presumably, the underestimation with the two-compartment model will be due to either a relatively early truncation in the curve, or to the fact that low flow gives a more symmetrical curve of longer duration certainly below 9.2 ml/s (Fig. 2B), or to a combination of both reasons.

Von Reth and Bogaard [10] stated from a theoretical study that the two-compartment model and the LDRW model are comparable to estimate cardiac output over a certain range of skewness (parameter  $\lambda$  in our calculations). For their studies they used the LDRW model to generate curves without noise, which were then fitted afterward by the two-compartment model. An explanation for the difference with our results could be influenced by the effect of noise on estimation of both the skewness ( $\lambda$ ) of the LDRW model and the parameters of the compartmental model.

Because the misfits of the log-normal distribution (2/112) and those of

the LDRW model (4/112) are about the same, we concluded that LDRW and log-normal approach are equally applicable. The log-normal one is a purely mathematical description without any physiological background. The LDRW approach is based on the lumping of compartmental aspects (mixing in the heart chambers), turbulence and Taylor dispersion into one effective diffusion coefficient, or dispersion coefficient [19, 21]. Certainly this approach, as with all distributions used until now, does not give a complete description of indicator transport. However, the parameters of the model can be linked to physiological mechanisms. Wise [19] suggested a general name for distributions such as the log-normal and LDRW distribution, namely "skew normal distributions," based on the comparable fitting properties of both for normally obtained curves with noise. This was confirmed by our study, which showed the superiority of the log-normal and LDRW to the compartmental model. The only difference was that the log-normal distribution could be fitted  $\sim 1.5$  times faster than the LDRW model. In situations where a link to the physiology is necessary the LDRW model will be preferred, and in situations where fitting time is important, the log-normal distribution could best be used.

For estimation of actual flow during inspiratory and expiratory pauses in mechanical ventilation, we recommend dilution curve analysis based on either the LDRW model or the log-normal distribution. Such cardiac output estimates might be useful for testing circulation under different circumstances, but do not necessarily reflect mean cardiac output. So the thermodilution estimates during an end-expiratory pause were found to be significantly higher than mean cardiac output calculated from the average of four estimates equally spread over the ventilatory cycle. This confirmed our previously published results based on EM recordings [15, 16] and is also illustrated by the EM recording of Fig. 1, where the mean over the ventilatory cycle will be found to be lower than the value during the end-expiratory phase because of the deficit during insufflation.

## References

- [1] Bassingthwaighe, J.B., T.J. Knopp, D.U. Anderson. Flow estimation by indicator dilution (Bolus Injection). Reduction of errors due to time-averaged sampling during unsteady flow. *Circ. Res.* 27: 277-291, 1970.
- [2] Bogaard, J. M., S. J. Smith, A. Versprille, M. E. Wise, and F. Hagemeyer. Physiological interpretation of the skewness of indicator-dilution curves; theoretical considerations and a practical application. *Basic Res. Cardiol.* 79: 479-493, 1984.



- [3] Bogaard, J. M., W. A. van Duyl, A. Versprille, and M. E. Wise. Influence of random noise on the accuracy of the indicator dilution method. *Clin. Phys. Physiol. Meas.* 6: 59-64, 1985.
- [4] Hasan, F. M., A. Malanga, W. M. Corrao, and S. S. Braman. Effect of catheter position on thermodilution cardiac output during continuous positive-pressure ventilation. *Crit. Care. Med.* 12: 387-390, 1984
- [5] Jansen, J. R. C., J. J. Schreuder, J. M. Bogaard, W. van Rooyen, and A. Versprille. The thermodilution technique for the measurement of cardiac output during artificial ventilation. *J. Appl. Physiol.* 51: 584-591, 1981.
- [6] Jansen, J. R. C., and A. Versprille. Improvement of cardiac output estimation by the thermodilution method during mechanical ventilation. *Int. Care. Med.* 12: 71-79, 1986.
- [7] Jardin, F., J. C. Farcot, P. Gueret, J. F. Prost, Y. Ozier, and J. P. Bourdarias. Cyclic changes in arterial pulse during respiratory support. *Circulation* 68: 266-274, 1983.
- [8] Newman, E. V., M. Merrel, A. Genecin, C. Monge, W. R. Milnor, and W. P. McKeefee. The dye dilution method for describing the central circulation; an analyses of factors shaping the time concentration curves. *Circulation* 4: 735-746, 1951.
- [9] Norwich, K. H., and S. Zelin. The dispersion of indicator in the cardiopulmonary system. *Bull. Math. Biophys.* 32: 25-43, 1970.
- [10] Reth, E. A. von, and J. M. Bogaard. Comparison of a two-compartmental model and distributed models for indicator dilution studies. *Med. Biol. Eng. Comput.* 21: 453-459, 1983.
- [11] Sheppard, C. W., and L. J. Savage. The random walk problem in relation to the physiology of the circulatory mixing. *Phys. Rev.* 83: 489-490, 1951.
- [12] Scheuer-Leeser, M., A. Morguet, H. Reul, and W. Irnich. Some aspects to pulsation error in blood-flow calculations by indicator dilution techniques. *Med. Biol. Eng. Comput.* 15: 118-123, 1977.
- [13] Schlossmacher, E. J., H. Weinstein, S. Lochaya, and A. B. Shaffer. Perfect mixers in series model for fitting venoarterial indicator dilution curves. *J. Appl. Physiol.* 22: 327-332, 1967.
- [14] Valentinuzzi, M., M. E. Valentinuzzi, and J. A. Poscy. Fast estimation of the dilution curve by a procedure based on a compartmental hypothesis. *J. Assoc. Adv. Med. Instrum.* 6: 335-343, 1972.
- [15] Versprille, A., and J. R. C. Jansen. Hemodynamic effects of PEEP and superimposed insufflation during CPPV. In: *Proc. Int. Symp. Intens. Care Emergency Med. 3rd Brussels 1983*, p. 184-187.

- [16] Versprille, A., and J. R. C. Jansen. Mean systemic filling pressure as a characteristic pressure for venous return. *Pflügers Arch.* 405: 226-233, 1985.
- [17] Vliers, A. C. A. P., K.R. Visser, and W .G. Zijlstra. Analysis of indicator distribution in the determination of cardiac output by thermal dilution. *Cardiovasc. Res.* 7: 125-132, 1973.
- [18] Wessel, H. U., M. H. Paul, G. W. James, and A. R. Grahn. Limitations of thermal dilution curves for cardiac output determinations. *J. Appl. Physiol.* 30: 643-652, 1971.
- [19] Wise, M. E. Tracer-dilution curves in cardiology and random walk and log-normal distributions. *Acta Physiol. Pharmacol. Neerl.* 14: 175-204, 1966.
- [20] Zierler, K. L. Theoretical basis of indicator dilution methods for measuring flow and volume. *Circ Res* 10: 393-407, 1962.
- [21] Zierler K. L. Circulation times and the theory of indicator dilution methods for determining blood flow and volume. In: Zierler KL (ed) *Handbook of physiology, Circulation*. Washington DC: Am. Physiol. Soc., sect. 1, vol. I, chapt. 18, p. 585, 1962.

## CHAPTER 6

# DISCREPANCIES BETWEEN MODELS AS A BASIS FOR CARDIAC OUTPUT ESTIMATION AND MEDICAL PRACTICE

J.R.C. JANSEN, J.M. BOGAARD AND A. VERSPRILLE

Pathophysiological Laboratory, Department of Pulmonary diseases,  
Erasmus University, P.O. Box 1738, 3000 DR Rotterdam, The Netherlands  
Published in *Modelling and Data Analysis in Biotechnology and Medical  
Engineering*. G. C. Vansteenkiste and P. C. Young (eds.), North-Holland  
Publishing Company, IFIP, 1983.

### 6.1 Introduction

THE APPLICATION OF THE INDICATOR-DILUTION TECHNIQUE to study the blood flow has been discussed in detail by Zierler [10]. The two main restrictions are that the flow through the system is constant and that complete mixing of indicator and blood occurs. If these conditions are fulfilled a variety of models (compartmental, distributed, or only mathematical descriptions) can be used as a fit to the undisturbed part of primary curves.

In clinical practice cardiac output is commonly estimated by injection of a bolus (delta function) of cold into the right atrium and by measuring the temperature-time curve in the pulmonary trunk. Then, a third restriction is introduced, i.e. the conservation of indicator injected. The loss of indicator is mainly estimated from the down slope extrapolation of the temperature-time curve, although a more accurate approach is given by integration of the curve for a predefined time [2]. Under circumstances of artificial ventilation the cardiac pulsations in flow are modulated [2, 3]. The amount of modulation appeared to be dependent on the level of the mean flow. In former investigations we have shown that the modulation of blood causes considerable errors in the estimation of mean flow by means of the thermodilution method. Differences of more than 100% between two observations were present in a hemodynamic stable situation [2]. The thermodilution estimates showed a shift in modulation with respect to the ventilatory cycle,

when the mean flow was changed. Due to this phase shift there is not one defined moment in the ventilatory cycle for estimation of cardiac output values with a systematic and constant difference from the mean.

The shape of the thermodilution curve is dependent on the modulation of flow; no reliable model fitting is possible under these circumstances.

The purpose of our study was firstly to analyse the errors due to modulation, and secondly, to test different analysis techniques for the estimation of mean cardiac output from a single dilution curve, when flow is modulated.

## 6.2 Methods

### 6.2.1 *Animal experiments*

The experiments were performed in anesthetized (pentobarbital sodium) pigs. <sup>1</sup> *After muscle relaxation (tubocurarine) mechanical ventilation was started using a computer controlled ventilator. The ventilation was set on 10 breath min<sup>-1</sup>, the pattern was a constant inspiratory flow (I) followed by a spontaneous expiration (E) after an inspiratory pause (IP) with a ratio I:IP:E of 25:5:70. Saline (0.5 ml) was injected into the right atrium with a detection of the temperature-time curve in the pulmonary trunk. 50 measurements, equally spread over the ventilatory cycle, were made in a random order. Comparisons were made with Fick's method for oxygen and in 2 experiments also with the cardiac output measured with an electromagnetic flow probe around the pulmonary artery.*

### 6.2.2 *Analysis of the thermodilution curves*

If the temperature-time function is denoted by  $\Delta T_b(t)$  then, according to the general theory as presented by Zierler [10] and furthermore considering  $\Delta T_b(t)$  to be proportional to the frequency distribution of transit times for volume elements of the solute, the "cold" balance for a bolus injection can be written as

$$V_i \rho_i S_i (T_b - T_i) = \int_{t_1}^{t_2} \Delta T_b(t) \dot{Q}(t) \rho_b S_b dt \quad (1)$$

where  $\dot{Q}(t)$  is the blood flow,  $V_i$  the effective injected volume of indicator,  $T_i$  is temperature of the indicator,  $\rho$  the density and  $S$  specific heat of the indicator ( $i$ ) and blood ( $b$ ) respectively.

---

<sup>1</sup>The part in italics is an extension of the original publication.

Assuming  $\dot{Q}$  is constant, the equation can be written in a generally accepted form.

$$\dot{Q} = \frac{V_i \rho_i S_i (T_b - T_i)}{\rho_b S_b \int_{t_1}^{t_2} \Delta T_b(t) dt} \quad (2)$$

The correction of the  $\Delta T_b$  values for heat loss from the injection catheter after injection based on an analysis of the thermal time constant of the double walled injection catheter [2].

### 6.2.3 Flow averaging of concentration and of time

When the flow is not constant, as shown in Fig. 3, the equation [1] might be rewritten as:

$$\rho_i S_i V_i (T_b - T_i) = \rho_b S_b \bar{Q} \int_{t_1}^{t_2} \Delta T_b(t) \cdot \frac{\dot{Q}(t)}{\bar{Q}} dt \quad (3)$$

$$\bar{Q} = \frac{\rho_i S_i V_i (T_b - T_i)}{\rho_b S_b \int_{t_1}^{t_2} \Delta T_b(t) \cdot \frac{\dot{Q}(t)}{\bar{Q}} dt} \quad (4)$$

Two approaches for solving equation [4] are schematically presented in Fig. 1:

The area found under the thermodilution curve after flow averaging is equal for both techniques. However, flow averaging of time gives the possibility of fitting the curves with distributions, describing the indicator transport as a function of real time.

For the flow averaging technique any variable which is proportional to or has a known functional relationship with  $\dot{Q}$  can be used. Another variable is necessary because in the intact individual no direct flow measurements are possible.

### 6.2.4 Pulse contour method

A proportional value for stroke volume ( $Q_{pc}$ ) (denoted as "stroke volume") was measured from the pulse contour of the pulmonary artery pressure. For the calculation of the quotient  $\dot{Q}(t) / \bar{Q}$  it is not necessary to estimate the real values of the stroke volumes. The derivation is given in Fig. 2.

For a more detailed description of the method we refer to Wesseling et al. [8]. The "stroke volumes" derived from the pulse contour method were compared with the result of simultaneously calculated "stroke volume" from the flow measured with an electromagnetic flow probe ( $Q_{EM}$ ). From

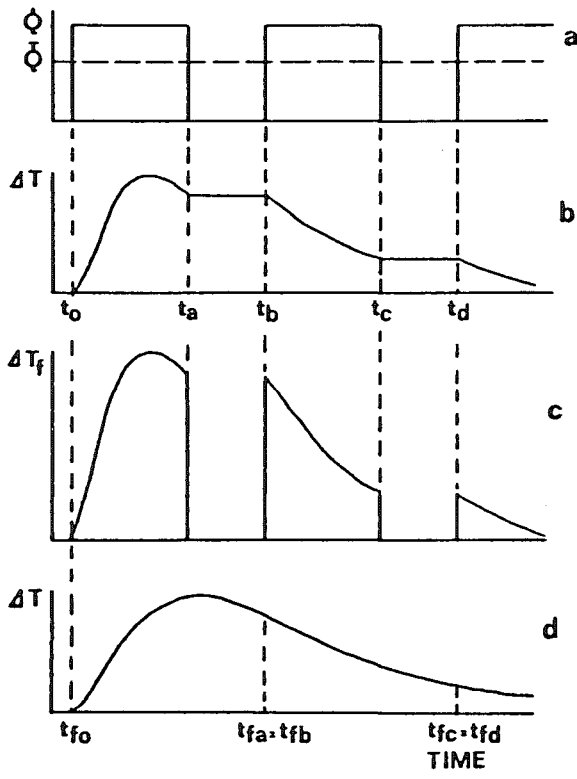
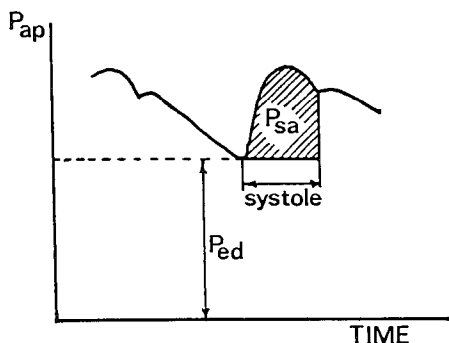


Fig. 1. Schematic diagram of flow averaging of concentration and of time. (a)  $\dot{Q}$  actual volume flow and  $\bar{Q}$  mean flow - - - - , (b)  $\Delta T$  temperature change of the blood after injection of a bolus of cold, (c)  $\Delta T_f = \Delta T_b(t) \cdot \frac{\dot{Q}(t)}{\bar{Q}}$  the value of blood temperature change after flow averaging, (d)  $\Delta T$  the real value of blood temperature, however as a function of time, which is transformed according to  $t_{fn} = t_{fn-1} + \frac{\dot{Q}(t)}{\bar{Q}} \cdot (t_n - t_{n-1})$ .



$$Q_{pc} = kP_{sa}$$

$$P_{sa} = \int_{ej} [P_{ap}(t) - P_{ed}] dt$$

Fig. 2. Determination of the individual beat to beat "stroke volume" ( $Q_{pc}$ ) from the pulmonary artery pressure.  $P_{sa}$  = area of the pressure curve during the right ventricular ejection phase ( $ej$ ) above the end-diastolic pressure level ( $P_{ed}$ ).  $k$  is a proportionally factor.

these results it was decided if the pulse contour method was applicable for calculating the relative changes of flow during the ventilatory cycle.

### 6.2.5 Model fitting

To determine the area under the primary curve we applied different approaches as suggested in the literature, before and after flow averaging of time or concentration.

1. The *log-normal distribution*. does not imply a physical model behind the processes of indicator transport. Instead it is based on a mathematical description of the curve [10].

$$\Delta T_b(t) = \Delta T_{b(max)} \exp -\{[\ln(t - t_0) - \ln t_L]^2 / 2\sigma^2\} \quad (5)$$

where  $\Delta T_{b(max)}$  is the maximum amplitude of dilution curve;  $\sigma$  is the standard deviation;  $t_L$  is the transformed time scale; and  $t_0$  is the *time 0* of the distribution, which is a virtual injection moment before the appearance of the curve.

2. A *compartmental distribution* for  $n$  mixing chambers in series. A compartmental distribution function for two mixing chambers in

series is described by the sum of two exponential washout processes in series [4, 5].

$$\Delta T_b(t) = c \left| \exp\left(-\frac{1}{\tau_1} t_n\right) - \exp\left(-\frac{1}{\tau_2} t_n\right) \right| \quad (6)$$

where  $t_n = t - t_a$ ,

and  $t_a$  is the appearance time;  $\tau_i$  is the time constant of a single chamber, volume-flow ratio;  $c$  is  $m/(V_1 + V_2)$  scaling factor, mass over volume ratio; and  $V_1, V_2$  are the volumes of the two mixing chambers.

3. A distribution function, local density random walk (LDRW) distribution [1].

$$\Delta T_b(t) = \alpha \frac{\exp(\lambda)}{\mu} \left| \frac{\lambda}{2\pi} \right|^{1/2} \left| \frac{\mu}{t'} \right|^{1/2} \exp\left| -1/2\lambda \left( \frac{t'}{\mu} + \frac{\mu}{t'} \right) \right| \quad (7)$$

where  $t' = t - t_0$ ,

and  $\Delta T_b$  is the blood temperature related to base-line value before injection of cold fluid;  $\alpha$  is the area under the curve;  $\lambda$  is the skewness parameter, increasing with decreasing asymmetry;  $\mu$  is the median transit time;  $t_0$  is the *time 0* of the distribution, which is a virtual injection moment before the appearance of the curve. Real injection time is no model parameter because of convective transport of indicator, (i.e., delay time).

4. *Integration of the total area*, after correction for the injection error

The estimates from 1, 2 and 3 are compared with those from 4.

### 6.3 Results

The cardiac output values, estimated with the thermodilution technique during artificial ventilation differ when injections are made at different moments in the ventilatory cycle. As measured with an electromagnetic flow probe (Fig. 3), the stroke volumes of the right ventricle, i.e. area of the  $\dot{Q}_{ap}$  curves ( $Q_{ap}$ ), are modulated by the ventilation. The ventilation is illustrated by the intrapulmonary pressure ( $P_T$ ). Stroke volume is smallest at peak insufflation. When the spontaneous expiration starts the stroke volume is rapidly increasing and is constant during the end-expiratory plateau after an overshoot. The mean value over the ventilatory cycles is constant.



Injection of a bolus of cold at 96%, 74% or 24% of the respiratory cycle time from the start of an inspiration gave an estimate of cardiac output of 17.4 ml/s, 28.2 ml/s respectively. Besides these differences also the shape of the thermodilution curve was changed, with the phase of the ventilatory cycle. During a period of low flow the concentration ( $\Delta T$ ) will be almost constant, whereas during an increasing flow a temperature-time curve will decline more rapidly.

Two temperature-time curves made by injection at 2% and 82% from the start of the ventilatory cycle, and fitted with the 3 models are shown in Figs. 4a en 4b. The recorded curves have apparently bimodal shapes and do not show reliable fits with any of the models. The 2 compartmental model fits worse compared to the LDRW and log normal models in case of a flat upstroke in the beginning of the ascending limb. There is hardly any difference in fit of the temperature-time curve by the log normal and LDRW model.

After flow averaging of the time the shape becomes unimodal and the area more equal for both curves. The fit with the three models is markedly improved, while the difference between the three models is decreased (Figs. 4c and 4d).

Figs. 5a, 5b and 5c shows 50 cardiac output estimates in an individual experiment after injections of cold, equally spread over the respiratory cycle. In Fig. 5a the area is obtained by integration of the total curve, in Fig. 5b by integration of the curve after flow averaging of concentration, and in Fig. 5c by a LDRW fit after flow averaging of the time. The mean value of cardiac output was calculated from all 50 measurements and taken as the 100% value. Each individual measurement was expressed as a percentage of this mean value. The individual estimations of cardiac output were spread between 65 and 125% of the mean dependent on the phase of the cycle. The values show a cyclic modulation related to the ventilatory cycle, with a relatively low random error superimposed on it.

After flow averaging of the concentration (Fig. 5b) there is hardly any modulation left. All estimations are within a range of 10% from the mean (SD  $\pm 5\%$ ). Flow averaging of the time and fitting the curves with a LDRW model shows a slightly larger variation (Fig. 5c).

The results of the calculation of "strokes volume" by the pulse contour method and by integration of the flow measured with an electromagnetic flow probe are compared in Fig. 6. Each point is representative for the individual "stroke volumes", as calculated with both techniques, at the same moment in the ventilatory cycle. The relationship over 6 ventilatory cycles shows a

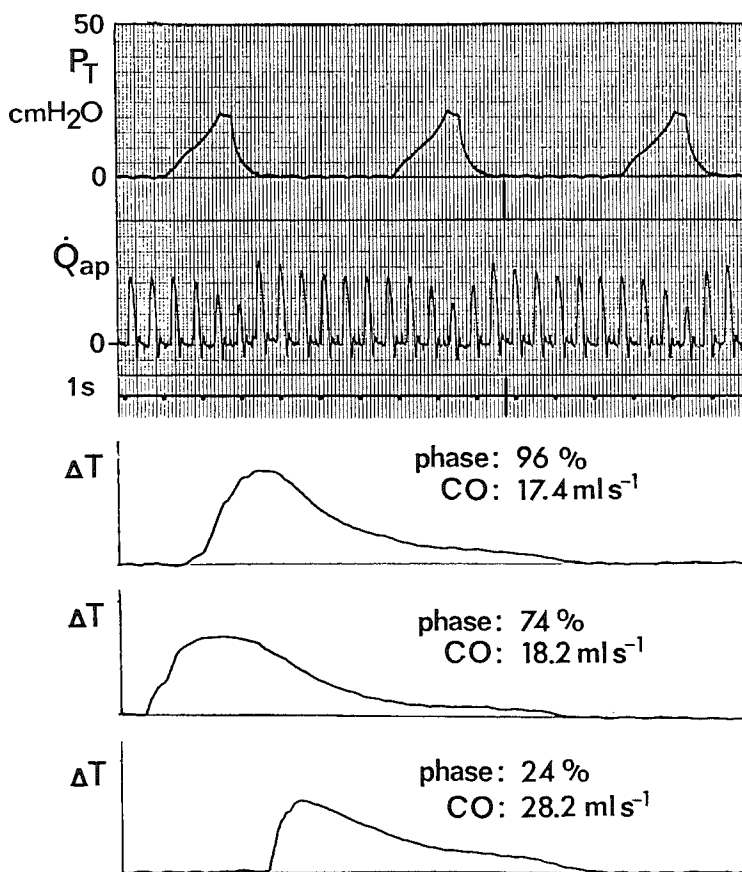


Fig. 3. Fluctuations of blood flow ( $\dot{Q}_{ap}$ ) in relation to the airway pressure ( $P_T$ ) during artificial ventilation and 3 estimates of cardiac output (CO) after injections at different moments in the ventilatory cycle.  $P_T$  is given in  $\text{cmH}_2\text{O}$ ,  $\dot{Q}_{ap}$  in arbitrary units.

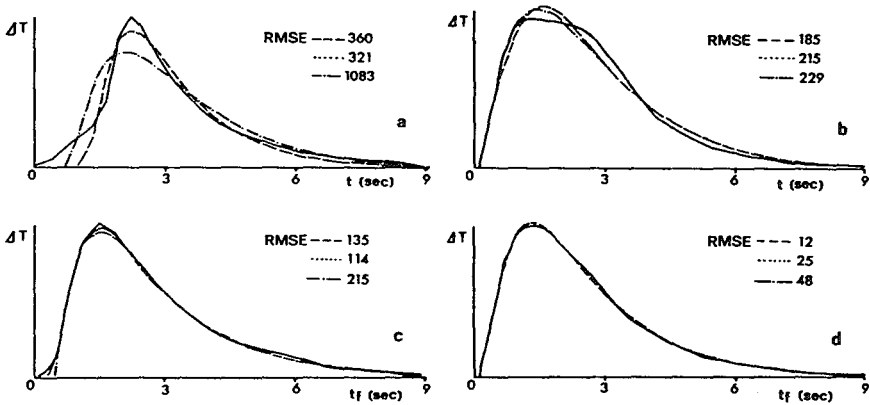


Fig. 4. Temperature-time curves obtained after injections at 2% (a) and 82% (b) of the respiratory cycle and the same curves after flow averaging of the time (c) and (d) respectively. The actual curves — were fitted with a two-compartment model — · — · —, a log-normal distribution · · · · · and a LDRW function — — —. RMSE is root mean square error.

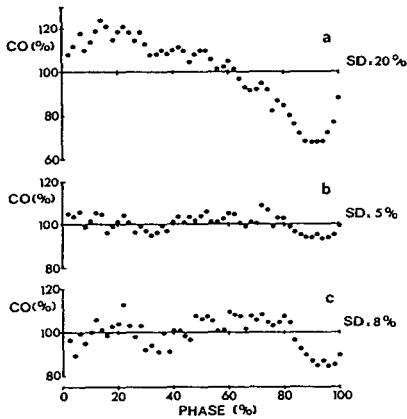


Fig. 5. Cardiac output estimates in a modulated flow.

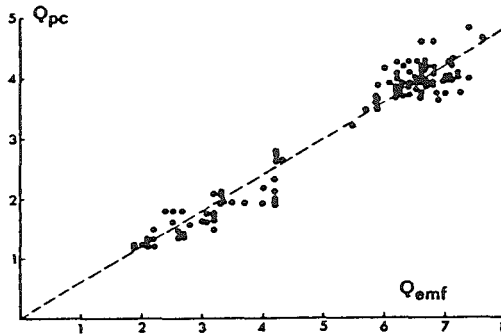


Fig. 6. Correlation of the "stroke volumes" estimated with the pulse contour method ( $Q_{pc}$ ) and by integration of the flow measured with an electromagnetic flow probe ( $Q_{EM}$ ). "Stroke volumes" in arbitrary units.

linear regression having a zero intercept.

Fig. 7 shows the same 50 cardiac output estimates as shown in Fig. 5, using the pulse contour estimates for flow averaging instead of the real flow. The results of the cardiac output estimates by integration of the temperature-time curve are given in Fig. 7a. The modulation in cardiac output estimates is strongly reduced after flow averaging using the pulse contour method. There is almost no difference in estimates after flow averaging of concentration (Fig. 7b) or of time and fitting the transformed curves with a LDRW model (Fig. 7c).

## 6.4 Discussion

### 6.4.1 *Flow averaging of time or concentration with a direct flow measurement*

In a former study [2] we have shown that during artificial ventilation large fluctuations exist in cardiac output estimates by thermodilution if injections of cold are performed at random in the respiratory cycle, however, appeared to be closely correlated with a cardiac output determined by Fick's method.

Because of the different and irregular shapes of the dilution curves, obtained at various moments in the ventilatory cycle, no reliable fit with any of the described models is possible. Certainly the two compartmental model is not able to fit such curves especially when these are more symmetrical [4].

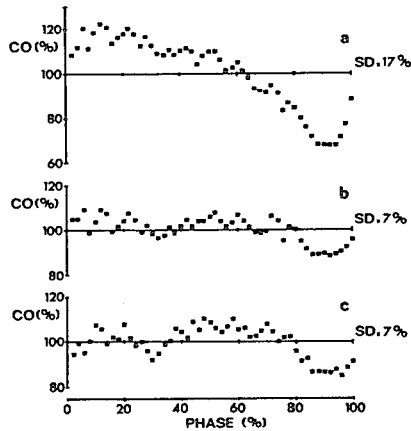


Fig. 7. Cardiac output estimates in a modulated flow (see text).

A fit of the models improved significantly when the curves are transformed by a flow averaging of the time. After this transformation, curves become unimodal again.

After flow averaging of the concentration ( $SD \pm 5\%$ ) the maximal deviation from the mean flow appeared to be only 10% of this mean. If an LDRW fit is applied to the time transformed curves there remains a small modulation of individual cardiac output estimates with respect to the mean. This may be explained by a varying instead of a constant effective longitudinal dispersion which is inherent to the application of distributed models. The variations in  $\dot{Q}$  may cause these variations in this effective longitudinal dispersion, causing the small modulation within a respiratory cycle.

#### 6.4.2 *Flow averaging of time or concentration with the pulse contour method*

In medical practice the thermodilution measurements are performed by application of a Swan-Ganz catheter, which has a lumen near the thermistor for monitoring the pulmonary artery pressure. From this pressure beat to beat "stroke volume" can be estimated by different pulse contour methods. The sources of errors in the various approaches are connected with the deviations from the assumptions which has to be fulfilled. We have used a model that considers the arterial system as a uniform transmission line with

a characteristic impedance ( $Z_0$ ) and terminated by a lumped resistance [8]. In our application one of the main assumptions is the constancy of  $Z_0$  over the ventilatory cycles during the period of the thermodilution measurement, considering that the time-constant of the control of  $Z_0$  by the central nervous system, is much greater than the respiratory cycle time.

From the close correlation between the areas of the pulmonary pressure curves and those of the flow curves, we concluded that the pulse contour estimates are suitable for the flow averaging technique (Fig. 6). The estimates of cardiac output showed a smaller modulation after flow averaging of the concentration by the flow itself (Fig. 5b) than by the pulse contour method (Fig. 7b). From this result we concluded that the error in estimation of the relative stroke volume by the pulse contour method is dependent of the ventilatory phase. The error is probably caused by the thermodilution of the pulmonary artery pressure baseline by the cyclic changing intrathoracic pressure. The application of the pulse contour method gave similar results when comparing flow averaging of concentration (Fig. 7b) with flow averaging of time and use of LDRW model fit (Fig. 7c). There is no difference in modulation after flow averaging of time by the pulse contour method (Fig. 7c) and by the real flow as measured with an electromagnetic flow probe (Fig. 5c). So, the thermodilution technique in combination with the pulse contour method is promising for clinical application.

In conclusion:

1. no reliable fit of the temperature-time curves with the three applied models is possible when flow is modulated;
2. flow averaging of time allows the use of models, based on stationary flow, to describe the thermodilution curves;
3. the estimation of mean flow by the thermodilution technique is markedly improved after flow averaging of concentration or of time, both by use of the real flow or of the pulse contour stroke volumes. A randomly performed thermodilution measurement gives estimates of the mean cardiac output, which are within 10% of the real value.

## References

- [1] Bogaard, J.M. Interpretation of indicator-dilution curves with a random walk model. Diss. abstr. int.; section C 1981, *Thesis* Erasmus University, Rotterdam, The Netherlands, 1980.

- [2] Jansen, J. R. C., J. J. Schreuder, J. M. Bogaard, W. van Rooyen, and A. Versprille. Thermodilution technique for measurement of cardiac output during artificial ventilation. *J. Appl. Physiol.* 51: 584-591, 1981.
- [3] Morgan, B. E., W. E. Martin, T. F. Hornbein, E. W. Crawford, and W. G. Guntheroth. Hemodynamic effects of intermittent positive pressure respiration. *Anesthesiology* 27: 584-590, 1966.
- [4] Reth, E. A. von, and J. M. Bogaard. Comparison between a two compartment model and distributed models for indicator-dilution studies. *Med. Biol. Eng. Comp.* 21: 453-459, 1983.
- [5] Schlossmacher, E. L., H. Weinstein, S. Lochaya, and A. B. Schaffer. Perfect mixers in series model for fitting venoarterial indicator-dilution curves. *J. Appl. Physiol.* 22: 327-332, 1967.
- [6] Vliers, A., K. Visser, and W. Zijlstra. Analysis of indicator distribution in the determination of cardiac output by thermal dilution. *Cardiovasc. Res.* 7: 125-132, 1973.
- [7] Wessel, H. U., M. H. Paul, G. W. James, and A. R. Grahn. Limitations of thermal dilution curves for cardiac output determinations. *J. Appl. Physiol.* 30: 643-652, 1971.
- [8] Wesseling, K. H., R. Purschke, N. Ty. Smith, and W. W. Nichols. Continuous monitoring of cardiac output. *Medicamundi* 21, no. 2, 1976.
- [9] Wise, M. E. The geometry of log normal and related distributions and an application to tracer-dilution curves. *Stat. Neerl.* 20: 119-142, 1966.
- [10] Zierler, K. L. Circulation times and the theory of indicator-dilution methods for determining blood flow and volume. In: Zierler KL (ed) *Handbook of physiology, Circulation*. Washington DC: Am. Physiol. Soc., sect. 1, vol. I, chapt. 18, p. 585-615, 1962.





# CHAPTER 7

## VERIFICATION OF THE EXPERIMENTAL RESULTS BY MODEL SIMULATIONS

### 7.1 Introduction

To have a better understanding of the errors made by the thermodilution technique in nonstationary flow the results of the animal studies, described in the chapters 3, 4, 5 and 6, will be compared to computer simulations based on a mathematical model of a part of the circulation. Such simulations are not required to estimate blood flow if the amount of injectate is well known, blood flow is constant, and the dilution curve is relatively free from noise due to pulsations or recirculation. However, when flow is cyclically modulated, as occurs during artificial ventilation (Ch. 5 and 6, [7]), the theoretical- and experimental analysis becomes more complex, and the aid of mathematical model simulations can be useful.

To study the effects of cyclic modulated flow, Bassingthwaight et al. [1] have proposed a model, based on a compartmental approach [4]. They used a transport compartment with dispersion properties and one ideal mixing chamber in series. Von Reth [5] also used a compartmental model, but he used two equal mixing chambers in series, with the injection of indicator in the first chamber. In both studies bolus injections were used.

For our simulations also a two-compartmental model was chosen, with the injection site in the inlet stream near the entrance of the first chamber but without the restriction of an ideal bolus injection as the input function. With this model simulations were done to study the effects of different conditions on the estimation of mean cardiac output by: changes in frequency and amplitude of the real flow modulation, the injection of indicator at different moment in the cycle i.e. ventilatory cycle, and by prolonging the duration of the injection of indicator.

### 7.2 Methods

The two-compartmental model is presented by the schematic drawing of figure 1. The tracer (cold saline in our experiments) is injected by a time related process ( $\dot{m}_i(t)$ ) into a bias flow  $\dot{Q}(t)$ . The indicator and blood will

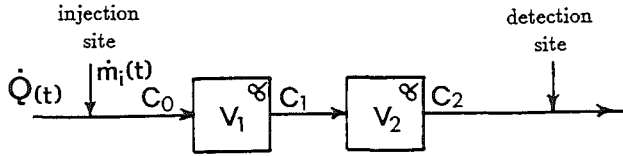


Fig. 1. Schematic diagram of a two-compartmental model. For abbreviations see text.

flows into a series of two ideal mixing chambers. The differential equations for the changes of indicator concentration with time are given by:

$$\frac{dC_1(t)}{dt} = \frac{\dot{Q}(t)}{V_1} [C_0 - C_1] \quad (1)$$

$$\frac{dC_2(t)}{dt} = \frac{\dot{Q}(t)}{V_2} [C_1 - C_2] \quad (2)$$

The concentration of the injectate at the inlet stream of the first mixing chamber is

$$C_0(t) = \frac{\dot{m}_i(t)}{\dot{Q}(t)} \quad \text{for } t_1 < t \leq t_1 + t_i \quad (3)$$

$$C_0(t) = 0 \quad \text{for } t < t_1 \text{ and } t > t_1 + t_i \quad (4)$$

The total amount of indicator injected is

$$m_i = \int_{t_1}^{t_1+t_i} \dot{m}_i(t) dt \quad (5)$$

where  $C_0(t)$  = concentration of indicator at the entrance of the first chamber [mass units/ml];  $C_1(t), C_2(t)$  = concentration of indicator in first and second mixing chamber, respectively [mass units/ml];  $V_1, V_2$  = volume of the first and second mixing chamber, respectively [ml];  $\dot{Q}(t)$  = volume flow of the medium [ml/s];  $\dot{m}_i(t)$  = injection rate of indicator [mass units/s];  $t$  = time since the start of the simulation [s];  $t_1$  = start of injection after the begin of the simulation [s];  $t_i$  = duration of the injection [s];  $\frac{V_1}{\dot{Q}_1}, \frac{V_2}{\dot{Q}_2}$  = time constant  $\tau_1$  and  $\tau_2$  of the first and second mixing chamber, respectively [s].

An instantaneous axial mixing is assumed at a cross section of the vessel at the injection site. As well as a flow/volume labeling of indicator [8]. The concentration of this distribution of indicator at the inlet is proportional to flow (flow proportional labeling [2, 3]) for a constant injection rate.

### 7.2.1 Constant blood flow and ideal bolus injections

For the specific situation of a constant blood flow and a bolus injection with a very short injection time ( related to a unit impulse or Dirac function  $\delta$  with area  $m_i$  and the moment of injection  $t_1$ ), the input becomes  $C_0(0) = 0$  and  $C_1(0) = m_i/V_1$ , the equations can be solved analytically. According to the model of Newman [4] the output for two mixing chambers is

$$C_2(t) = \frac{m_i}{V_1 - V_2} \left[ \exp\left(-\frac{\dot{Q}}{V_1}t\right) - \exp\left(-\frac{\dot{Q}}{V_2}t\right) \right] \quad (6)$$

This equation has been used to describe the indicator dilution curves in order to extrapolate the downslope of the curves, as described in chapter 5, and to test the influence of flow averaging of time on the shape of the indicator dilution curve, as in chapter 6.

### 7.2.2 Nonstationary flow

Under circumstances of artificial ventilation the cardiac output is modulated by the ventilation (Ch. 5 and 6, [7]). For these circumstances flow  $\dot{Q}(t)$  can be described by

$$\dot{Q}(t) = \bar{\dot{Q}}[1 + K f(t)] \quad (7)$$

where  $\bar{\dot{Q}}$  is the mean flow,  $f(t)$  the periodic time varying function, with zero mean value, and  $K$  representing the amplitude of the variation.

For the simulations the flow was chosen to be sinusoidal, because every periodic flow pattern can be constructed by the sum of sinusoidal curves. In case of a linear system, as the two-compartmental model, also the output response of the model for the different sinusoidal input curves can be summed.

$$\dot{Q}(t) = \bar{\dot{Q}}[1 + K \sin(\omega t)] \quad (8)$$

in which  $K = (\dot{Q}_{max} - \bar{\dot{Q}})/\bar{\dot{Q}}$  is the amplitude of the sinusoidal modulation,  $\omega$  is the angular frequency of the oscillation in flow (rad/s).  $\dot{Q}_{max}$  is the maximal flow value,  $\dot{Q}(t)$  was limited to positive values.  $t_c = 2\pi/\omega$ , where  $t_c$  is the cycle time of the modulation.

### 7.2.3 The simulation model

The set of nonlinear differential equations were solved numerically on a PDP11/23 computer by use of a simulation program (TUTSIM) of the Technical University of Twente, The Netherlands.

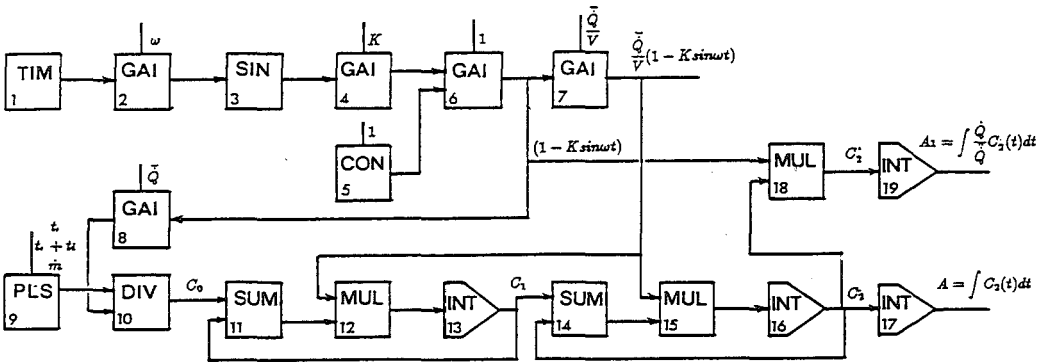


Fig. 2. TUTSIM block diagram of the two-compartmental model. TIM, time function; GAI, gain function; SIN, sine function; CON, constant; PLS, pulse function; DIV, divide function; SUM, summation function; MUL, multiply function; INT, integrator. A, area under dilution curve and  $A_1$ , area under corrected dilution curve.

The simulation program is an interactive program that mainly solves differential equations. The block diagram for the differential equation is given in Fig. 2. The blocks 1 to 6 generate the relative changes in flow  $(1 + K \sin \omega t)$ . In which block 2 adjusts the frequency and block 4 the relative amplitude of the modulation. Block 9 simulates a constant rate of injection of cold in the flow stream, whereas the blocks 8 and 10 provide the flow equivalent labeling of indicator. The blocks 7, 11, 12 and 13 simulate the first mixing chamber and the blocks 7, 14, 15 and 16 the second mixing chamber. Integrator 17 gives the area under the dilution curve of  $C_2$ . Flow averaging of the sampled concentration is obtained by block 18 and the area under the curve is integrated by block 19. The simulated cardiac output estimates were calculated according to the Stewart-Hamilton equation, from the total injected amount of indicator ( $m_i$ ) and the area under curve of  $C_2$  and the flow averaged curve  $C_2'$ ,  $CO = m_i/A$  or  $CO' = m_i/A_1$  respectively.

The calculated variables at each step of the simulation procedure are denoted in the figure.

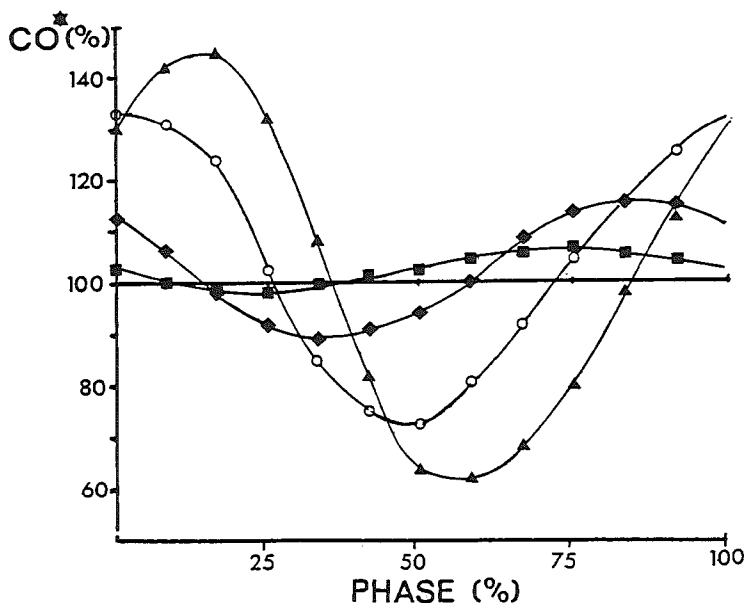


Fig. 3. Cardiac output ( $CO^*$ ) estimated by the model, as a percentage of the mean or stationary value  $\bar{Q}$ , plotted against the moment of injection as a phase of the modulation (ventilation) cycle  $PHASE = (t_1/t_c) \cdot 100\%$  for 4 different cycle times ( $t_c$ ).  $\blacktriangle = 12$  s;  $\circ = 6$  s;  $\blacklozenge = 3$  s;  $\blacksquare = 1.5$  s. Duration of injection = 0.3 s.

### 7.3 Results

#### 7.3.1 Variation of cardiac output with the moment of injection in the cycle

Dilution curves were simulated for 12 different cycle times of modulation ranging from 20 s to 1 s. To describe the range of the estimates of mean cardiac output, 12 equidistant moments in the cycle were chosen for injection of indicator. Mean cardiac output ( $\bar{Q}$ ) was determined by a simulation during of constant blood flow, i.e. the amplitude of modulation  $K = 0$  (equation 8). The individual simulated estimates were expressed as a percentage  $CO^*$  of this mean.

For all simulations parameters close to normal values in the pulmonary circulation of the pig were used, observed in our own laboratory. Volume of the two mixing chambers  $V = 20$  ml, mean blood flow  $\bar{Q} = 25$  ml/s (resulting in a time constant,  $\tau = 0.8$  s for each chamber), amplitude of

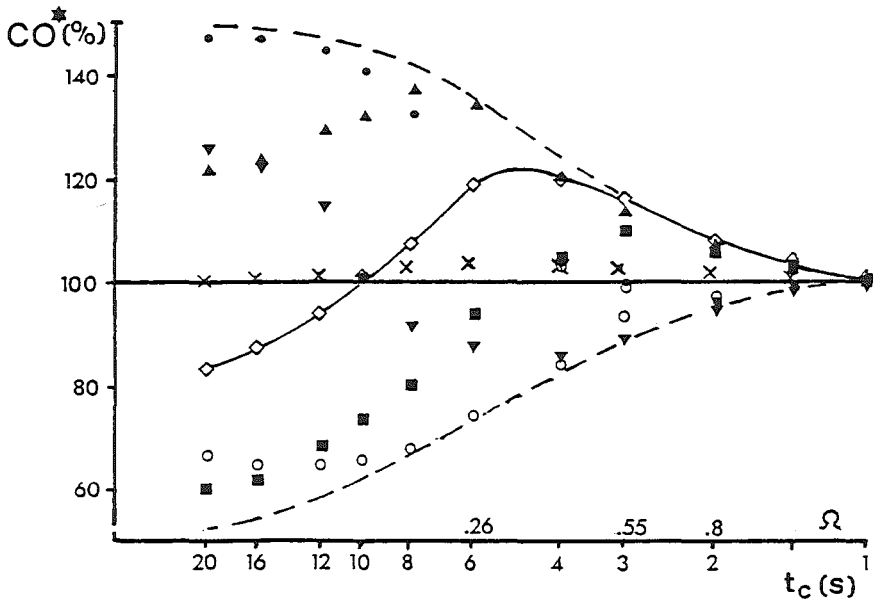


Fig. 4 Cardiac output ( $CO^*$ ) plotted versus the cycle time of modulation for 6 different phases of injection of indicator.  $\blacktriangle = 0\%$ ;  $\bullet = 16\%$ ;  $\blacktriangledown = 33\%$ ;  $\circ = 50\%$ ;  $\blacksquare = 66\%$ ; and  $\diamond = 83\%$   $\times =$  mean from the 12 estimates at one modulation frequency.

modulation  $K = 0.5$ , and a duration of injection  $t_i = 0.3$  s.

The estimates of cardiac output, by the model ( $CO^*$ ), versus the moment of injection in the modulation cycle were plotted in Fig. 3 for cycle times of  $t_c = 12, 6, 3$  and  $1.5$  s respectively.

The results demonstrate a cyclic modulation of the estimates with the same periodicity as the applied sinusoidal input flow. However, the pattern of the estimates is not sinusoidal. This is shown by the difference between the maximal positive and the maximal negative deviation. For a cycle time of 6s, for instance, these deviations were 32% and 28% ( $CO^* - 100$ ) of the mean respectively. There is also a difference in the downward slopes and upward slopes to observe. The amplitude of the modulation of the estimates decreased with a decrease in the ventilatory cycle-time ( $t_c$ ). Furthermore, there was a forward shift in the pattern of modulation when  $t_c$  was increased.

Another presentation of the range of  $CO^*$  is given in Fig. 4, for 12 dif-

ferent cycle times. In order to make the interpretation of this figure more general we have normalized for different time constants of the mixing chambers by indicating on the abscis also the quotient ( $\Omega$ ) of total time constant,  $2\tau = 1.6$  s, and the cycle time of the modulation ( $t_c$ ). At higher frequencies the deviations from the mean are negligible. At lower frequencies there is an increase in the range of CO\* estimates. At very low frequencies the actual flow during the duration of the dilution curve is estimated. However, great uncertainty exists about what is estimated in the middle range of cycle times, nor actual flow neither the mean flow. To test the averaging procedures as used in chapter 4, also all averaged values of each 12 estimates at the different phases of the modulation cycle are indicated in Fig. 4. These averages were equal to or larger than 100%. The maximal deviation of the averaged value from the mean was found in the middle range of the modulation cycle times. For the given set of simulation parameters the maximal deviation of the average was 4.6%.

### 7.3.2 *Effect of the amplitude of modulation of flow on the cardiac output estimates*

The range of the cardiac output estimates after injection at different phases of the cycle increased with the amplitude of flow modulation ( $K$ ) Fig. 5. For the simulation of this relationship the model parameters were:  $\tau = 0.8$  s,  $t_c = 6$  s,  $t_i = 0.3$  s, and the amplitude of modulation  $K = 0.0$  to  $0.9$ .

The amplitude of the CO\* estimates increases with increasing amplitude of the flow modulation, but not linearly. There is an asymmetrical distribution of the deviations with respect to the mean for the different injection phases in the modulation cycle. This causes an overestimation of the mean cardiac output. At an amplitude of  $0.9$  the overestimation, of the averaged value was 10%.

### 7.3.3 *Prolonging the injection time*

To study the effects of the duration of the injection of indicator on the CO\* estimates, four different injection times were simulated (Fig. 6). The rate of injection was kept constant during the injection period. The model settings were:  $t_c = 6$  s,  $\tau = 0.8$  s, and  $K = 0.5$ . It is clear that the range of the CO\* estimates decreased with an increase of the injection time. No deviations from the mean were found when an injection time of  $6$  s was simulated. The average of the 12 estimates equally spread over the ventilation cycle

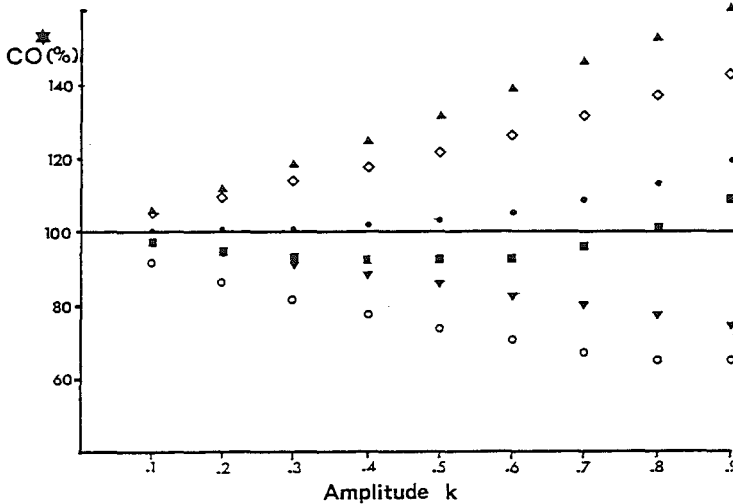


Fig. 5. Cardiac output ( $CO^*$ ) plotted against the amplitude ( $K$ ) of the flow modulation for 6 different phases of injection of indicator, see Fig. 4. The model parameters were:  $\tau = 0.8$  s,  $t_c = 6$  s and  $t_i = 0.3$  s.

overestimated mean flow i.e. 4.6% with an injection time ( $t_i$ ) of 0.25 s, 2.1% with  $t_i = 2$  s, 0.8% with  $t_i = 3$  s, and 0.0% with  $t_i = 6$  s.

## 7.4 Discussion

An appropriate mathematical model to describe the basic mechanisms of the indicator dilution technique should not only simulate the shape of an dilution curve, but it should also be based on parameters with a physiological significance. Such models, as suggested in literature, have been subdivided into two categories: compartmental and distributed models. Both categories of models have similar abilities to fit experimental data [4]. They, however, imply different conditions: the compartmental models are based on a highly concentrated mixing at a site in the vascular system, and the distributed models, as a local density random walk (LDRW) or diffusion with drift model, imply that mixing is uniformly distributed throughout the vascular system.

Our preference for a distributed model (Ch. 5) was mainly based on its greater similarity with the physiological system. However, for the approach in this chapter we have chosen for a two-compartmental model. The



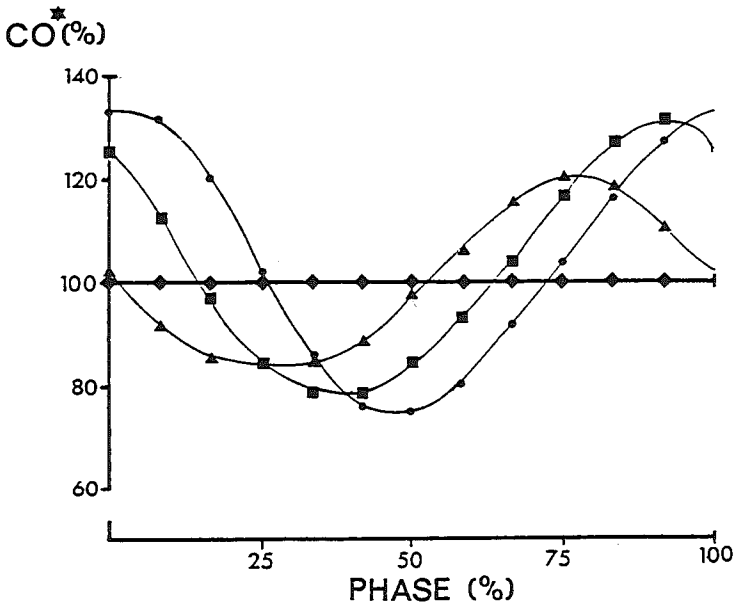


Fig. 6. Effect of the injection time ( $t_i$ ) on the  $CO^*$  estimates for a cycle time  $t_c = 6$  s.  $\circ t_i = 0.25$  s;  $\blacksquare t_i = 2$  s;  $\blacktriangle t_i = 3$  s; and  $\blacklozenge t_i = 6$  s.

compartmental model was mainly chosen because it is less complex in the computations. It enables simulations, when blood flow and input of indicator are a function of time.

Our model is an extension of Bassingthwaigte's model [1] from one to two mixing chambers. It is also an extension of Von Reth's model [5] with respect to the injection duration, from an ideal impulse function into a time consuming injection. Besides this difference the injection site was chosen near the entrance of the first mixing chamber instead of a injection into the first mixing chamber. As a consequence computations of the differential equations were adapted.

The results of our simulations and those of Bassingthwaigte et al. [1] and Von Reth [6] were in general agreement with the data obtained from the studies in pigs, chapters 3, 4, 5 and 6. Therefore, we concluded that the compartmental models provide an acceptable approach to study the effects of nonstationary flow on the estimation of cardiac output. These models, however, remain an approximation, e.g. the volume between injection and detection sites (i.e. right atrium, right ventricle, and pulmonary artery) in the animal varies with flow, whereas in all models a constant volume is assumed.

From our experimental data (Ch. 3 and 4) and the simulations (Fig. 3, 4 and 5) we conclude that the modulation in flow is a prominent source of error for the estimation of mean flow. The deviation from mean flow appeared to be dependent on frequency and amplitude of modulation, and on the moment of injection in the ventilatory cycle used. Our simulations indicated also that the duration of the injection is a source of error (Fig. 6).

The large amplitudes of the cardiac output flow oscillations caused by each heart beat were not of any importance on the estimation of mean flow, because the cardiac rate was relatively high (Fig. 3 and 4). Such a result was also reported before by Scheuer-Leeser et al. [7].

#### 7.4.1 *Estimation of mean cardiac output under changing circumstances*

Changes in ventilatory frequency, amplitude and duration of the injection period, have led to a change in the phase of the pattern of CO estimates (Figs. 3, 4, 5 and 6). Therefore, not one common moment in the ventilatory cycle could be pointed to as an accurate moment for the estimation of mean cardiac output under different circumstances. This conclusion is similar to the conclusion from experimental data obtained in pigs (Ch. 3, Fig. 3), and (Ch. 4, Fig. 4 and 5).

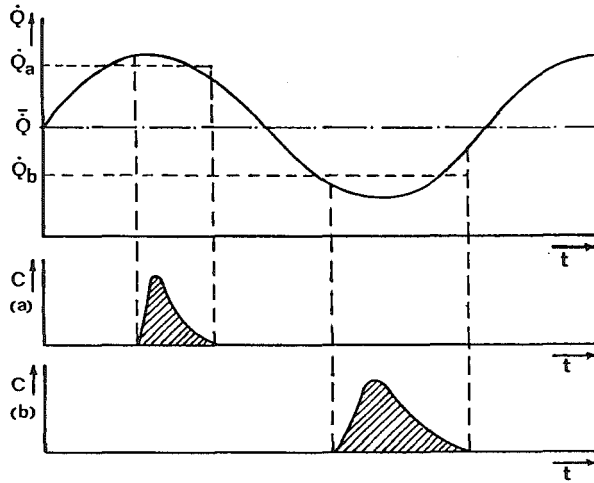


Fig. 7. Schematic representation of two cardiac output estimates  $\dot{Q}_a$  and  $\dot{Q}_b$  during high flow (a) and low flow (b), respectively.

#### 7.4.2 Improvement of cardiac output estimation

The analyses of our experimental data and the data obtained from the simulations revealed a number of methods to improve the accuracy of the estimation of mean cardiac output.

- *An increase in the ventilatory frequency.* At a higher respiratory frequency the amplitude of the real flow modulation will be smaller due to a lower tidal volume. This improves the estimation of mean cardiac output (Figs. 4 and 5, and Ch. 4, Fig. 4). Although this could be a recommendable mode of diminishing the effects of artificial ventilation, a change in the ventilatory settings also will influence gas transport mechanisms and the hemodynamic status of a patient or animal.
- *Breathhold procedures.* During a prolonged expiratory pause as well as during inspiratory hold maneuvers constant hemodynamic conditions were found (Ch. 5). The cardiac output estimates during a prolonged end-expiratory pause were significantly higher than mean cardiac output. Therefore, this method will not precisely estimate mean flow. However, inspiratory- and end-expiratory breathhold maneuvers can be very useful for testing the condition of the systemic circulation, as

was demonstrated by Versprille and Jansen [7].

- *Extending the duration of injection.* The simulations with different injection times (Fig. 6) have demonstrated that a longer injection time decreases the range of the estimates of mean cardiac output. When the duration of the injection was equal to the cycle time of modulation (i.e. the time of the ventilatory cycle) then the deviations were reduced to zero. For these simulations we have assumed no recirculation, and no influence on the biological system of the injected cold indicator. In pigs we found this injection mode to disturb hemodynamic stability and no reliable cardiac output estimate could be obtained (unpublished data). Thus, although injection with a duration equal to the ventilation cycle should be a good solution theoretically, for practical reasons we warn to be careful in the application of this method.
- *Averaging of estimates.* The average of the model estimates equally spread over the ventilatory cycle overestimates mean cardiac output (Figs. 4 and 5). The overestimation is caused by different indicator-passage times at the sampling site during low flow and high flow parts of the cycle (Fig. 7). During low flow the indicator is more spread out than during high flow. This causes a larger contribution of moments with higher flow to the curve which coincides mainly with low flow (Fig. 7b) than the moments of low flow do to the area of the curve which coincides with high flow (Fig. 7a). A corresponding result was reported by Von Reth [5]. In chapter 4 an improvement in the estimation of mean cardiac output was found when randomly performed estimates were averaged. But a much better result appeared when estimates equally spread over the ventilatory cycle were averaged. The average of two measurements equally spread over the ventilatory cycle was better than the mean of five random estimates. Experimentally we did not find an overestimation of mean cardiac output, because there was no significant difference between the average of equally spread estimates and mean cardiac output estimated by the Fick method. There was one exception. During hypovolemic conditions an overestimation of 13% was found (Ch. 4, Tabel 1). The hypovolemic situation is characterized by a low mean flow and an extended amplitude of the real flow modulation. In our simulations the extended amplitude of the flow modulation resulted in an increase of the overestimation of mean cardiac output (Fig. 5). The low mean cardiac output causes a wider dilution curve and thus a slight reduction in the overestimation

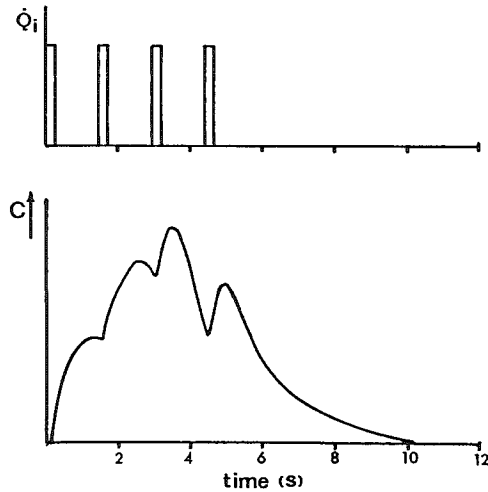


Fig. 8. Simulation of 4 injections equally spread within one ventilatory cycle.

of the average of the equidistant performed estimates (Fig. 4).

At the injection site one injection with a duration of 6 s can be considered to be equal to 12 injections of 0.5 s consecutively performed. As mentioned the average of such a series of 12 simulations overestimated mean cardiac output. The simulated estimate of cardiac output from one injection with a duration equal to the ventilatory cycle did not differ from the mean (Fig. 6). To study this discrepancy the response of four simulated injections equally spread in one ventilatory cycle (Fig. 8) was compared to the result of four injections also equally spread over the ventilatory cycle but consecutively performed in separate ventilation cycles. The parameters for the model simulations were  $t_i = 0.25$  s,  $t_c = 6$  s,  $n \cdot \tau = 2 \times 0.8$ ,  $\bar{Q} = 25$  ml/s, and the amount of injected indicator was 12.5 units on an arbitrary scale.

The cardiac output calculated from the four injections within one cycle was equal to 100% of the mean cardiac output, whereas the averaged value of the four separately performed simulations was 103.4% of the mean, i.e.  $12.5 \times (1/0.656 + 1/0.480 + 1/0.381 + 1/0.490)/4 = 25.85$  ml/s or 103.4%. The estimate of the averaged area under the curve of the four separate simulations is  $2.008/4 = 0.502$  units.s giving a

mean flow of  $12.5/0.502 = 24.9$  ml/s. This appeared to be close to the mean cardiac output ( $24.9/25.0 = 0.997$ ).

Although it is not theoretically proven we conclude that the averaging technique gives the best results when the arithmetic mean of the area under the curve is used instead of the harmonic mean. This conclusion could induce the suggestion that the averaging technique proposed in chapter 4 should be adapted because there the harmonic mean of the area has been used. However, this mean was very close to the mean estimated by the Fick method. Therefore, it is an open question whether the arithmetic mean will be superior to the harmonic mean in experimental as well as in medical studies.

- *Flow averaging of concentration.* During all simulations the technique of flow averaged sampling has been carried out. For all simulations the model estimates were found to be equal to mean cardiac output. Measurements in pigs (Ch. 6) also showed a reduction in the spread of cardiac output estimates, but not to zero. We have explained this remaining modulation by a varying effective longitudinal dispersion of indicator, causing a flow dependent distribution of indicator transit times. No deviations were found in the simulations with the compartmental approach which does not incorporate dispersion of indicator. This supports the explanation for the discrepancy with the experimental results, and the conclusion that the compartmental approach is not completely suitable to describe the indicator transport in the right ventricle and pulmonary circulation. A conclusion which is in agreement with the results found in comparative studies of three models (Ch. 5).

## References

- [1] Bassingthwaite, J. B., T. J. Knopp, and D. U. Anderson. Flow estimation by indicator dilution (bolus injection). Reduction of errors due to time-averaged sampling during unsteady flow. *Circ. Res.* 27: 277-291, 1970.
- [2] Castellana, F. S., S. M. Snapinn, S. Y. Tam, and R. B. Case. Inlet and intrachamber concentration distributions in tracer studies of the canine central circulation and their relation to the isotope dilution residue function. *Circ. Res.* 47: 10-20, 1980.
- [3] González-Fernández, J. M. Theory of the measurement of the dispersion of an indicator in indicator-dilution studies. *Circ. Res.* 10: 409-427, 1962.
- [4] Harris, T. R., and E. V. Newman. An analysis of mathematical models of circulatory indicator-dilution curves. *J. Appl. Physiol.* 28: 840-850, 1970.
- [5] Reth, E. A. von. Assessment of the indicator-dilution technique in nonstationary flow. In: *Thesis*, Technische Hogeschool Eindhoven, 1984.

- [6] Scheuer-Leeser, M., A. Morquet, H. Reul, and W. Inrich. Some aspects to the pulsation error in blood-flow calculations by indicator-dilution technique. *Med. Biol. Eng. Comput.* 15: 118-123, 1977.
- [7] Versprille, A., and J. R. C. Jansen. Mean systemic filling pressure as a characteristic pressure for venous return. *Pflügers Archiv* 405: 226-233, 1985.
- [8] Zierler, K.L. Circulation times and the theory of indicator-dilution methods for determining blood flow and volume. In: *Handbook of Physiology, Circulation*. Washington, DC: Am. Physiol. Soc., sect. 1, vol. I, chapt. 18, p. 585-615, 1962.





# Summary

## *Chapter 1*

Starting from a review of historical aspects of the indicator dilution method the theory of this technique has been summarized for the bolus injection method. The blood circulation is generally considered as stationary and linear in its variables. Under these conditions the Stewart-Hamilton equation can be used to calculate mean cardiac output. However, during mechanical ventilation blood flow is modulated with a periodicity equal to the ventilation cycle and, under these conditions, the system cannot be regarded as stationary and linear, as has been shown by several authors. Therefore, the application of the Stewart-Hamilton equation is not strictly valid. Nevertheless, the thermodilution technique and the application of the Stewart-Hamilton equation is widely used and accepted in patient care even when blood flow is modulated by mechanical ventilation. This is particularly because of a lack of better alternative. Consequently, this thesis is devoted to (i) the estimation of mean cardiac output by the thermodilution method in pigs under mechanical ventilation (chapters 3 and 4) and (ii) the consideration of several new approaches to improve the accuracy of the estimation of mean cardiac output (chapters 4, 5, 6 and 7).

## *Chapter 2*

The design of a microcomputer controlled ventilator for automatic performance of lung function and circulatory tests has been described. It incorporates the characteristics of normal mechanical ventilation and also allows one to perform a multitude of test procedures for lung function and circulatory studies in paralyzed animals. The major components of the set-up are a pump assembly with solenoid valves to direct gas flow, an electro-mechanical servo system and an MS-DOS microcomputer system. The pump assembly has been constructed as a relatively simple device. Great versatility is created by the use of a microcomputer for the control of the ventilator. The software can be easily adapted to several other types of experimental studies. Besides the keyboard input the ventilator can be controlled by a remote computer system. This allows one to run an experimental protocol automatically and to use it in closed loop servo ventilation. The flexibility in the choice of the respiratory parameters makes the ventilator suitable for

lung function and circulatory studies during artificial ventilation. The ventilator has been successfully used in different animal studies during the last 6 years.

### *Chapter 3*

The feasibility of using the thermodilution method to monitor cardiac output during artificial ventilation was studied in anesthetized pigs. Normal saline (0.5 ml) at room temperature was injected into the left ventricle or the right atrium. The dilution curves were detected in the aortic arch and the pulmonary artery, respectively. The ventilation rate was 10 cycles/min at end-expiratory pressures of 0, 5, 10 and 15 cmH<sub>2</sub>O. For each level, 50 measurements of cardiac output were performed at regular intervals over the ventilatory cycle. The order of measurements were randomly selected. The average of each series of 50 measurements showed excellent correlation with the estimates of cardiac output based on the direct Fick method for oxygen. The maximum difference between the values of cardiac output randomly measured by the thermodilution method was 40% for the left side of the heart and 70% for the right side. However, when the values of cardiac output were sorted according to the specific phases of the respiratory cycle, there was a systemic variation with a small random error. For the left side of the heart a satisfactory moment of injection for estimation of mean cardiac output values at the right side did not reveal any satisfactory moment for injectate administration under changing circumstances, e.g., positive end-expiratory pressure.

### *Chapter 4*

The reliability of cardiac output estimation by thermodilution during artificial ventilation was studied in anesthetized pigs at the right side of the heart. The estimates exhibited a cyclic modulation related to the ventilation. The amplitude of the modulation was independent of the level of positive end-expiratory pressure, ventilatory pattern and volemic loading of the animals. However, a non-constant phase relation existed between the ventilatory cycle and the modulation. Single observations at a fixed moment in the ventilatory cycle are therefore not appropriate for estimation of mean cardiac output neither for studying its relative changes.

The averaging of estimates spread equally over the ventilatory cycle led to a much larger reduction in the deviation of the averages from the mean cardiac output than an averaging procedure of randomly selected estimates.

The accuracy of estimation of mean cardiac output by two estimates equally spread in the ventilatory cycle was equal to the accuracy obtained by averaging five randomly selected estimates.

Averaging four estimates, equally spread in the cycle, appeared to be the optimal procedure. For 89% of all averages an accuracy of 5% around the mean was obtained and for 99% an accuracy of  $\pm 10\%$ .

### *Chapter 5*

The feasibility of three mathematical models to extrapolate the tail of thermodilution curves, when flectures are present in the descending limb, was tested in anesthetized pigs. The models were a local random walk model (LDRW), a log-normal distribution, and a two-compartmental model. First, the accuracy of the extrapolation of the tail by each model was tested on two undisturbed curves by taking the truncation at five different points on the descending limb. The extrapolated curve area obtained from each model was compared with total area of the undisturbed curve. Next, dilution curves obtained during inspiratory hold maneuvers and characterized by deflection points were analyzed, taking the truncation just before deflection. The estimates of cardiac output by the models were compared with electromagnetically measured flow in the pulmonary artery. The area of the dilution curve was estimated more accurately when more information on the descending limb was available. The LDRW model and the log-normal distribution were superior to the two-compartment model regarding accuracy of cardiac output estimation and root-mean-square errors of the fit. Both models estimated curve area with an error  $< 5\%$  when truncation of the descending limb occurred below 60% of the peak value. In circumstances of mechanical ventilation, where only short periods of constant flow will be present, analyses of dilution curves based on the LDRW model or the log-normal distribution are recommended.

### *Chapter 6*

The feasibility of the thermodilution method for estimation of cardiac output was studied in anesthetized and artificially ventilated pigs. A series of 50 thermodilution measurements each, equally distributed over the ventilatory cycle, were performed randomly. These estimates were spread between 65-125% of the mean. After sorting the estimates with respect to the ventilatory cycle, a cyclic modulation appeared. Fitting the temperature-time curves with each of 3 models (log-normal, local density random walk and

two compartmental) did not give reliable results. To improve the reliability of cardiac output estimates we transformed the thermodilution curves by either flow averaging of time or flow averaging of concentration. For this averaging technique the flow measured with an electromagnetic flow probe ( $Q_{emf}$ ) was used. After this test we used the pulse contour of the pulmonary artery pressure to estimate the relative change in stroke volume of the heart instead of  $Q_{emf}$ . From these results it appeared that flow averaging of time improves the accuracy of the fit by the 3 models (mean RMSE 2.5 times smaller). Flow averaging of concentration or of time decreased significantly the modulation of the cardiac output estimates by the respiratory cycle. Estimation of mean cardiac output with one randomly performed thermodilution measurement is possible in this way. Using the flow averaging technique the mean cardiac output could be estimated with an SD of 7%.

### Chapter 7

For a better understanding of the errors made in the estimation of mean cardiac output by the thermodilution method, mathematical simulations were compared to the experimental results. A two-compartmental model was used to describe the indicator dilution process. The results of the model simulations were found to be similar to the experimental data. A cyclic pattern of cardiac output estimates appeared when injections were simulated at different phases of the ventilation cycle. This cyclic pattern was found to be dependent of the cycle time and amplitude of the real flow, and the duration of the injection of indicator. The phase of the pattern of estimates shifted when the conditions were changed, therefore the conclusion was confirmed that not one defined moment in the ventilatory cycle could be used to estimate mean cardiac output. The accuracy of the estimation of mean cardiac output was improved by averaging estimates equally spread over the ventilatory cycle, as was also found in the animal studies. However, in the model simulations an overestimation of the mean occurred. This overestimation appeared to be less when the arithmetic mean of the areas under the dilution curve was used instead of the harmonic mean. The application of injections with a duration equal to the cycle time of the flow modulation showed to be a theoretically good solution for the estimation of mean cardiac output. The calculations of mean cardiac output after flow averaging of the concentration of the indicator were correct during simulation under all circumstances, which was already found experimentally.

# Samenvatting

## *Hoofdstuk 1*

De thermo-dilutiemethode wordt heden ten dage veelvuldig in kliniek en laboratorium toegepast. In dit hoofdstuk wordt allereerst een beknopt overzicht gegeven van de ontwikkelingen die geleid hebben tot de thermo-dilutiemethode. De theorie van de indicator-dilutiemethode werd samengevat voor een circulatiesysteem waarvan de parameters constant en lineair zijn. Bij deze aanname kan het gemiddelde hartminuutvolume (HMV) berekend worden op grond van de Stewart-Hamilton vergelijking.

Tijdens beademing is de bloedstroomsterkte niet constant maar wordt gemoduleerd met een frequentie, die gelijk is aan die van de beademing. Onder deze omstandigheden kan het circulatiesysteem dan ook niet als constant en lineair in zijn parameters beschouwd worden. Toepassing van de Stewart-Hamilton vergelijking tijdens beademing is dus op theoretische gronden onjuist. Niettemin wordt dit toch gedaan in de kliniek, bij gebrek aan beter.

Daarom werden in dit proefschrift allereerst de fouten bestudeerd die men dan maakt bij het schatten van het gemiddelde HMV tijdens beademingsomstandigheden (hoofdstukken 3 en 4). Vervolgens werden verschillende benaderingen getest, die de fouten reduceren en daarmee de nauwkeurigheid verbeteren waarmee het HMV kan worden geschat (hoofdstukken 4, 5, 6 en 7).

## *Hoofdstuk 2*

Voor het bestuderen van de afwijkingen die ontstaan in de schatting van het gemiddelde HMV tijdens beademing was het nodig om op elk gewenst moment in de beademingscyclus een bepaling van de bloedstroomsterkte te kunnen uitvoeren. Mede met dit doel werd in samenwerking met de centrale research werkplaats van de EUR op het eigen laboratorium een beademingsapparaat ontwikkeld. Dit beademingsapparaat heeft o.a. de volgende mogelijkheden:

- uitvoering van conventionele beademing met een in te stellen beademingspatroon naar keuze.
- inpassing tijdens genoemde conventionele beademing van een enkele beademingscyclus met een gekozen patroon zowel voor de inspiratie

als ook voor de expiratie.

- gegevensuitwisseling met een andere computer.
- het starten van een HMV-bepaling m.b.v. de thermo-dilutiemethode op elk gewenst moment in de beademingscyclus. Dit gebeurt door de injectie van een kleine hoeveelheid koude vloeistof in de bloedstroom en de daardoor ontstane thermo-dilutiecurve te analyseren met een speciaal daarvoor geschreven programma voor een PDP 11/23 computer.

De belangrijkste onderdelen van de ventilator zijn: twee blaasbalgen met electromagnetische kleppen om de gastroom te besturen, een electro-mechanisch servosysteem en een MS-DOS computer (Fig. 1 en 2, pag. 12 en 13). Het mechanische gedeelte werd zo eenvoudig mogelijk gehouden. Door gebruik te maken van een microcomputer voor de besturing van het mechanische gedeelte werd de ventilator algemeen toepasbaar gemaakt voor velerlei doeleinden, dankzij aanpassing van de computerprogramma's aan de experimentele vraagstellingen. De invoer voor zo'n programma gebeurt via een toetsenbord of via een andere computer. Door invoer via deze andere computer is het mogelijk om geheel automatisch een experimenteel protocol uit te voeren. Hierbij kunnen uiteenlopende ventilatieprocedures aan het proefdier worden opgelegd. Tevens kan via deze invoerweg een zogenaamde gesloten lus beademing gemaakt worden. Hierbij voert de ventilator een opdracht uit, de reacties hierop van het proefdier worden gemeten en deze meetsignalen worden via een andere computer geanalyseerd. Deze rekent dan op basis van de verkregen gegevens en de opgelegde ventilatie criteria een nieuwe lijst van invoergegevens voor de ventilator uit. De ventilator heeft goed gefunctioneerd gedurende de voorbije 6 jaar dat deze in gebruik is.

### *Hoofdstuk 3*

Bij genarcotiseerde biggen werd de bruikbaarheid van de thermo-dilutiemethode onderzocht voor het bepalen van het gemiddelde hartminuutvolume. Allereerst werd gezocht naar het meest geschikte moment in de beademingscyclus voor het uitvoeren van een thermo-dilutiemeting. Hiertoe werden op verschillende momenten in de beademingscyclus HMV-metingen gedaan. Vervolgens werd bestudeerd of een gekozen moment in de beademingscyclus onafhankelijk was van de hemodynamische conditie. Deze conditie werd beïnvloed door het opleggen van een positieve eind-expiratoire

druk (PEEP) van 0, 5, 10, en 15 cmH<sub>2</sub>O. De proefdieren werden beademd met een frequentie van 10 per minuut.

Voor dit onderzoek kon gebruik gemaakt worden van de computergestuurde ventilator uit hoofdstuk 2. Dit onderzoek is juist mede aanleiding geweest voor de ontwikkeling van een dergelijke ventilator. Voor de beademing werd gebruik gemaakt van een Starling pomp, waarvan het inspiratie patroon half- sinusvormig was en de inspiratie en expiratie tijd respectievelijk 44% en 56% van de beademingscyclustijd duurden. De beademingscyclus werd in 100 gelijke intervallen verdeeld (procenten) door de ventilator te voorzien van een mechanisch-electronische schakeling (Fig. 1, pag. 30). Bij iedere ingestelde PEEP-waarde werd een serie van 50 thermo-dilutiemetingen gedaan, met tussen iedere bepaling een wachtperiode van een halve minuut. De bepalingen werden op alle even waarden van de fase van de beademingscyclus (2%, 4%, .. 100%) gedaan. De metingen werden in willekeurige volgorde uitgevoerd.

Een meting werd uitgevoerd door 0,5 ml fysiologisch zoutoplossing in te spuiten in het linker ventrikel of het rechter atrium, waarbij de dilutiecurve werd gemeten in respectievelijk de aorta en de arteria pulmonalis. Bij de analyse van de thermo-dilutiecurve werden correcties aangebracht voor temperatuurverlies in de katheter, cyclische temperatuurveranderingen ten gevolge van de beademing en langzaam optredende veranderingen in de lichaamstemperatuur.

Het gemiddelde van de 50 HMV-bepalingen bleek identiek aan het gemiddelde HMV bepaald met de directe Fick methode voor zuurstof (Fig. 4, pag. 37). De maximale afwijking van het gemiddelde was echter 35% voor metingen aan de rechterzijde van het hart en 25% voor die aan de linkerkant (Fig. 2, pag. 36). Op grond van deze resultaten kon geconcludeerd worden dat de thermo-dilutiemethode ongeschikt is om het gemiddelde HMV nauwkeurig te bepalen met één enkele willekeurige meting. Werden echter de 50 HMV-bepalingen gesorteerd naar het moment van injectie in de beademingscyclus, dan werd een systematische afwijking ten opzichte van het gemiddelde zichtbaar (Fig. 2, pag. 36). Het patroon van de HMV-bepalingen was gelijk in frequentie aan die van de beademingscyclus. Werd de serie van 50 thermo-dilutiemetingen aan de rechterzijde van het hart op een ander PEEP-niveau uitgevoerd, dan verschoof het cyclisch patroon van de afwijkingen (Fig. 3, pag. 36). Ten gevolge van deze faseverschuiving was het niet mogelijk één moment in de beademingscyclus aan te geven voor een goede schatting van het gemiddelde HMV. Bij metingen aan de linkerzijde van het hart werd deze verschuiving bij toenemende PEEP niet waargenomen.

#### *Hoofdstuk 4*

In dit onderzoek werd de invloed van de experimentele condities op het patroon van HMV schattingen verder onderzocht, door veranderingen in zowel het patroon, de frequentie en de amplitude van de werkelijke bloedstroomsterkte te veroorzaken. Dit werd gedaan door het kiezen van verschillende patronen en frequenties van beademen en het introduceren van drie bloedvullings-toestanden. In dit onderzoek werd gebruik gemaakt van de computergestuurde ventilator uit hoofdstuk 2. Vervolgens werd onderzocht in welke mate middelingsmethoden een verbetering van de schatting van het gemiddelde HMV gaven. Hierbij werden 2750 thermo-dilutiebepalingen gebruikt.

Zoals in het onderzoek van hoofdstuk 3 werden ook hier fase-verschuivingen van het patroon van schattingen van het gemiddelde HMV gevonden bij veranderende condities (Fig. 4 en 5, pag. 51 en 53). Dit illustreerde nogmaals dat men niet een vast moment in de beademingscyclus kan kiezen om het gemiddelde HMV te schatten en ook niet om het verloop in het gemiddelde HMV te volgen als daarbij de conditie van het proefdier verandert.

Het gemiddelde van 2 tot 6 op willekeurige momenten in de beademingscyclus uitgevoerde bepalingen gaf een verbetering in de nauwkeurigheid waarmee het gemiddelde HMV geschat wordt. Een nog veel beter resultaat werd bereikt door het gemiddelde van gelijk over de beademingscyclus verdeelde metingen te nemen (Fig. 2, pag. 48 en Tabel 1, pag. 52). De nauwkeurigheid van het gemiddelde van twee gelijk over de beademingscyclus uitgevoerde metingen (b.v. op 5% en op 55% van de cyclus) is even groot als dat van 5 metingen op willekeurige momenten. Voor biggen bleek het gemiddelde van 4 metingen, gelijk over de ademcyclus verdeeld, de meest optimale procedure. Hierbij viel 89% van de waarden binnen een nauwkeurigheidsgrens van  $\pm 5\%$  en 99% binnen een nauwkeurighedsinterval van  $\pm 10\%$ .

#### *Hoofdstuk 5*

Gedurende een korte ademstilstand (10 - 12 s) is de bloedstroomsterkte constant. In dat geval kan bij een indicator-dilutiemeting de Stewart-Hamilton vergelijking voor het schatten van het gemiddelde HMV worden toegepast. De periode van de ademstilstand is echter in vele gevallen te kort om de indicator de meetplaats volledig te laten passeren (Fig. 1, pag. 65). Met behulp van wiskundige modellen kan zo'n curve gecorrigeerd worden, alsof de stationaire toestand blijft voortduren, door de curve te extrapoleren voorbij



de duur van de ademstilstandperiode.

Bij genarcotiseerde biggen werden inspiratoire en eind-expiratoire ademstilstandprocedures uitgevoerd. Tijdens deze ademstilstandprocedures werden thermo-dilutiecurven gemeten. De volgende drie mathematische modellen werden onderzocht op de bruikbaarheid: een "local density random walk" (LDRW)-model, een log-normale distributie functie en een tweemengkamermodel.

Om de nauwkeurigheid van de extrapolatietechniek te onderzoeken werden de drie modellen aangepast ("best fit") aan twee complete en ongestoorde curven, waarbij in 5 stappen steeds minder informatie over het dalende been van de curve werd meegegeven. Dat wil dus zeggen dat vanaf de piekwaarde van de curve het afdalende been steeds korter werd gekozen. (Fig. 2, pag. 68) Het oppervlak onder de op grond van het model aangepaste dilutiecurve werd vergeleken met het oppervlak onder de ongestoorde volledige curve (Tabel 1, pag. 66). Hieruit bleek dat de log-normale distributie en het LDRW-model nauwkeuriger zijn dan het tweemengkamermodel, vooral bij dilutiecurven die meer symmetrische zijn en waarbij minder informatie over het verloop van het afdalende been beschikbaar is.

Vervolgens werden de dilutiecurven geanalyseerd die tijdens de beademingsstilstand-procedures werden verkregen. Deze dilutiecurven waren gekenmerkt door een afbuigpunt in het dalende been. De gegevensinvoer voor het aanpassen van de modellen aan de curven ("best fit") werd gestopt juist voor dit afbuigpunt.

De HMV-waarden, die met behulp van de drie modellen werden geschat, werden vergeleken met de bloedstroomsterkte-waarden gemeten met een electromagnetische stroomsterktemeter. Geconcludeerd werd dat een betere schatting van het HMV met behulp van de modellen gemaakt kan worden naarmate er meer informatie over het dalende been van de curve beschikbaar is. Ook hier voldeden de log-normale distributie en het LDRW-model beter dan het tweemengkamermodel, gelet op de nauwkeurigheid waarmee het HMV geschat werd en de kleinste kwadratensom van de modelaanpassing (Fig. 3, 4, 5, pag. 69 en 70). Geconcludeerd werd dat bij korte momenten van constante bloedstroomsterkte, de analyse van een dilutiecurve het best gebaseerd kan zijn op een log-normale distributie of het LDRW-model.

De HMV-waarden, verkregen gedurende een eind-expiratoire ademstilstand, bleken in alle experimenten het gemiddelde HMV tijdens beademing te overschatten (Tabel 2, pag. 70). De mate van overschatting bleek afhankelijk van het niveau van het HMV. Deze ademstilstand-procedure lijkt dan ook niet geschikt om veranderingen in het HMV te volgen.

## Hoofdstuk 6

Om het HMV te schatten uit een enkele thermo-dilutie bepaling kan, naast het middelen van een aantal gelijk over de beademingscyclus verspreide metingen, óók voor het aanpassen van de berekeningsmethode gekozen worden. De Stewart-Hamilton vergelijking dient dan te worden aangepast door òf de indicator-concentratie òf de tijdschaal eerst te vermenigvuldigen (wegen) met de relatieve verandering in de bloedstroomsterkte en vervolgens de getransformeerde curve te integreren. Een dergelijke methode van wegen werd allereerst getest met het werkelijke stroomsterktesignaal dat met een electromagnetische stroomsterktemeter werd opgenomen (Fig. 5, pag. 85). Daarna werd de methode getest met een gemakkelijker verkrijgbaar substituuat voor het stroomsterktesignaal, en wel de druk in de a. pulmonalis, geanalyseerd volgens de pulscontour-methode (Fig. 7, pag. 87).

Het transformeren van de tijdschaal van de dilutiecurve leverde een dilutiecurve op die aanzienlijk beter met de wiskundige modellen, zoals beschreven in hoofdstuk 5, kon worden geanalyseerd dan de curve vóór de transformatie. De kleinste kwadratensom van de afwijking tussen model en meetpunten verbeterde ca. 2,5 keer door de transformatie (Fig. 4, pag. 84). Het wegen van de indicator-concentratie of de tijdschaal verminderde de grootte van de modulatie van de HMV-schattingen aanzienlijk. Door deze weegmethode werd het gemiddelde HMV geschat met een nauwkeurigheid van 7% voor 1 SD (Fig. 7, pag. 87), bij toepassing van een serie van 50 metingen gelijk over de cyclus verdeeld. Het bleek aldus mogelijk met slechts één willekeurig in de tijd uitgevoerde meting het HMV met aanvaardbare nauwkeurigheid te schatten. Deze nauwkeurigheid was echter iets minder dan die van het gemiddelde van 4 metingen gelijkelijk verspreid over de beademingscyclus.

## Hoofdstuk 7

Om beter te kunnen begrijpen waardoor en in welke mate er fouten bij het schatten van het HMV gemaakt worden, zijn de resultaten van wiskundige modelsimulaties vergeleken met de dierexperimentele bevindingen uit de hoofdstukken 3, 4, 5 en 6. Voor het simuleren van het indicator-dilutieproces werd gebruik gemaakt van een twee-mengkamermodel. Er werd een grote mate van overeenkomst gevonden tussen de modelsimulaties en de dierexperimentele resultaten. Een cyclisch patroon in de HMV (model-) waarden werd aangetoond, wanneer deze werden uitgezet tegen het moment van injectie in de beademingscyclus. De amplitude en de fase van dit cyclisch

patroon bleken afhankelijk te zijn van de amplitude en de cyclustijd van de werkelijke stroomsterktemodulatie en de duur waarover geïnjecteerd werd (Fig. 3, 4, 5 en 6, pag. 95, 96, 98 en 99).

De conclusie - in hoofdstuk 3 - dat er geen moment in de ademcyclus is aan te geven waarop onder alle condities het gemiddelde HMV geschat kan worden, werd met deze model-simulaties bevestigd. De nauwkeurigheid kon aanzienlijk verhoogd worden door een aantal gelijk over de beademingscyclus verdeelde thermo-dilutiemetingen te middelen, zie ook hoofdstuk 4. In de modelsimulaties werd hierbij echter een kleine doch systematische overschatting van het werkelijke gemiddelde gevonden.

Het model leverde een goede schatting van het gemiddelde HMV op als de injectieduur gelijk werd gekozen aan de duur van de beademingscyclus. Na het wegen van de indicator-concentratie of de tijdschaal met de relatieve bloedstroomsterkte werden bij simulatie met het wiskundige model HMV-waarden berekend die onder alle omstandigheden exact overeenkwamen met de opgelegde HMV-waarden. Ook in de dierexperimentele situatie werd een verbetering van de nauwkeurigheid met deze methode gevonden (hoofdstuk 6).



## Curriculum vitae

Naam	Jozef Reinier Cornelis Jansen
Geboren	11 maart 1944 te Noordwijkerhout
1962-1967	H.T.S. elektrotechniek te Breda
1967-1970	1e assistent van het hoofd van de afdeling marine luchtvaartdienst bij het ministerie van defensie, met als taken de coördinatie van de opleiding van technici en het toezicht op het onderhoud van en onderzoek naar apparatuur benodigd voor onderzeeboot-bestrijding.
1970-1971	Geluids- en belichtingstechnicus bij de productie van een film over de sociale en psychologische situatie van langdurig zieken, gesubsidieerd door het voormalige Ministerie van C.R.M.
1971-1974	Systeemanalist/elektronicus bij het Klinisch Fysiologisch Laboratorium van de afdeling Kindergeneeskunde, Rijks Universiteit Leiden (hoofd: Dr. A. Versprille).
1974-heden	Systeemanalist, stafid van het pathofysiologisch laboratorium (hoofd: prof.dr. A. Versprille) van de afdeling Longziekten (hoofd: prof.dr. C. Hilvering) van de Erasmus Universiteit te Rotterdam. Hij is o.a. als projectleider verantwoordelijk voor het onderzoek naar de toepassingsmogelijkheden van de thermodilutie-methode, in een samenwerkingsverband met de Werkgroep Biomedische Instrumentatie TNO(BMI) en de afdeling anesthesiologie, beide gehuisvest in het Academisch Medisch Centrum te Amsterdam.

## Nawoord

Dit proefschrift is tot stand gekomen met de hulp van anderen. Ik wil hen hiervoor bedanken.

De computergestuurde ventilator werd ontwikkeld in samenwerking met medewerkers van de centrale research werkplaatsen.

Voor de "hardware" zorgden o.a. de heren W.J. v. Alphen, A. Drop, H.R. Thon en Ir. R. Niesing.

De "software" werd op overzichtelijke wijze geschreven en gebruikersvriendelijk gemaakt door Ing. E. Hoorn. Drs. J. v. Goudoever zorgde voor enkele uitbreidingen van het programma.

Onvermoeibare steun tijdens de experimenten kreeg ik van de heer A. Drop. Stimulerende discussiepartners waren Dr. J.J. Schreuder, Dr. A. Zwart, Ir. J. Settels en Ir. K. Wesseling.

Creatieve impulsen voor een goede opzet en verwerking van de experimenten tot artikelen heb ik ontvangen van mijn promotor Prof. Dr. A. Versprille en co-promotor Dr. J.M. Bogaard.

Mevr. L. Molenaar bedank ik voor haar betrokkenheid bij mijn promotie en haar zorg besteed aan het manuscript.

## List of abbreviations frequently used:

A	area of temperature-time curve
C	concentration
$C_0$	concentration at the entrance of first mixing chamber
$C_1, C_2$	concentration in first and second mixing chamber resp.
$C_2'$	concentration after flow averaged sampling
CO	cardiac output
CO*	CO normalized to the mean CO value
CO <sub>TH</sub>	CO estimated by the thermodilution method
CO <sub>Fick</sub>	CO estimated by the Fick method for oxygen
$\overline{CO}_{TH}$	mean cardiac output from (50) measurements
CPPV	continuous positive pressure ventilation
ECG	electro cardiogram
h	hour
$h_{max}$	peak value dilution curve
$h_{tp}$	height of curve at the truncation point
Hb	hemoglobin
I	inspiration
IP	inspiratory pause
IPPV	intermittent positive pressure ventilation
K	amplitude of sinusoidal modulation
E	expiration
ERR	root mean square error of fit
LDRW	local density random walk model
LOGN	log-normal distribution
$m_i$	mass of indicator injected
$P_{ao}$	aortic pressure
$P_{ap}$	pulmonary artery pressure
$P_{cv}$	central venous pressure
$P_T$	tracheal pressure
$P_{CO_2}$	partial pressure of carbon dioxide
$P_{O_2}$	partial pressure of oxygen
PEEP	positive end expiratory pressure
$\dot{Q}$	flow
$\dot{Q}_i$	injectate rate
$\dot{Q}_{EM}$	electromagnetically measured flow
$\dot{Q}_{err}$	underestimation of CO when base-line is neglected
$\dot{Q}_{rv}$	right ventricular outflow

$\overline{\dot{Q}_{TH,4}}$	mean of 4 estimates equally spread over ventilatory cycle
$\dot{Q}_{TH,ee}$	cardiac output estimate during an end expiratory pause
RR	respiration rate
SD	standard deviation
s	time
$S_b, S_i$	specific heat of blood and injectate resp.
$T_b, T_i$	temperature of blood and injectate resp.
t	time
$t_c$	cycle time of flow modulation
$t_i$	duration of injection
$V_i$	volume of injected indicator
$V_D$	volume of intracorporeal part injection catheter
$\dot{V}_{O_2}$	oxygen uptake
$V_1, V_2$	volume of first and second mixing chamber, resp.
v	velocity
W	weight
wk	week
ZEEP	zero end expiratory pressure
2-comp	two-compartmental model
$\alpha$	scaling factor dilution curve
$\Delta T$	temperature change after injection
$\lambda$	skewness parameter
$\mu$	median transit time
$\sigma$	standard deviation
$\tau$	time constant of a mixing chamber
$\rho_b, \rho_i$	specific gravity of blood and injectate resp.
$\omega$	angular frequency of the oscillation
$\Omega$	dimensionless frequency